

APPENDIX L

GROUNDWATER FLOW FIELD DEVELOPMENT

This appendix describes the development of a regional-scale groundwater flow field for the Hanford Site. A groundwater flow field is a time-dependent, spatially varying representation of the direction and magnitude of groundwater flow. The Hanford groundwater flow field was critical to the evaluation and comparison of the potential long-term impacts of *Tank Closure and Waste Management Environmental Impact Statement for the Hanford Site, Richland, Washington* alternatives, and evaluation of the long-term cumulative impacts, on resources related to groundwater.

L.1 INTRODUCTION

This *Tank Closure and Waste Management Environmental Impact Statement for the Hanford Site, Richland, Washington (TC & WM EIS)* is being prepared in accordance with the National Environmental Policy Act (NEPA) of 1969, as amended (42 U.S.C. 4321 et seq.); U.S. Department of Energy (DOE) implementing procedures for NEPA (10 CFR 1021); and Council on Environmental Quality (CEQ) regulations for implementing the procedural provisions of NEPA (40 CFR 1500–1508). These regulations require that an environmental impact statement evaluate short- and long-term environmental impacts of the alternatives and their cumulative impacts. This *TC & WM EIS* evaluates the impacts of Tank Closure, Fast Flux Test Facility (FFTF) Decommissioning, and Waste Management alternatives on land resources, infrastructure, noise, air quality, geology and soils, water resources, ecological resources, cultural resources, socioeconomics (e.g., employment, regional demographics, housing and community services), public and occupational health and safety, environmental justice, and waste management activities. Contaminants in groundwater at the Hanford Site (Hanford) could potentially impact water resources, ecological resources, cultural resources, public health and safety, and environmental justice over the long term. In particular, the Columbia River and its associated ecological resources are highly valued resources that could be impacted by contaminants transported from Hanford through groundwater.

This *TC & WM EIS* quantifies impacts on the human and natural environment to the extent practicable, consistent with DOE's sliding-scale approach, taking into account available project information and design data. This approach to NEPA analysis implements CEQ's instruction to "focus on significant environmental issues and alternatives" (40 CFR 1502.1) and discuss impacts "in proportion to their significance" (40 CFR 1502.2[b]). This *TC & WM EIS* acknowledges uncertainty and incompleteness in the data and, where the uncertainty is significant or a major factor in understanding the impacts, explains how the uncertainty affects the analysis. Reasonably varied analyses are used to identify the range of potential flow fields consistent with the available data (see Section L.2). Thus, this *TC & WM EIS* balances the dual goals of accuracy and comparability against the available information and the need for timely decision-making.

L.1.1 Purpose

The purpose of this appendix is to describe the development of the model that simulates the groundwater flow field for Hanford. The groundwater pathway is one of the major pathways affecting the evaluation of the impacts of alternative and cumulative impacts at Hanford. The importance of the groundwater pathway is the connectivity between the waste disposal areas at the ground surface, the aquifer beneath Hanford, and the receptors exposed to that aquifer. The groundwater flow field is a calculation of the direction and rate of water movement in the aquifer. The groundwater flow field provides the connection between the source locations evaluated in the *TC & WM EIS* alternative and cumulative impact sources and the lines of analysis at which impacts are reported.

The groundwater flow field was calculated prior to simulation of contaminant transport in the vadose zone and unconfined aquifer. The groundwater flow field provides the numerical representation of water table

elevations and velocities that provided inputs to the vadose zone transport model STOMP [Subsurface Transport Over Multiple Phases] (see Appendix N) and the saturated zone transport model (see Appendix O). A well-calibrated groundwater flow field provides connection and consistency between the vadose zone and saturated zone transport models that are used to evaluate alternative and cumulative impacts.

Distinct flow fields resulting from different encoded data or assumptions, called design variants, were developed to span the range of expected conditions at Hanford. These reasonably varied design variants are used to assess the uncertainty of key flow field parameters, the sensitivity of simulated long-term impacts of *TC & WMEIS* alternatives to flow field parameters, and the effect reasonably foreseeable future scenarios would have on the flow field (see Section L.2).

Three key criteria were considered in the development of the *TC & WMEIS* groundwater flow field design variants based on NEPA requirements:

- The flow field must provide a basis for an unbiased evaluation of the impacts of the *TC & WMEIS* alternatives for the 10,000-year period of analysis (1940–11,940).
- The flow field must provide a basis for understanding the *TC & WMEIS* alternatives in the context of cumulative impacts.
- An evaluation and discussion of the effects of uncertainties and gaps in input data (e.g., spatial distribution of well borings across the study area), modeling assumptions (e.g., conceptualizing the top of basalt as a no-flow boundary), and numerical error (e.g., head and water balance residuals) must be provided.

This appendix describes how the *TC & WMEIS* groundwater flow field was developed to meet these requirements.

L.1.2 Scope

In describing the development of the *TC & WMEIS* groundwater flow field for Hanford, this appendix presents the following:

- The fundamental features of the regional-scale flow field model specific to Hanford
- Two design variants to evaluate the long-term impacts of *TC & WM EIS* alternatives
- The data sources, data, and representation (encoding) of the data in the flow field model
- Model parameters and settings
- Algorithms selected for the model
- Multiple phases of calibration to existing water-level data and the results of the preliminary and automated calibration processes

The model simulating the flow field was built incrementally as validated data became available; preliminary assumptions were tested, rejected, or finalized; and the interactions between release, vadose zone, and groundwater transport models were defined. This development history is not presented unless it informs the justification for the final model configuration. Similarly, numerous calculations were performed to evaluate the sensitivity of the simulated flow field to uncertainties in input parameters. This appendix describes the results where the calculations suggested that the groundwater flow field was

sensitive to changes in input parameters; other calculations are included in separate project documentation.

L.1.3 Technical Guidance

The *Technical Guidance Document for Tank Closure Environmental Impact Statement, Vadose Zone and Groundwater Revised Analyses (Technical Guidance Document)* (DOE 2005) provides technical assumptions, model input parameters, and methodologies for proceeding with *TC & WM EIS* vadose zone (area of unsaturated soil and rock between ground surface and water table) and groundwater analyses. The technical bases supporting many of the assumptions result from various multiyear field- and science-based activities consistent with the Hanford Federal Facility Agreement and Consent Order, also known as the Tri-Party Agreement (Ecology, EPA, and DOE 1989); the Record of Decision for the *Tank Waste Remediation System, Hanford Site, Richland, Washington, Final Environmental Impact Statement (TWRS EIS)* (62 FR 8693); and the National Research Council's review of the *Draft TWRS EIS* (National Research Council 1996). This appendix indicates where design features or input data used in the development of the flow field are specified by the *Technical Guidance Document*.

The *Technical Guidance Document* specifies five key requirements for development of the *TC & WM EIS* groundwater flow field, as follows:

1. The flow field should be transient (i.e., change with time).
2. The factor driving the transient behavior should be operational recharge to the aquifer rather than time-changing boundary conditions.
3. The sitewide natural recharge rate should be 3.5 millimeters (0.14 inches) per year.
4. Both a Base Case and a Sensitivity (Alternate) Case should be investigated; the difference between the two cases should take into account the uncertainty in the top of basalt (TOB) elevation in the Gable Mountain–Gable Butte Gap (Gable Gap). The intent of the *TC & WM EIS* is to illustrate any potential differential effects this uncertainty might have on simulated alternative impacts. This approach was preferred (as opposed to presentation of results for all alternatives for each flow field) for brevity and clarity of presentation.
5. Flow field development should be consistent with the frameworks for vadose zone and contaminant transport modeling.

The *TC & WM EIS* groundwater flow model and simulated flow field meet these specifications.

L.2 DESIGN VARIANTS TO ADDRESS UNCERTAINTY AND SENSITIVITY

Groundwater at Hanford is found in a zone of permeable gravels, sands, silts, and clays that lie on top of multiple basalt flows and in interbed sediments (i.e., zones between basalt flows). The upper, fluvial (river-deposited) and lacustrine (lake-deposited) sediments on top of the basalt are referred to as suprabasalt sediments which are conductive and contain the upper, unconfined aquifer. The contact of the water-saturated suprabasalt materials with the relatively impermeable basalt is of particular importance at Hanford. For example, in the Gable Gap area near Gable Mountain and Gable Butte, the elevation of the basalt/suprabasalt sediment interface is uncertain. The difference between the top of basalt elevation and the water table elevation is an important factor governing groundwater flux through Gable Gap and consequently, the predominant direction of flow from the central plateau to the Columbia River. To address this uncertainty, two different flow fields were simulated.

The two flow fields, the Base and Alternate Cases, span the range of expected conditions at Hanford (see Sections L.2.1 and L.2.2). These cases result from different representations of the TOB elevation in the Gable Gap area. A third flow field was developed to evaluate the effect of a reasonably foreseeable future scenario—construction of the Black Rock Reservoir west of Hanford. Development of the Black Rock Reservoir case flow field and related analysis are described in Appendix V.

As discussed in Section L.1.3, the *Technical Guidance Document* (DOE 2005) specified development of two flow fields to take into account the uncertainty in the TOB surface in the Gable Gap area. The goal was to design two model variants that would perform the following actions:

- Simulate water table elevations during the operational period (1944–2006) equally well
- Exhibit different long-term (e.g., post-2006) flow directions and velocities in and around the Core Zone

For the purpose of this regional-scale model, the water balance in the unconfined aquifer beneath Hanford is assumed to have remained relatively constant since 1940, except for anthropogenic recharges resulting primarily from operations at Hanford. The basis for this modeling assumption is the *Technical Guidance Document* (see Section L.1.3). These operational recharges produced groundwater mounds beneath the 200-East and 200-West Areas on the Central Plateau of Hanford (see Section L.4.2.4). The dissipation of these mounds in terms of the long-term flow directions and velocities is strongly influenced by the TOB cutoff elevation in the Gable Gap area. If the TOB cutoff elevation in the Gable Gap area is high (relative to the water table), long-term flow from the Core Zone will be predominantly to the east. Conversely, lower TOB cutoff elevations in the Gable Gap area lead to long-term flow from the Core Zone that is predominantly to the north, through the Gable Gap.

The TOB surfaces in both the Base and Alternate Cases were produced by an analysis of approximately 850 point measurements of TOB elevations derived from boring logs and surface recordings. The analysis is discussed in detail in Section L.4.3.2.1 and is summarized here to develop the discussion of the Base and Alternate Cases. Each point measurement was assigned an uncertainty based on professional judgment of the quality of the record, the drilling method, the topography of the surface terrain, and the description of the contact between the suprabasalt sediments and basalt. The uncertainties in TOB elevation ranged from 1 to 30 meters (3.3 to 98.4 feet). All references to elevations in this appendix are relative to the North American Vertical Datum of 1988. From the best point estimates of TOB elevation and uncertainty, 100 sets (realizations) of point estimates were generated by adding a random variation (based on the uncertainty) to the best estimate of TOB elevation. A geostatistical analysis was used to create 100 TOB surfaces, one from each random realization. The TOB cutoff elevation in the Gable Gap area was identified for each realization.

L.2.1 Base Case

Because of the topology of the point estimates and their uncertainties, the TOB cutoff elevations in the Gable Gap area were not normally distributed. The distribution of cutoff elevations showed two reasonably strong tendencies: one approximately 118 meters (387 feet), and a second between 121 meters (397 feet) and 122 meters (400 feet) above mean sea level (amsl). A realization was chosen with a cutoff elevation of 121.5 meters (398.5 feet) amsl and encoded as the Base Case TOB surface. The Base Case represents the most likely TOB cutoff elevation in the Gable Gap area given the individual TOB measurements and their uncertainties.

L.2.2 Alternate Case

The Alternate Case was designed to have a lower TOB cutoff elevation in the Gable Gap area to increase the opportunity for long-term flow from the Core Zone to be predominantly northward, through the

Gable Gap. Ninety-five percent of the TOB surfaces had cutoff elevations greater than 118 meters (387 feet) amsl. The realization selected for the Alternate Case had a TOB cutoff elevation of 117.8 (387 feet) amsl. This model surface approaches the lower limit for the Gable Gap cutoff elevation that can be considered reasonably consistent with the measurements of TOB elevations.

L.3 MODEL DEVELOPMENT FRAMEWORK

The *TC & WM EIS* groundwater flow model simulates the time-varying spatial distribution of the rate and direction of water movement in the unconfined aquifer. Groundwater flow through the unconfined aquifer is simulated using the U.S. Geological Survey (USGS) MODFLOW [modular three-dimensional finite-difference groundwater flow model] 2000 Engine, Version 1.15.00 (USGS 2004). The commercial version used in this *TC & WM EIS* is Visual MODFLOW, Version 4.2 (WHI 2006). The resulting time-varying groundwater flow field is then used to simulate the transport of contaminants from their points of contact with the groundwater at various times in the history of the site to various receptor locations, including the Columbia River (see Appendix O).

The *TC & WM EIS* groundwater flow model was built using the best available information for Hanford. The development of the groundwater flow model was based, in part, on the Site-Wide Groundwater Model (e.g., Thorne et al. 2006), when features of the work were adequately documented, traceable, and independently verifiable. Previously compiled site data were used when they could be traced to a source and were judged to be adequate. When compiled site data were unavailable or inadequate for the development methodology used, historical primary data were obtained and processed for use or additional data were collected. Published conceptualizations informed some modeling decisions when neither compiled site data nor historical primary data were available for direct use or as input to associated models. When the above sources did not provide the necessary information, the required inputs were derived through engineering judgment or became model calibration parameters. MODFLOW groundwater flow model inputs derived both directly and indirectly from site data and knowledge are described in Section L.4. Model calibration data are described in Section L.6.1.

The MODFLOW groundwater flow model was developed in an incremental fashion, proceeding through a preliminary two-layer, steady state realization to the final transient, multilayered, calibrated, and parameterized model. This appendix presents the final version, describing the technical bases for model modifications, as well as the preliminary (see Section L.7), automated (see Section L.8), and Monte Carlo (see Section L.9) model calibration processes.

At key points during development of the MODFLOW groundwater flow model, technical reviews were performed to identify issues and concerns with important features of the model, provide suggestions for resolution of problem areas, and develop and understand alternative ways to conceptualize and encode model features. The technical review process had three major components:

- Review and comment by the Washington State Department of Ecology (Ecology), a cooperating agency on this *TC & WM EIS*
- Review and comment by a Local Users' Group (LUG), which consists of hydrogeologists and geologists from the Hanford community (modelers and field scientists)
- Review and comment by the MODFLOW Technical Review Group (MTRG), four experts with commercial, governmental, and academic experience in groundwater modeling and/or environmental engineering

During each review cycle, the *TC & WM EIS* groundwater modeling team presented status briefings to Ecology and LUG. Written comments from these two groups were solicited and provided to MTRG for their consideration and response, as they deemed appropriate. The *TC & WM EIS* groundwater modeling

team also presented the model development status briefing to MTRG. These presentations were open to the public. The *TC & WM EIS* groundwater modeling team and MTRG then spent several days discussing details of the model development effort and considering comments from Ecology and LUG. Finally, the MTRG provided their comments and suggestions in a closeout meeting, which was open to the public.

L.3.1 MODFLOW 2000

Per direction from the DOE Office of River Protection, the numeric engine selected for simulating groundwater flow was MODFLOW 2000, Version 1.15.00 (USGS 2004). A numeric engine performs the calculations to solve the equations describing water flow through the unconfined aquifer. MODFLOW 2000, a modular three-dimensional finite-difference groundwater flow model, describes the flow of groundwater into and out of every active finite model cell for each discrete time step and along all three dimensions: two horizontal and the vertical.

L.3.2 Visual MODFLOW 4.2

Per direction from the DOE Office of River Protection, the MODFLOW interface software selected for this *TC & WM EIS* was Visual MODFLOW, Version 4.2 (WHI 2006), a product that supports MODFLOW 2000 by providing tools for data input, model control, and presentation of model output. The MODFLOW 2000 numerical engine and its parameter settings in Visual MODFLOW, Version 4.2, are discussed further in Section L.5.3.

L.3.3 Parameter Estimation Module

The initial approach to model calibration included the use of Parameter Estimation Module (PEST) to determine the optimum set of hydraulic parameter values that would yield the best overall match of simulated head values to field-observed head values over the calibration period (1948–2006). This technical approach was implemented but resulted in unrealistically low uncertainty estimates for the range of optimum hydraulic parameter values. This result led the *TC & WM EIS* groundwater modeling team to believe that there may be multiple optimum sets of parameter values that are not related linearly. In other words, the objective function space is bumpy with several local minimums but not a single best minimum. The PEST process and results are discussed in more detail in Section L.8.

L.3.4 Monte Carlo Optimization

The PEST calibration process was useful in understanding the topography of objective function space but was not sufficient for determining an optimum set of hydraulic parameter values because this optimum set of values is non-unique. The *TC & WM EIS* groundwater modeling team then considered alternate methods to achieve the model calibration. They opted to perform a Monte Carlo optimization, selecting a random range of hydraulic parameter values around a specified mean value for each material type, then randomly combining these random sets of values together and completing a model run for that set. Thousands of model runs (6,660 cases for the Base Case model and 5,395 cases for the Alternate Case model) were completed with randomly selected hydraulic parameter values, and the root mean square (RMS) error (simulated heads compared to field-observed heads) for each model run was observed and tallied to determine which sets of random values produced the lowest RMS error. This approach to head calibration confirmed that there are many sets of reasonable hydraulic parameter values for the Base Case and Alternate Case models. This Monte Carlo optimization process is discussed in more detail in Section L.9.

L.4 MODEL INPUTS–CONCEPTUALIZATION, CHARACTERIZATION, AND ENCODING

This section describes the model inputs for defining the model grid design, cell properties, and flow boundary conditions. The encoding of these features of the *TC & WM EIS* groundwater flow model captures a conceptualization of the unconfined aquifer, its geomorphology, the hydrogeostratigraphic structure of the unconsolidated sediments, and its gross water budget based on underlying principles, data, and interpretation.

L.4.1 Discretization

“Discretization” of the groundwater flow model refers to the specification of the model domain (extent) and the compartmentalization (gridding) of the model domain in three dimensions: two horizontal and the vertical. Defining the model extent and the model grid is a matter of convenience informed by model purpose and computational considerations.

L.4.1.1 Extents

The *TC & WM EIS* groundwater flow model extents are determined by the Columbia and Yakima Rivers and by the top of the uppermost layer of basalt beneath the unconfined aquifer at Hanford.

The horizontal extents of the MODFLOW groundwater flow model are defined on the north, east, and south by the Columbia and Yakima Rivers. Review of hydrographs from wells along the river and comparison to river stage showed that the Columbia River is a reasonable hydrologic boundary. Coordinates for the Columbia and Yakima Rivers within the model domain were collected off shore within 25 meters (82 feet) of the nearshore bank using a global positioning system device in April 2006. The resulting river trace is shown in Figure L–1. The model extent on the west side is arbitrarily set at easting 557000, which is west of the Hanford boundary and the basalt ridge, Rattlesnake Mountain.

The minimum vertical extent is set at –90 meters (–295 feet) amsl, based on the lowest observed TOB elevation from boring logs for Hanford boreholes. The deepest estimated TOB elevation is –91 meters (–299 feet) amsl, which is rounded to –90 meters (–295 feet) in the model, given the uncertainties in elevation estimates. The maximum extent in the vertical direction is set at +165 meters (+541 feet) amsl, which is arbitrarily set above the maximum water table elevation (150 meters [492 feet]) for Hanford (Thorne et al. 2006:Figure 7.23).

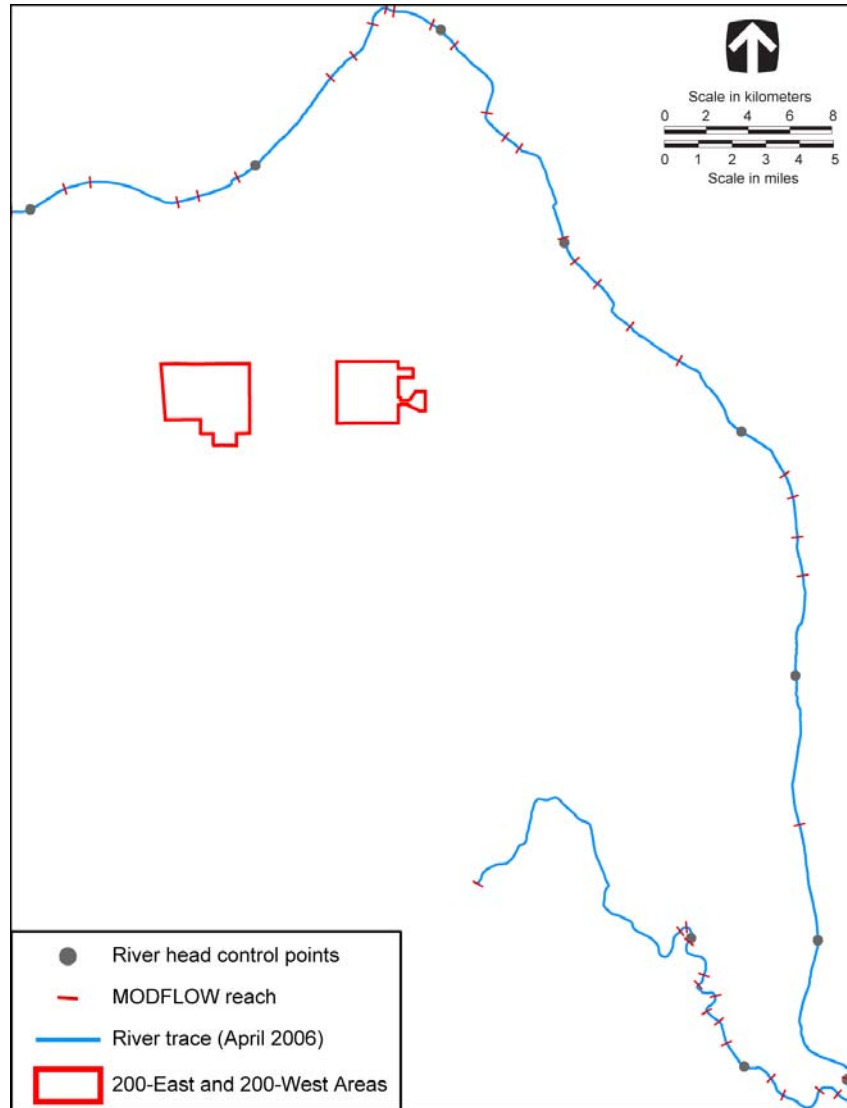


Figure L-1. MODFLOW Groundwater Flow Model Domain, Columbia and Yakima River Reaches, and River-Head Control Points

L.4.1.2 Gridding

The *TC & WM EIS* MODFLOW groundwater flow model divides Hanford within the model domain into three-dimensional blocks or cells. The model domain is divided into a 200- by 200-meter (656- by 656-foot) horizontal grid, with a “fringe” of partial cells on the northern, eastern, and southern sides. The sizes of the partial cells are defined by the distance between the last full-size row and column and the model extent. The horizontal grid and the fringe on the eastern and southern edges of the *TC & WM EIS* MODFLOW groundwater flow model are depicted in Figure L-2.

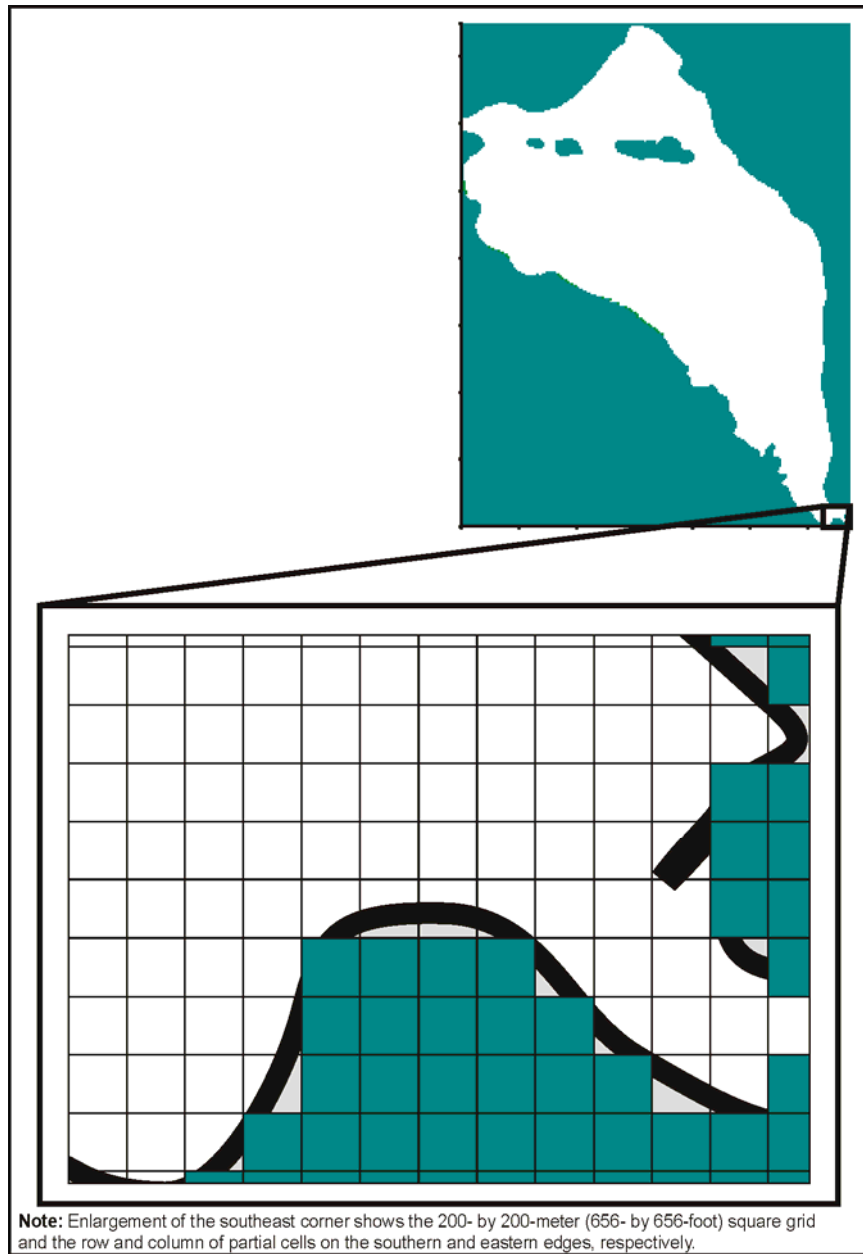


Figure L-2. Plan View of MODFLOW Horizontal Gridding

The interpolated elevation of the TOB surface in Gable Gap is not sensitive to the cell size of the horizontal grid. The lowest TOB elevation in Gable Gap (i.e., the “cutoff” elevation) determines the water level at which flow through the gap is possible. A comparison of 31 variants of the interpolated TOB surface for both a 200- by 200-meter (656- by 656-foot) grid and a 100- by 100-meter (328- by 328-foot) grid (see Section L.2.2) found that the elevation of the TOB surface in Gable Gap was not sensitive to grid size (see Table L-1). This finding justifies a uniform 200- by 200-meter (656- by 656-foot) grid across the entire model domain.

**Table L-1. Top of Basalt “Cutoff”^a Elevation in Gable Mountain–Gable Butte Gap
by Grid Size and Aggregation Mean**

Run	Description	Elevation (meters)	
		100- by 100-meter grid ^b	200- by 200-meter grid ^c
Default	Geostatistical Analyst (Johnston et al. 2001) default settings.	121	121
Variant 1	Reduce major range from default (22,580 m) to 22,354 m.	121	121
Variant 1a	Reduce major range from default (22,580 m) to 21,451 m.	121	121
Variant 2	Reduce minor range to 22,354 m; model direction = 0 degrees.	121	121
Variant 2a	Reduce minor range to 21,451 m. Major range = 22,580 m and model direction = 0 degrees.	120	120
Variant 3	Minor range = 22,354 m; model direction = 356 degrees.	121	121
Variant 3a	Reduce minor range to 21,451 m and change model direction to 352 degrees (or 172 degrees).	121	121
Variant 4	Reduce partial sill from default (12,519 m) to 12,394 m.	121	121
Variant 4a	Reduce partial sill from default (12,519 m) to 11,893 m.	121	121
Variant 5	Increase nugget from default (0 m) to 15 m.	121	121
Variant 5a	Increase nugget from default (0 m) to 150 m.	121	120
Variant 6	Partial sill = 12,394 m; increase nugget to 125 m; constant sill.	121	120
Variant 6a	Reduce partial sill from default (12,519 m) to 11,893 m and increase nugget to 626 m.	120	120
Variant 7	Increase neighbors to include per sector from default (5) to 6, “Include at Least” 2.	120	120
Variant 7a	Increase number of neighbors to include per sector from default (5, “Include at Least” 2) to 7, “Include at Least” 2.	120	120
Variant 8	Reduce lag size from default (4,859.2 m) to 4,810.7 m.	121	121
Variant 8a	Reduce lag size from default (4,859.2 m) to 4,616 m.	121	121
Variant 9	Increase number of lags to 13.	121	121
Variant 9a	Increase number of lags to 14.	121	121
Variant 10	Lag size 4,810.7 m; number of lags 13.	121	121
Variant 10a	Reduce lag size from default (4,859.2 m) to 4,616 m and increase number of lags to 14.	121	121

Table L–1. Top of Basalt “Cutoff”^a Elevation in Gable Mountain–Gable Butte Gap by Grid Size and Aggregation Mean (continued)

Run	Description	Elevation (meters)	
		100- by 100-meter grid ^b	200- by 200-meter grid ^c
Random 1	Random Realization No. 1.	121	120
Random 2	Random Realization No. 2.	121	121
Random 3	Random Realization No. 3.	120	120
Random 4	Random Realization No. 4.	121	121
Random 5	Random Realization No. 5.	121	121
Random 6	Random Realization No. 6.	120	120
Random 7	Random Realization No. 7.	120	120
Random 8	Random Realization No. 8.	122	122
Random 9	Random Realization No. 9.	118	118
Random 10	Random Realization No. 10.	121	120

^a Lowest maximum elevation along MODFLOW flow path through Gable Mountain–Gable Butte Gap.

^b ESRI default mean.

^c Harmonic mean.

Note: To convert meters to feet, multiply by 3.281.

Key: m=meters; MODFLOW=modular three-dimensional finite-difference groundwater flow model.

The *TC & WMEIS* MODFLOW groundwater flow model is divided into 31 layers in the vertical direction. Each layer is a uniform (constant) thickness across the entire model domain in the horizontal directions. The layers range in thickness from 1 meter (3.281 feet) to 40 meters (131 feet). The layering of the *TC & WMEIS* MODFLOW groundwater flow model is depicted in Figure L–3. The model has 1-meter (3.281-foot) thick layers at depths between 115 and 125 meters (377 and 410 feet) amsl, where the TOB surface is near the water table. These high-resolution layers span the TOB elevations simulated to occur in Gable Gap. Water levels fluctuate between these depths during the model simulation period. The thickest layers, which are greater than 15 meters (49.2 feet) thick, occur deep in the aquifer, where less resolution is required.

L.4.2 Boundary Conditions

The boundary conditions for the *TC & WMEIS* groundwater flow model are defined by the Yakima and Columbia Rivers, the subsurface influx of water into the unconfined aquifer along Rattlesnake Mountain, the basalt layer beneath the unconfined aquifer, and recharge (anthropogenic and natural) at the ground surface. The Columbia and Yakima Rivers and naturally occurring subsurface influxes of groundwater to the unconfined aquifer at three discrete locations along the western boundary are modeled as Generalized Head Boundaries (GHBs). With the exception of the discrete GHB-encoded areas along the western boundary where mountain-front recharge is thought to occur (see Section L.4.2.3), the basalt layer beneath the unconfined aquifer is assumed to be a no-flow boundary, i.e., no water enters the unconfined aquifer from the underlying basalt. For the *TC & WMEIS* groundwater flow model, the rivers, subsurface influx, basalt “basement,” and natural recharges are taken as constant. The only time-varying fluxes of water across the model boundary are anthropogenic areal recharges. These boundary conditions are discussed below.

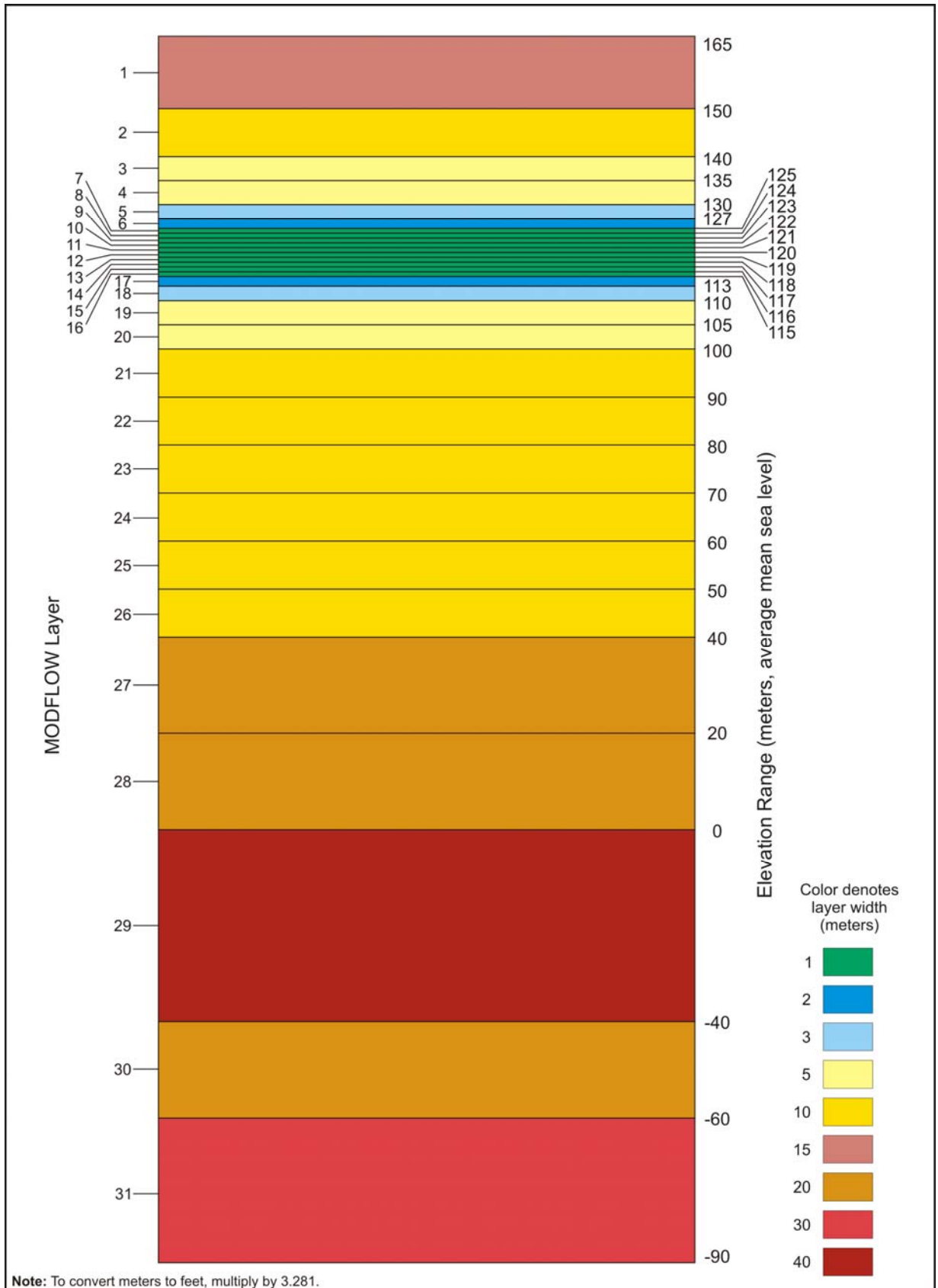


Figure L-3. Cross-Section View of MODFLOW Vertical Grid

L.4.2.1 Basalt Surface (No-Flow Boundary)

Massive basalts beneath the unconfined aquifer at Hanford define a no-flow boundary (aquiclude) in the *TC & WMEIS* groundwater flow model. A no-flow boundary represents a limit to flow within the unconfined aquifer. In this MODFLOW groundwater flow model, no water enters the unconfined aquifer from the underlying basalt. Except for a ridge of basalt in Gable Gap, the model cell in which the TOB surface (see Section L.2.2) is assigned and all lower cells are encoded in the model as “inactive.” Inactive cells do not allow water to flow to neighboring cells and do not accept flow coming from neighboring cells. For the ridge of basalt in Gable Gap, only cells at 115 meters (377 feet) amsl and below are encoded as inactive; these elevations correspond to MODFLOW Layers 16 through 31. Cells above 115 meters (377 feet) amsl that are encoded as basalt are made active, with a hydraulic conductivity 500 times smaller than that of Hanford and Ringold muds (0.001 meters [0.00328 feet] per day). This active status prevents the MODFLOW cells from drying out during fluctuations of the water table which causes model instabilities (see Section L.5.1.1).

L.4.2.2 Columbia and Yakima Rivers (River Package)

The *TC & WMEIS* groundwater flow model uses the Visual MODFLOW river package to encode the Columbia and Yakima Rivers. This package encodes surface-water/groundwater interaction via a seepage layer (riverbed) separating the surface-water body from the groundwater aquifer. The portions of the Columbia and Yakima Rivers in the *TC & WMEIS* MODFLOW groundwater flow model domain (see Figure L-1) are encoded in the model as an unbroken sequence of cells sharing a face or vertex. Each 200- by 200-meter (656- by 656-foot) cell encoded as river is assigned to a reach, and each reach is assigned a conductance, which is an inverse measure of the resistance to flow between the streambed and the underlying aquifer. For the *TC & WMEIS* groundwater flow model, conductance is a calibration parameter.

In the MODFLOW river package, conductance is a function of the length and width of a reach and the thickness and conductivity of the streambed. The *TC & WMEIS* MODFLOW groundwater flow model sets streambed thickness at 2 meters (6.6 feet) and conductivity at 0.0004 meters (0.0013 feet) per second. Reach width is a uniform 200 meters (656 feet). Reaches of different lengths are defined on the basis of slope. Because the length and width of each reach are fixed, adjusting conductance during calibration implies an adjustment of the ratio of streambed conductivity to streambed thickness.

In the *TC & WMEIS* MODFLOW groundwater flow model domain, 27 reaches, each with a relatively constant slope, are defined on the Columbia River, and 14 reaches are defined on the Yakima River (see Figure L-1). Elevations were assigned to coordinates along the trace by interpolating from existing river elevation data developed by Pacific Northwest National Laboratory (PNNL) (Thorne et al. 2006). Elevations were assigned assuming constant slope between PNNL data points. The PNNL data set contains 700 data points for the Columbia River and 44 points for the Yakima River within the model extent. The entire Yakima River within the model domain is not modeled because the river upstream of Horn Rapids is assumed not in communication with the unconfined aquifer at Hanford.

The specified river stages, river bed thicknesses, and river bed conductances govern the interactions of the Columbia and Yakima Rivers with the unconfined aquifer. When the river stage is greater than the head in the aquifer immediately below, water flows from the river into the aquifer. The flow is reversed when the river stage is lower than the head in the aquifer immediately below. The former condition is described as a losing reach of the river, and the latter as a gaining reach. In general, the Columbia River gains throughout the modeled domain, and the Yakima River loses.

L.4.2.3 Mountain-Front Recharge (Generalized Head Boundary)

Groundwater is thought to enter the unconfined aquifer at Hanford from the underlying basalt layer in defined areas along the western boundary—Cold Creek Valley, Dry Creek Valley, and Rattlesnake Hills (Thorne et al. 2006). Well-documented springs occur in Cold Creek Valley and Dry Creek Valley. Runoff from the eastern face of Rattlesnake Hills is the third source of subsurface influx of groundwater along Hanford’s “upstream” boundary.

These three examples of mountain-front recharge are encoded in the *TC & WM EIS* groundwater flow model using the Visual MODFLOW GHB package (see Figure L-4). With the GHB package, one defines groups of cells (zones) with specific values for head and parameters affecting conductance, the resistance to water flow into the cells of the zone. The head and conductance parameters for each of the three GHB zones in the *TC & WM EIS* MODFLOW groundwater flow model are varied to calibrate the model to observed water levels (see Section L.7).

L.4.2.4 Natural Areal Recharge (Recharge Boundary)

The *TC & WM EIS* groundwater flow model incorporates natural recharge at the rates specified in the *Technical Guidance Document* (DOE 2005). Cribs and trenches receive 50 millimeters (2 inches) per year, and tank farms receive 100 millimeters (4 inches) per year. Fifty millimeters per year is equivalent to 50 liters (13.2 gallons) per square meter per year. A fixed infiltration rate, 3.5 millimeters (0.14 inches) per year, representing precipitation on natural surfaces, is applied to the remaining areas not otherwise specified. Recharge in the city of Richland and surrounding agricultural land is a calibration parameter. These natural infiltration rates are also used in the STOMP vadose zone models (see Appendix N).

L.4.2.5 Artificial Recharge (Recharge Boundary)

Anthropogenic recharge associated with Hanford operations and, to a lesser extent, extraction (water withdrawal) and irrigation beyond the Hanford boundary represents the important time-varying fluxes of water into and out of the aquifer during the model period of analysis (1940–11,940). Water originally taken from the Columbia River was discharged onto the ground surface during operations. These anthropogenic recharge sources are the time-varying inputs that drive the transient behavior of the *TC & WM EIS* groundwater flow model.

Values for over 200 sources (or sinks) of water were taken from the Cumulative Impacts Inventory Database (SAIC 2006) and encoded into the model. These fluxes are encoded as constant flux boundary conditions in the MODFLOW cells that contain the sources and release sites. These recharge fluxes are also modeled using STOMP to simulate transport of contaminants through the vadose zone to the groundwater.

Of all the anthropogenic liquid sources identified in the Hanford inventory database, eight sites account for 88 percent of the total site recharge (see Table L-2). The volumes released at these sites range from 41 billion liters (10.8 billion gallons) at the 216-S-16 P Pond to 300 billion liters (79.3 billion gallons) at the 116-K-2 Trench. All eight sites combined released roughly 1.43 trillion liters (0.38 trillion gallons). Five of these sites are located in the 200 Areas, and they were major contributors to the mounds of water that built up beneath the 200-East and 200-West Areas during operations from 1945 through the mid-1990s.

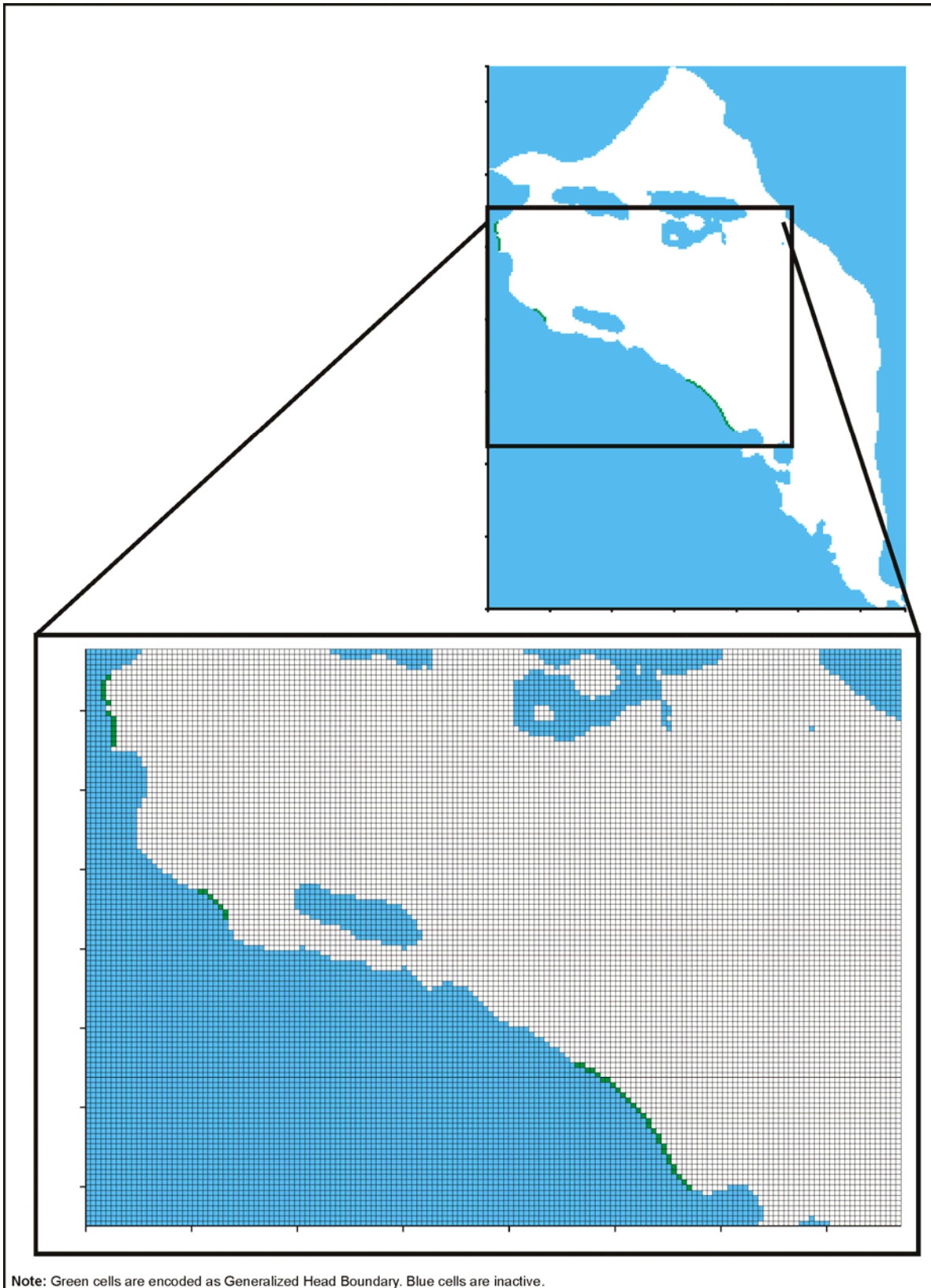


Figure L-4. Mountain-Front Recharge Zones

Table L-2. Major Total Recharge Sources on the Hanford Site (1940–Present)

WIDS ID	Site Type	Source Type	Centroid Easting	Centroid Northing	Volume (liters)	Cumulative Fraction
116-K-2	Trench	Liquid	569801	147701	300,000,000,000	0.21
216-A-25	Pond	Liquid	574970	139650	293,899,037,982	0.42
216-B-3	Pond	Liquid	576898	136687	282,689,367,700	0.61
216-U-10	Pond	Liquid	566318	134602	159,859,250,966	0.73
116-N-1	Crib	Liquid	571534	149782	83,700,000,000	0.78
316-1	Pond	Liquid	594283	116106	51,116,602,319	0.82
216-T-4A	Pond	Liquid	566475	137133	42,826,720,640	0.85
216-S-16P	Pond	Liquid	565412	133192	40,723,265,275	0.88

Note: To convert liters to gallons, multiply by 0.26417.

Key: WIDS ID=Waste Information Data System Identification.

Anthropogenic areal recharge is encoded in the model in 1-year stress periods beginning in 1944. The model applies the estimated annual flux to the water table from each site in the appropriate 1-year stress periods, beginning the first year of operations at the site and ending in the final year of operations. The total recharge applied to the water table in a given stress period fluctuates from year to year as the number of contributing sites and their fluxes vary. For example, Figures L-5 and L-6 show the timing and magnitude of flux from the dominant anthropogenic recharge sources in the 200-East and 200-West Areas, respectively.

In addition to the liquid inventory sources, the model boundaries comprise three city of Richland water system well fields: North Richland, 1100B, and Wellsian Way. The pump houses at the North Richland and 1100B fields were constructed in 1978. Retention basins at these sites received Columbia River water, which was allowed to infiltrate to groundwater. Reference data for recharge from the

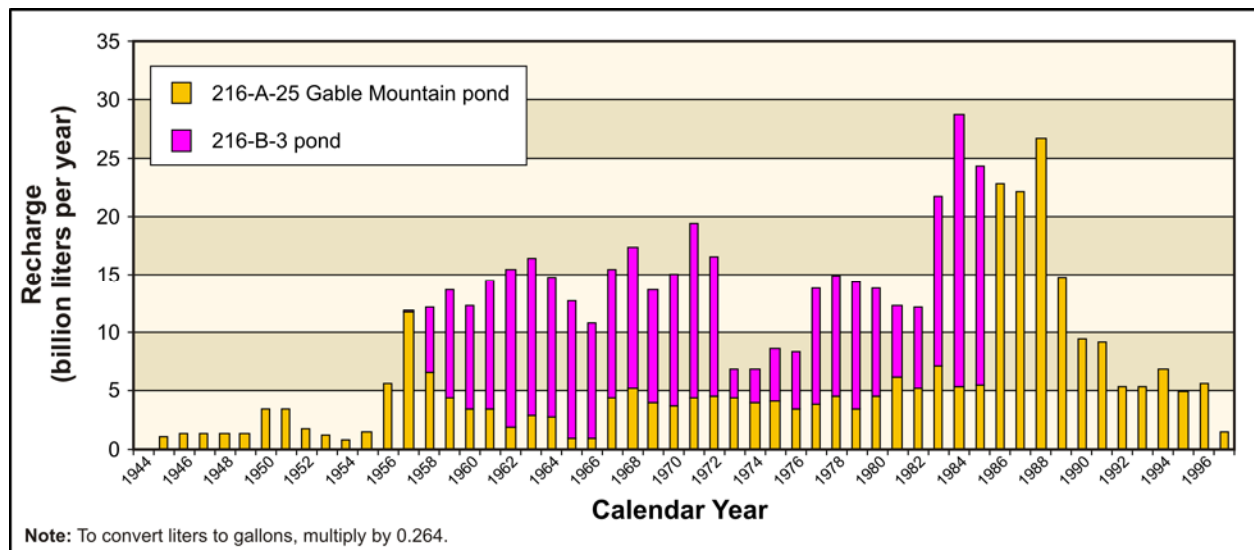


Figure L-5. Major Anthropogenic Recharge Sources in the 200-East Area

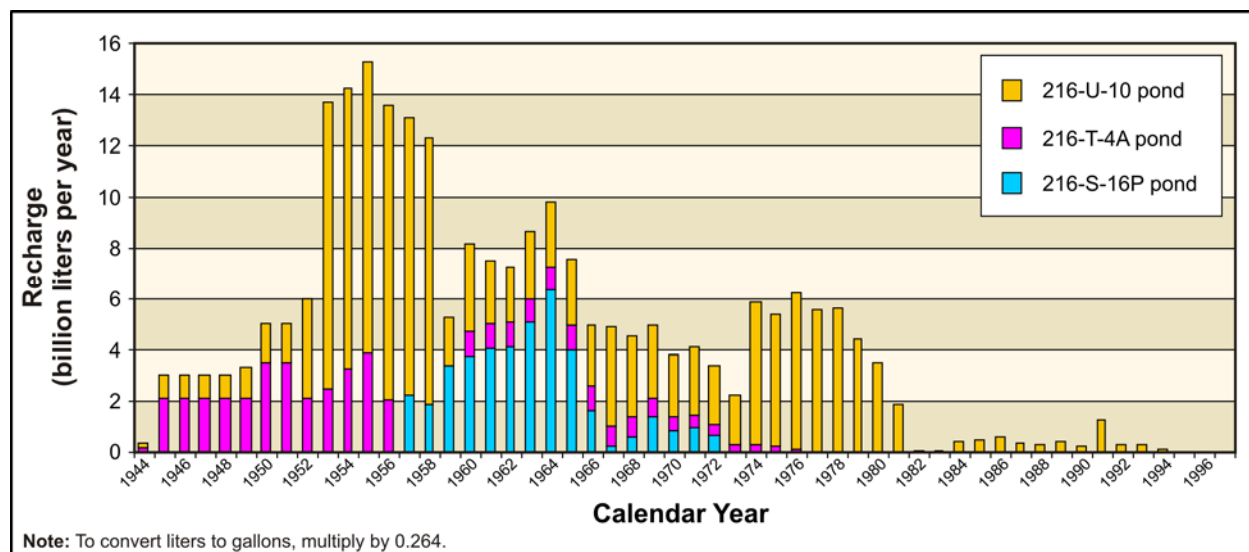


Figure L-6. Major Anthropogenic Recharge Sources in the 200-West Area

retention basins and production wells were obtained from city of Richland water system reports dating from 1981 to 2006 (see Table L-3). Based on information provided in the water system reports, a 95th percentile upper confidence limit on mean net recharge was calculated and used for the time period from 1978 to 1981. For the purposes of this analysis, future anthropogenic recharges were estimated based on past usage. The 95th percentile upper confidence limit on the mean was used for the years 2006 through 11,940 for all three city of Richland well field locations.

L.4.3 Lithology

Three major lithologic units that occur beneath Hanford are encoded in the *TC & WM EIS* groundwater flow model: Elephant Mountain basalt, Ringold Formation, and Hanford formation. The Elephant Mountain basalt represents the bottom of the unconfined aquifer (see Section L.4.3.2.1). The unconsolidated sediments of the Ringold and Hanford formations constitute the unconfined aquifer. The sediments of these two formations comprise the saturated zones through which groundwater flow is modeled.

L.4.3.1 Hydrogeologic Unit Definition

The *TC & WM EIS* groundwater flow model recognizes two major lithologic formations in the unconfined aquifer above the basalt, Hanford and Ringold, and two minor formations, Cold Creek and Plio-Pleistocene (PP) units. The Ringold Formation is the lower geologic unit of the unconfined aquifer, and, where it occurs, it sits on top of the underlying basalt. The Hanford formation is situated above the Ringold Formation where the latter occurs and directly above the basalt where the Ringold is missing. Between the Hanford and Ringold formations, the Cold Creek and PP units (formerly pre-Missoula/PP/early Palouse soil units) occur in some places at Hanford. Both the Hanford and the Ringold formations consist of fluvial and lacustrine sequences of mud, silt, sand, and gravel. The coarse-grained multifacies of the Cold Creek and PP units are thought to be more like Hanford formation gravel and sand than the harder, more-cemented Ringold Formation Gravel and Sand (Thorne et al. 2006).

Table L-3. City of Richland Water Supply Data – Annual Summary Report

Year	Extraction North Richland (Mgal)	Extraction 1100B (Mgal)	Positive Recharge (Mgal) ^a	Positive Recharge/ Extraction	Net Recharge (Mgal)	Net Recharge (gal)
1978	9.13×10 ²	6.86×10 ¹	3.70×10 ^{3b}	3.77	2.72×10 ³	2.72×10 ⁹
1979	9.13×10 ²	6.86×10 ¹	3.70×10 ^{3b}	3.77	2.72×10 ³	2.72×10 ⁹
1980	9.13×10 ²	6.86×10 ¹	3.70×10 ^{3b}	3.77	2.72×10 ³	2.72×10 ⁹
1981	9.13×10 ²	6.86×10 ¹	3.66×10 ³	3.73	2.68×10 ³	2.68×10 ⁹
1982	9.13×10 ²	6.86×10 ¹	2.36×10 ³	2.40	1.38×10 ³	1.38×10 ⁹
1983	9.13×10 ²	6.86×10 ¹	2.76×10 ³	2.82	1.78×10 ³	1.78×10 ⁹
1984	5.31×10 ²	0.00×10	3.61×10 ³	6.79	3.07×10 ³	3.07×10 ⁹
1985	5.42×10 ²	0.00×10	2.72×10 ³	5.01	2.17×10 ³	2.17×10 ⁹
1986	3.99×10 ²	1.08×10 ²	2.35×10 ³	4.63	1.84×10 ³	1.84×10 ⁹
1987	5.11×10 ²	1.02×10 ²	2.33×10 ³	3.80	1.72×10 ³	1.72×10 ⁹
1988	5.39×10 ²	1.08×10 ¹	1.94×10 ³	3.53	1.39×10 ³	1.39×10 ⁹
1989	1.08×10 ³	7.19×10	2.92×10 ³	2.69	1.83×10 ³	1.83×10 ⁹
1990	1.45×10 ³	4.07×10	2.70×10 ³	1.86	1.25×10 ³	1.25×10 ⁹
1991	1.13×10 ³	1.02×10 ¹	2.77×10 ³	2.44	1.64×10 ³	1.64×10 ⁹
1992	8.39×10 ²	4.35×10 ¹	1.71×10 ³	1.93	8.23×10 ²	8.23×10 ⁸
1993	6.01×10 ²	1.57×10 ¹	3.30×10 ³	5.35	2.68×10 ³	2.68×10 ⁹
1994	1.34×10 ³	6.17×10 ¹	2.64×10 ³	1.89	1.24×10 ³	1.24×10 ⁹
1995	5.72×10 ²	6.00×10 ¹	1.86×10 ³	2.94	1.23×10 ³	1.23×10 ⁹
1996	5.03×10 ²	5.84×10 ¹	2.34×10 ³	4.16	1.77×10 ³	1.77×10 ⁹
1997	6.23×10 ²	6.84×10 ¹	1.90×10 ³	2.75	1.21×10 ³	1.21×10 ⁹
1998	1.33×10 ³	1.47×10 ²	1.86×10 ³	1.26	3.85×10 ²	3.85×10 ⁸
1999	7.46×10 ²	1.11×10 ²	1.61×10 ³	1.88	7.54×10 ²	7.54×10 ⁸
2000	7.65×10 ²	3.64×10 ¹	1.83×10 ³	2.29	1.03×10 ³	1.03×10 ⁹
2001	5.34×10 ²	7.47×10 ¹	1.48×10 ³	2.44	8.76×10 ²	8.76×10 ⁸
2002	1.19×10 ³	6.85×10 ¹	3.05×10 ³	2.43	1.80×10 ³	1.80×10 ⁹
2003	5.35×10 ²	1.76×10 ¹	2.67×10 ³	4.83	2.12×10 ³	2.12×10 ⁹
2004	4.10×10 ²	5.79×10 ¹	1.69×10 ³	3.61	1.22×10 ³	1.22×10 ⁹
2005	5.39×10	1.33×10 ²	2.61×10 ³	18.86	2.47×10 ³	2.47×10 ⁹
2006–11,940	9.13×10 ²	6.86×10 ¹	3.70×10 ^{3b}	3.77	2.72×10 ³	2.72×10 ⁹
			Count	24.00		
			SD	1.35		
			Average	3.23		
			95% UCL	3.77		

^a Positive recharge taken from city of Richland water system reports for years 1981–2005.

^b Used the 95th percentile UCL ratio.

Note: To convert gallons to liters, multiply by 3.7854.

Key: %=percent; gal=gallon; Mgal=million gallons; SD=standard deviation; UCL=upper confidence limit.

L.4.3.2 Hydrogeologic Unit Encoding

The *TC & WM EIS* groundwater flow model has been encoded with hydrogeologic data for the entire model domain, developed from Hanford well borings completed as of September 2005. Approximately 5,000 boring logs were reviewed to determine if the geologic units and discrete hydrostratigraphic layers could be recognized from the geologic descriptions. When multiple logs existed for a borehole, higher credibility was given to those descriptions recorded by a professional geologist. Logs were reviewed for specific identification of the Elephant Mountain basalt, Hanford and Ringold formations, and Cold Creek

and PP units. The logs were further examined to discern textural types among the sedimentary units: mud, silt, sand, and gravel. Each of the resulting hydrogeologic units is encoded with unique properties (see Section L.4.4). The development of the hydrogeologic data for use in the *TC & WM EIS* groundwater flow model is described in the following sections.

L.4.3.2.1 Basalt Surface

The TOB surface encoded in the *TC & WM EIS* groundwater flow model was derived from boring logs, surface measurements, and geostatistical interpolation. Approximately 5,000 boring logs from Hanford and its surroundings were reviewed to determine if the geologic descriptions accompanying the boring logs indicated the depth of the uppermost basalt layer underlying the unconfined aquifer. When multiple logs existed for a borehole, higher credibility was given to those lithological descriptions recorded by a professional geologist. Only boreholes whose locations (coordinates) were known with some confidence were used. The TOB surface elevations at basalt outcroppings on or near Hanford were measured using a global positioning system device. Some TOB surface elevation values were taken from USGS topographic maps of Gable Mountain, Gable Butte, and Rattlesnake Mountain, which are massive outcroppings of the Elephant Mountain basalt, the formation underlying the unconfined aquifer at Hanford. Uncertainty estimates were assigned to each TOB elevation value.

The TOB surface encoded in the *TC & WM EIS* MODFLOW groundwater flow model is a geostatistical interpolation of the basalt-elevation data points from approximately 850 Hanford boring logs and 18 control points (see Figure L-7). Of the 18 control points, 12 are “structural,” representing site knowledge about TOB surface elevation where there were limited or no data available and 6 are “visual,” added to improve the depiction of the TOB surface. Nine of the 12 structural control points were added along the Columbia River where it enters Hanford to position the TOB surface beneath the river. The other 3 structural control points were added at borehole (well) locations where the boring did not extend completely to the basalt but only to the Ringold Formation Lower Mud Unit, which lies atop the basalt where it occurs. At these 3 locations, the TOB surface was estimated from other nearby borings that went deep enough to encounter the Ringold Formation Lower Mud Unit and the underlying basalt. Four of the 6 visual control points were added north of Gable Butte and Gable Mountain along the known position of the Gable Mountain Fault (see Figure L-7). The visual control points along the Gable Mountain Fault do not affect the simulated elevation of the TOB surface in Gable Gap (see Table L-4). The other 2 visual control points were added at Yakima Ridge. These 2 visual control points are not expected to affect the flow field in the operational areas of the site because of their distance from the operational areas (several kilometers to the south), and the predominant direction of groundwater flow (easterly).

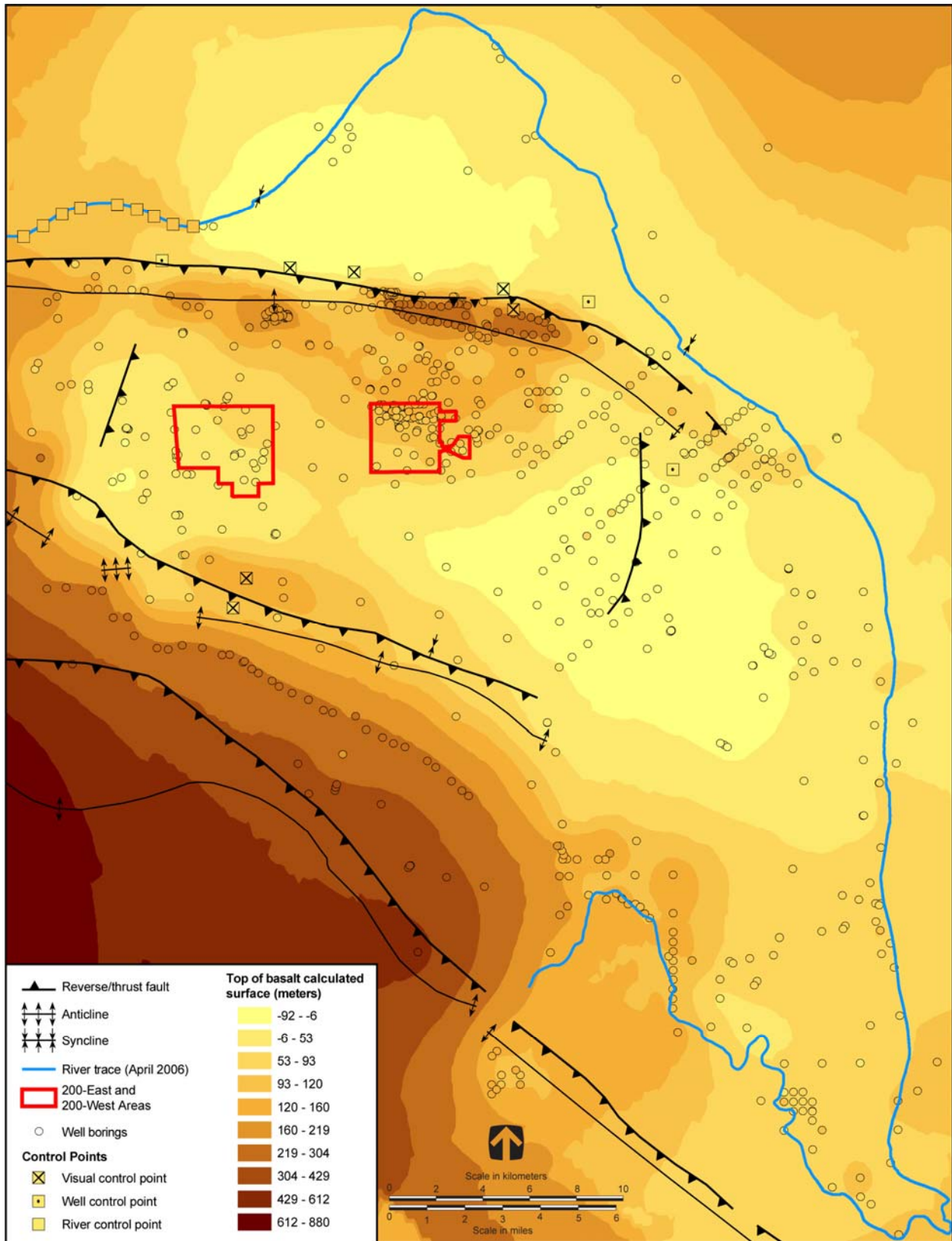


Figure L-7. Interpolated Top of Basalt Surface at the Hanford Site, Showing Faults, Anticlines, and Synclines

Table L–4. Effect of Visual Control Points on Top of Basalt “Cutoff”^a Elevation in Gable Gap

Visual Control Points	Gable Gap Cutoff Elevation ^a (meters)	MODFLOW Layer (elevation in meters)	Notes
None	120.8407	11 (120–121)	–
5	120.8409	11 (120–121)	Includes new visual control points YRCP-1, YRCP-2, GMFCP-1, GMFCP-2, and GMFCP-3
6	120.8412	11 (120–121)	Includes five visual control points listed above and GMFCP-4 (closest to Gable Gap)

^a Lowest maximum elevation along MODFLOW flow path through Gable Gap.

Note: To convert meters to feet, multiply by 3.281.

Key: Gable Gap=Gable Mountain–Gable Butte Gap; MODFLOW=modular three-dimensional finite-difference groundwater flow model.

The TOB surface encoded into the *TC & WMEIS* groundwater flow model was interpolated from the data and control points using ArcGIS Version 9.1, ArcInfo Level with Geostatistical Analyst Extension (Johnston et al. 2001). The interpolated TOB surface is not sensitive to the parameter settings assigned in ArcGIS. To make this determination, the TOB surface for the MODFLOW flow field model domain was interpolated by ordinary kriging using ArcGIS for the cases listed in Table L–5. The resulting TOB Gable Gap cutoff elevations, also shown in Table L–5, indicate that the interpolated TOB surface is insensitive to the parameter settings assigned in ArcGIS.

Table L–5. Top of Basalt “Cutoff”^a Elevation in Gable Mountain–Gable Butte Gap Based on ArcGIS Parameter Settings

Run	Description	Top of Basalt Elevation (meters) ^b
Default	Geostatistical Analyst (Johnston et al. 2001) default settings.	121
Variant 1	Reduce major range from default (22,580 m) to 22,354 m.	121
Variant 1a	Reduce major range from default (22,580 m) to 21,451 m.	121
Variant 2	Reduce minor range to 22,354 m; model direction = 0 degrees.	121
Variant 2a	Reduce minor range to 21,451 m. Major range = 22,580 and model direction = 0.	121
Variant 3	Minor range 22,354 m; model direction = 356 degrees.	121
Variant 3a	Reduce minor range to 21,451 m and change model direction to 352 degrees (or 172 degrees).	121
Variant 4	Reduce partial sill from default (12,519 m) to 12,394 m.	121
Variant 4a	Reduce partial sill from default (12,519 m) to 11,893 m.	121
Variant 5	Increase nugget from default (0 m) to 15 m.	121
Variant 5a	Increase nugget from default (0 m) to 150 m.	121
Variant 6	Partial sill 12,394; increase nugget to 125 m; constant sill.	121
Variant 6a	Reduce partial sill from default (12,519 m) to 11,893 m and increase nugget to 626 m.	120
Variant 7	Increase neighbors to include per sector from default (5) to 6, “Include at Least” 2.	120
Variant 7a	Increase number of neighbors to include per sector from default (5, “Include at Least” 2) to 7, “Include at Least” 2.	120

Table L-5. Top of Basalt “Cutoff”^a Elevation in Gable Mountain–Gable Butte Gap Based on ArcGIS Parameter Settings (*continued*)

Run	Description	Top of Basalt Elevation (meters) ^b
Variant 8	Reduce lag size from default (4,859.2 m) to 4,810.7 m.	121
Variant 8a	Reduce lag size from default (4,859.2) to 4,616 m.	121
Variant 9	Increase number of lags to 13.	121
Variant 9a	Increase number of lags to 14.	121
Variant 10	Lag size 4,810.7 m; number of lags 13.	121
Variant 10a	Reduce lag size from default (4,859.2 m) to 4,616 m and increase number of lags to 14.	121

^a Lowest maximum elevation along MODFLOW (modular three-dimensional finite-difference groundwater flow model) flow path through Gable Mountain–Gable Butte Gap.

^b Grid is 200-by-200 m (harmonic mean).

Note: To convert meters to feet, multiply by 3.281.

Key: m=meter; MODFLOW=modular three-dimensional finite-difference groundwater flow model.

The final TOB surface was interpolated using ordinary kriging with the default settings (see Figure L-8). The resulting TOB surface was output to a raster file containing the elevation of the center point of each cell of the 200- by 200-meter (656- by 656-foot) grid of the *TC & WM EIS* groundwater flow model. These values were used to encode the TOB surface at the proper vertical layer in the MODFLOW groundwater flow model. For each MODFLOW cell, the TOB surface was assigned to the layer containing the TOB elevation if the TOB elevation was greater than the midpoint of the layer; otherwise, the TOB surface was assigned to the next-lower layer. The cell to which the TOB surface was assigned and all lower cells were made inactive, i.e., assigned the “no-flow” condition.

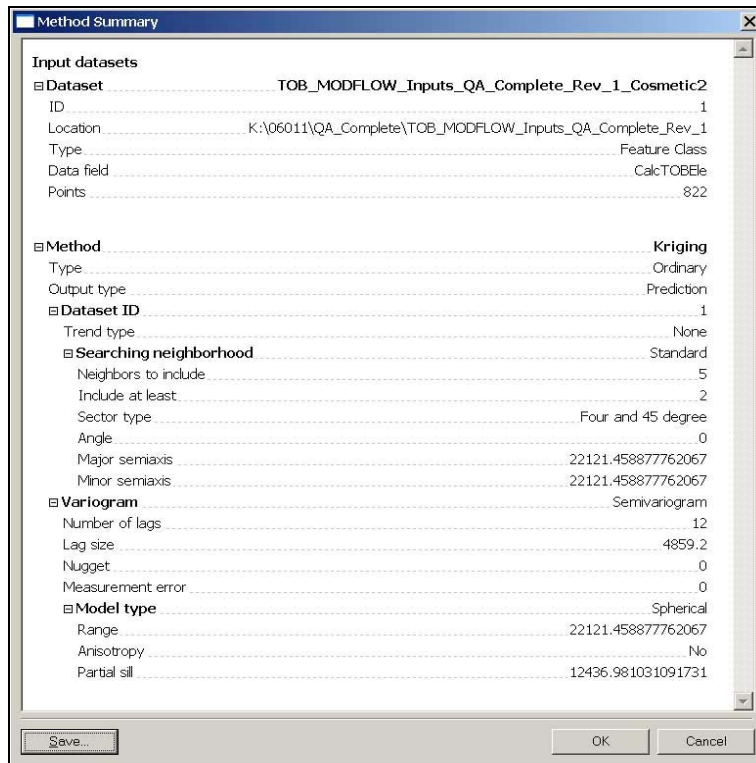


Figure L-8. Screen Print of Default Settings From Top of Basalt Surface Interpolation Using ArcGIS Geostatistical Analyst

The impact on the flow field of lower TOB elevations in Gable Gap is evaluated in this appendix (see Sections L.2.2 and L.10.2). The lowest TOB elevation in Gable Gap, i.e., the “cutoff” elevation, determines the water level at which flow to the north through the gap is possible. One hundred TOB surfaces were created by randomly selecting the TOB elevation for each of the 849 borings and 12 structural control points from a normal distribution, with the mean equal to the reported TOB elevation and the interval size equal to twice the elevation uncertainty estimate. The results indicated that there are multiple possible locations for the gap to occur, with different elevation values. The mean elevations of the three most frequent locations correspond to cutoffs encoded in the groundwater flow model at approximately 118 meters (387 feet), 121 meters (397 feet), and 122 meters (400 feet) amsl. Less than 5 percent of the realizations have a cutoff elevation lower than 118.5 meters (389 feet) amsl. The TOB surface encoded in Gable Gap for the *TC & WMEIS* groundwater flow model Alternate Case (see Section L.2.2) was interpolated from a random TOB elevation data set with a cutoff value of 117.8 meters (387 feet) amsl.

L.4.3.2.2 Suprabasalt Sedimentary Layers

Hanford boring logs were examined to discern textural layers of mud, silt, sand, and gravel within the Hanford and Ringold formations and Cold Creek and PP units. Individual layers are assigned to 1 of 13 material types (see Table L–6). The resulting lithological profiles—well name, well location, ground surface elevation, starting and ending depths of each layer, and each layer’s assignment to the textural types—were imported into a database program that generates geologic cross sections.

**Table L–6. Abundance of Textural Types in MODFLOW Groundwater
Flow Model: Base Case**

Textural Type (Model Material Type Zone)	Unweighted (Cells)	Unweighted Percent	Weighted (km ³)	Weighted Percent
Hanford mud (1)	245	0.05	0.05	0.04
Hanford silt (2)	2,238	0.43	0.30	0.28
Hanford sand (3)	33,237	6.38	8.71	8.06
Hanford gravel (4)	132,943	25.52	17.87	16.53
Ringold Sand (5)	27,333	5.25	10.27	9.51
Ringold Gravel (6)	168,246	32.29	37.39	34.60
Ringold Mud (7)	52,638	10.10	20.98	19.41
Ringold Silt (8)	1,757	0.34	0.47	0.43
Plio-Pleistocene sand (9)	115	0.02	0.06	0.05
Plio-Pleistocene silt (10)	186	0.04	0.09	0.09
Cold Creek sand (11)	3,444	0.66	0.40	0.37
Cold Creek gravel (12)	31,724	6.09	2.35	2.18
Highly conductive Hanford gravel(13)	65,933	12.65	9.10	8.42
Activated basalt (14) ^a	967	0.19	0.04	0.04

^a Zone 14 (Activated basalt) was assigned to mitigate rewetting problems (see Section L.5.1.1) and was encoded over nine model layers.

Note: To convert cubic kilometers to cubic miles, multiply by 0.2399.

Key: km³=cubic kilometers; MODFLOW=modular three-dimensional finite-difference groundwater flow model.

Hydrostratigraphic cross sections were constructed using HydroGeo Analyst, Version 3.0 (WHI 2005). Transects for these cross sections are located in the exact middle of a MODFLOW grid row (or column), and have a 100-meter (328-foot) buffer on either side. Thus, each cross section represents one row

(or column) of the *TC & WM EIS* groundwater flow model. Transect length varies, but generally cross sections do not span the entire model domain. Lithological profiles for boreholes located within the buffer area are projected onto the cross section for stratigraphic interpretation and interpolation. Elevations of contacts between the discrete geologic layers are determined by the resulting cross sections. Geologic layers within the cross section are encoded into the groundwater flow model based on elevation, from 165 meters (541 feet) amsl down to the TOB surface. If more than one geologic layer is contained within one MODFLOW cell, the cell is assigned the properties of the hydrostratigraphic type with the largest total thickness over the range of elevations represented by the MODFLOW layer. At elevations near the water table (115 to 125 meters [377 to 410 feet]), this approach allows encoding of features on the order of several meters in thickness. At elevations deeper in the aquifer, the vertical grid spacing increases, and the minimum thickness of features that can be represented in the model ranges from several to tens of meters (see Figure L-3). The overall thickness of the model domain is approximately 250 meters (820 feet). At a minimum, features with thicknesses of about 10 percent of the overall model domain (25 meters [82 feet]) are represented in the model, which is appropriate for a regional-scale representation.

The hydrostratigraphy encoded into the *TC & WM EIS* groundwater flow model on the basis of HydroGeo Analyst cross sections was fine-tuned to remove artifacts associated with the encoding of adjacent transects, to ensure consistency with the final TOB surface, to eliminate rewetting problems (see Section L.5.1.1), and to add zonation within textural types. Fine-tuning involved re-encoding the MODFLOW stratigraphy to achieve the following:

- Remove incongruities due to extrapolation from borehole out to edge of transect (seam).
- Remove incongruities due to truncation of lithology that should extend out to seam.
- Remove incongruities due to extrapolation of lowest layer of borehole down to TOB surface.
- Remove incongruities due to incorrect assignment to textural types.
- Remove inconsistent assignment to mud or silt from same formation.
- Eliminate disconnects due to lack of shared face at seam (edge contact only).
- Extend lithology laterally or vertically to TOB surface.
- Activate basalt in the Gable Gap area at elevations where water table fluctuates to mitigate rewetting problems. Refer to Section L.5.1.1 for more detailed information.
- Add zone of high hydraulic conductivity extending from north of Gable Gap, and through the Gable Gap, as well as south and southeast through the central area of the model domain. This change was a result of Local User Group input, MODFLOW Technical Review Group input, and testing which improved the match between model-simulated hydraulic heads and field-observed hydraulic heads across the model domain.

L.4.4 Material Properties

The different textural types in the Hanford, Ringold, and other sedimentary hydrostratigraphic units are characterized by different material properties. Material properties required for the groundwater flow model include hydraulic conductivity, specific storage, and specific yield. Hydraulic conductivity is a measure of how easily water moves through pore spaces. Specific storage of a saturated aquifer is the amount of water that a given volume of aquifer material will release under a unit change in hydraulic

head. Specific yield is the volumetric fraction of the bulk aquifer volume that an aquifer will yield when all the water is allowed to drain out of it under the forces of gravity.

Material properties for unconsolidated sediments below the water table are required for MODFLOW calculations. In MODFLOW, material of a given type can have only one value for a property, e.g., hydraulic conductivity. Each of the 14 material types encoded in the *TC & WM EIS* groundwater flow model (see Table L-6) has a unique combination of values for the several material properties. Material properties in this model are calibration parameters with the exception of Zone 14—activated basalt (refer to Section L.5.1.1 for more detailed information on activated basalt); the value for a given material type everywhere in the model is adjusted within some realistic range until simulated water levels are calibrated to observed water levels (see Sections L.7, L.8, and L.9).

L.5 MODEL INPUTS – ALGORITHM SELECTION, PARAMETERS, AND SETTINGS

Some model inputs are independent of site data. These inputs include initial conditions and settings specifying how to make the calculations and how to modify the model to eliminate numerical instabilities that may arise. Some of the inputs are required by the MODFLOW software, e.g., rewetting rules, while others are common to all groundwater simulation models, e.g., time-stepping settings and initial conditions. These data-independent model inputs are discussed in the following sections.

L.5.1 Rewetting Methods

MODFLOW allows for cells to become dry (inactive) if the simulated head falls below the elevation of the cell bottom. Conversely, if the simulated head rises above the cell bottom or the laterally adjacent cells are wet, a currently dry cell can become wet. This process is called rewetting. The rewetting rules and parameters used to develop the *TC & WM EIS* groundwater flow model were generally the default parameters of MODFLOW 2000 (USGS 2004). The settings selected in Visual MODFLOW for the *TC & WM EIS* groundwater flow model are given in Table L-7.

Table L-7. Visual MODFLOW Rewetting Settings

Option	Setting
Activate cell wetting	On
Wetting threshold	0.1
Wetting interval	1 (iteration)
Wetting method	From below
Wetting head	Calculated from neighboring cells
Head value in dry cells	-1×1030 (meters)
Minimum saturated thickness for bottom layer	0.01 (meters)

Note: To convert meters to feet, multiply by 3.281.

Key: MODFLOW=modular three-dimensional finite-difference groundwater flow model.

L.5.1.1 Mitigation of Rewetting Problems

Rewetting problems emerged during model development that required mitigating actions. The rewetting problems were encountered in areas within the model where the water table and the TOB (inactive model cells) were at or near the same elevation and resulted in dry model cells in areas that should have been wet, based on the elevation of the water table in surrounding active model cells. Based on the model's rewetting settings, once an active model cell becomes dry it can only be rewet from an active wet model cell below the active dry model cell. In our problem cases, the cell below the active dry model cell was an inactive cell that represented the TOB in that area within the model. This configuration would not allow the active dry model cell to rewet even though water table elevations in surrounding active wet

model cells would normally result in rewetting of the problem dry model cell. This problem was significant enough that mitigation was required in the area of the model that represents Gable Gap.

To mitigate the rewetting problem in the Gable Gap area within the model, inactive cells that represented the TOB were made active and assigned hydraulic conductivity values that are more than 500 times smaller than that of Hanford and Ringold Muds (0.001 meters [0.00328 feet] per day). Making the inactive cell active and using a low hydraulic conductivity value allowed the active water table cells above the TOB to rewet from below but also maintained the TOB as an impermeable boundary.

The TOB was activated in the Gable Gap area within the model between 124 meters (407 feet) amsl and 115 meters (377 feet) amsl.

L.5.2 Time-Stepping Settings

The *TC & WM EIS* groundwater flow model period of analysis is 10,000 years, from 1940—prior to the start of operations—to 11,940. The model is preconditioned by simulating the years 1940 through 1943 (pre-Hanford) in transient mode prior to the occurrence of any anthropogenic recharge influxes (see Section L.4.2.5). The model then continues running in transient mode to capture the time-varying anthropogenic recharge influxes and the resulting water table fluctuations. Anthropogenic inputs are applied in 1-year stress periods beginning in 1944. The final stress period begins in 2022 and ends in 11,940.

L.5.3 Numerical Engine Selection and Parameterization

The numeric engine selected for simulating groundwater flow was MODFLOW 2000, Version 1.15.00 (USGS 2004), which is public domain software supported by Visual MODFLOW, Version 4.2. The settings selected in Visual MODFLOW for the *TC & WM EIS* groundwater flow model are given in Table L-8.

Table L-8. Visual MODFLOW Numerical Solution Settings

Option	Setting
Simultaneous equation solver	Preconditioned conjugate-gradient (PCG2)
Preconditioning method	Modified incomplete Cholesky
Cholesky relaxation parameter	0.98
Maximum outer iterations	500
Maximum inner iterations	200
Head change criterion	0.01 (meter)
Residual criterion	5,000
Damping factor	1
Printout interval	10 (time steps)

Note: To convert meters to feet, multiply by 3.281.

Key: MODFLOW=modular three-dimensional finite-difference groundwater flow model.

The preconditioned conjugate-gradient package for solving simultaneous equations is described in USGS Water-Resources Investigations Report 90-4048 (Hill 1990). Modified incomplete Cholesky preconditioning of the hydrogeologic parameter matrix is efficient on scalar (non-vector) computers (WHI 2006). Outer iterations vary the preconditioned matrix of hydrogeologic parameters of the flow system, e.g., transmissivity, saturated thickness, in an approach toward the solution. Inner iterations continue until the user-defined maximum number of inner iterations has been executed or the final convergence criteria are met. Outer iterations continue until the final convergence criteria are met on the first inner iteration after an update. Both the head-change and residual criteria determine convergence of the solver. The head change criterion is used to judge the overall solver convergence; the residual

criterion is used to judge the convergence of the inner iterations of the solver. The damping factor allows the user to reduce the head change calculated during each successive outer iteration.

L.5.4 Initial Head Distribution

Pre-Hanford head observation data are not available. The *TC & WM EIS* groundwater flow model was assigned an initial arbitrarily high water table and run in transient mode for 500 years to simulate pre Hanford (1940–1943) conditions with only natural recharges applied per the *Technical Guidance Document* (DOE 2005). This initial 500-year model run approached long-term steady state conditions, which is assumed to represent pre-Hanford conditions.

L.6 CALIBRATION STRATEGY

The *TC & WM EIS* groundwater flow model is calibrated to heads observed beginning in 1948. Artificial recharges during Hanford operations, especially those from 1944 to the mid-1990s, produced mounding of groundwater underneath the 200-East and 200-West Areas on the Central Plateau of Hanford (see Section L.4.2.4). Groundwater mounding influenced the local direction of flow and transport and consequently needs to be accurately represented in the long-term groundwater flow model.

Model calibration to head is conducted in four process steps:

1. Prepare a calibration data set consisting of observed groundwater (head) levels across Hanford during the calibration period, 1948–2006, including the pre-conditioning period of 1940–1943.
2. Specify the model calibration criteria, that is, how similar model results need to be compared with the observations in the calibration data sets.
3. Conduct a preliminary model calibration to heads, during which the model parameters are adjusted manually to provide a reasonable starting point for the head calibration.
4. Conduct final model calibration using gradient-based and Monte Carlo optimization methods.

The technical approach to these tasks and the results are discussed below.

L.6.1 Calibration Data Set

The *TC & WM EIS* groundwater flow model is calibrated to head data collected between 1948 and 2006 for a large number of selected wells scattered across the site. The data came from the HydroDat database of measured water table elevations provided by PNNL and accepted by the *TC & WM EIS* team as quality-assurance complete (PNNL 2006). This database includes approximately 127,000 observations at approximately 1,800 discrete locations. Wells were excluded from use in the head observation data set under the following conditions:

- Closer than 600 meters (1,969 feet) to the Columbia River, to remove the periodic fluctuations in the river stage from the head observation data
- Outside the active model domain, because the model is not being calibrated in these areas
- Screened in basalt, because these observations measure head values within confined aquifers that are not part of this flow model calibration
- Obvious data recording or entry errors

Table L–9 details the number of well locations and head observations that were removed from the original head observation data set.

Table L–9. Number of Well Locations and Head Observations Removed from Original Head Observation Data Set

Change	Number of Observations Remaining	Number of Wells Remaining
Original head observation data set	127,063	1,805
Removes wells outside of the horizontal model domain	126,551	1,737
Remove observations with head values of greater than 165 meters (541 feet) or less than 100 meters (328 feet)	126,149	1,699
Remove wells screened in basalt	119,619	1,599
Remove wells located within 600 meters (1,968 feet) of the Columbia River	88,699	1,274
Average the observations for each well, screen, and year such that each well and/or screen has a single observation for each year	20,921	1,274
Retain the well and/or screen with the largest number of averaged observations	20,112	1,174
Edit well locations and observations per detailed hydrograph review	19,299	1,119

The data from the remaining wells were partitioned into four approximately equal sets for final calibration. The data assigned to each data set were selected at random, with the restriction that no more than one observation well could be assigned to any given MODFLOW cell. One data set (approximately 25 percent of the observation wells) was selected and set aside for validation. The remaining three data sets (approximately 75 percent of the observation wells) were used in independent calibrations to test the robustness of the calibration parameters. A common set of observation wells and their head observation data were assigned to all four calibration data sets to ensure representation across the model domain in each of the calibration data sets. The distribution of the number of wells and the number of observations assigned to each of the three calibration data sets and the validation data set are detailed in Table L–10.

Table L–10. Number of Well Locations and Head Observations Assigned to Calibration and Validation Data Sets

Head Observation Data Set	Number of Observations	Number of Wells
Calibration Data Set # 1	5,005	274
Calibration Data Set # 2	5,563	279
Calibration Data Set # 3	5,230	270
Validation Data Set # 4	4,482	264

L.6.2 Calibration Criteria

The calibration data sets are used to assess the ability of the model to accurately simulate water levels and flow direction in the past, which is an indication of its ability to accurately simulate water levels and flow direction in the future. The calibration criteria define acceptable model performance in terms of measures of similarity (difference) between observed and simulated values. The model calibration criteria are as follows:

- Residuals (differences between observed and modeled heads) should be reasonably distributed.
 - Residual distribution should be reasonably normal.

- The mean residual should be approximately 0.
- The number of positive residuals should approximate the number of negative residuals.
- The correlation coefficient (calculated versus observed) should be greater than 0.9.
- The RMS error (calculated versus observed) should be less than 5 meters (16.4 feet), approximately 10 percent of the gradient in the water table elevation.
- The residual distribution should meet the needs of this *TC & WM EIS*.
 - Residuals in the 200-East Area should be distributed similarly to those in the 200-West Area.
 - The residuals should be evenly distributed through time.
 - The residuals should be evenly distributed across the site.
- The calibrated parameters should compare reasonably well with field-measured values.
- Parameters should be reasonably uncorrelated. Correlation among the parameters is a symptom of a poorly posed problem with many non-unique solutions.

These criteria are used to assess the final head calibrations.

L.6.3 Development of Objective Function

The groundwater flow model is calibrated to observed hydraulic heads across Hanford during the calibration period (1948–2006). The objective of the head calibration was to minimize the difference between the model-simulated head values and the field-observed head values during the calibration period. All head observation wells used in the head calibration were weighted equally. No concentration calibration was performed as part of the flow model development. Concentration calibration of the groundwater transport model is discussed in Appendix O.

L.7 PRELIMINARY CALIBRATION

The goal of preliminary head calibration is to produce a reasonable starting point for the gradient-based head calibration and Monte Carlo optimization. The most important prerequisites for these are a working model and parameters that are reasonably close to the expected solution and reasonably stable in parameter space, with the important components of parameter variability defined and understood. In the transient *TC & WM EIS* MODFLOW simulation, the goal was to obtain an initial head distribution in the aquifer that reasonably represented the boundary conditions at the start of the simulation.

The head distribution in 1940 represents the starting point for the transient simulation. The model was first preconditioned by simulating the year 1940 (pre-Hanford) by running the model for 500 years in transient mode without any anthropogenic recharge influxes. This approach resulted in initial heads that are believed to reasonably represent the pre-Hanford water table. These initial heads were used as the starting point for the model simulation. The model was then run in transient mode through an additional preconditioning period (1940–1943), followed by the various stress periods (each of which is about 1 year during the Hanford operational period). Stress periods between 1944 and the mid-1990s represent changes in operational discharges to the aquifer, which caused mounding of the water table. Stress periods following the mid-1990s allowed the mound to dissipate as operational discharges ceased. Subsequently, the head distribution relaxed to a long-term steady state distribution that is consistent with the boundary conditions. This long-term steady state distribution closely matched the initial condition. The primary difference between the initial condition and the long-term steady state condition is the city of Richland long-term extractions and recharge.

The steps in the preliminary head-calibration process are:

1. Generate an initial list of parameters that are important to examine.
 - a. Hydraulic conductivities of all of the hydrostratigraphic units
 - b. Storage properties of all of the hydrostratigraphic units
 - c. Conductance values of the riverbeds in each reach of the Columbia and Yakima Rivers
 - d. Conductance values and heads of the GHBs representing mountain-front recharge
2. Generate an initial estimate for each parameter. The initial estimates for material properties (i.e., steps 1a and 1b above) come from site-specific studies. The initial estimates for conductance values of the riverbeds and GHBs are set to large values. The initial estimates for GHB heads are set to values consistent with observed heads near the GHB locations along the western edge of the active model domain.
3. Precondition the model to obtain the initial (1940) head distribution. This task is achieved with a 500 year preconditioning model run as described earlier in this section. Compare the head distribution to the 2006 water table elevation distribution—the best, albeit very rough, estimate of the long-term steady state head distribution. Iterate through this step, adjusting the parameters to provide reasonable agreement with the 2006 water table elevation distribution.
4. When the parameter settings are reasonably correct and the resulting initial head distribution is obtained, run the model in transient mode from 1940–2006, including the preconditioning period from 1940–1943. Compare the calculated and observed heads for the preliminary set of calibration parameters encoded in Visual MODFLOW. Iterate through this step, adjusting the material properties and conductance values to provide reasonable agreement between the observed and calculated heads.

Once preliminary head calibration met the calibration criteria for reasonable agreement between the observed and calculated heads (see Section L.6.2), the gradient-based head calibration and Monte Carlo optimization began.

The results of the preliminary calibration are discussed below.

L.7.1 Potential Calibration Parameters

Calibration parameters are adjustable model settings that allow the user to control model behavior during the model simulation. For the *TC & WM EIS* groundwater flow model, some calibration parameters were specified in the *Technical Guidance Document* (DOE 2005), some were provided by available data, some were not used, and the remaining parameters were adjusted to achieve the head calibration. Table L–11 lists the potential calibration parameters and how they were applied during calibration.

Table L–11. Potential Calibration Parameters

Potential Calibration Parameter	How Specified or Used
Initial heads	500-year model run to establish pre-Hanford heads
Natural recharge	Specified by the <i>Technical Guidance Document</i> (DOE 2005)
Anthropogenic recharge	Specified by data (SAIC 2006)
River head	Specified by data (Thorne et al. 2006)
River conductance	Adjustable calibration parameter
Mountain-front recharge head	Adjustable calibration parameter
Mountain-front recharge conductance	Adjustable calibration parameter
Flow storage properties of material types	Adjustable calibration parameter
Hydraulic conductivity properties of material types	Adjustable calibration parameter

Key: Hanford=Hanford Site; *Technical Guidance Document*=*Technical Guidance Document for Tank Closure Environmental Impact Statement, Vadose Zone and Groundwater Revised Analyses*.

These calibration parameters were encoded if specified by data or adjusted within reasonable ranges to achieve the groundwater flow model calibration. Details of the calibration are included in the following sections.

L.7.2 Sensitivity Analysis

During the preliminary calibration, model runs were made to determine the model’s sensitivity to the adjustable calibration parameters. This sensitivity analysis is discussed in the following sections.

L.7.2.1 River Conductance

The Columbia and Yakima Rivers are modeled using the MODFLOW river package, which applies these boundaries as a GHB. River conductance values were initially set to arbitrarily high values, which resulted in the rivers behaving as constant head boundaries. This setting provided stability in the early stages of model development. Model runs were made, adjusting river conductance values over several orders of magnitude to determine the model’s sensitivity to this parameter. The results of this analysis concluded that the head calibration was not highly sensitive to river conductance. The model’s convergence behavior is sensitive to river conductance. In general, lower river conductance values resulted in greater model instability. The river conductance values derived during preliminary calibration ranged from 2.74×10^5 square meters (2.95×10^6 square feet) per year to 9.78×10^7 square meters (1.05×10^9 square feet) per year. Because the model is not sensitive to this parameter, these values were adopted for the Base and Alternate Case models.

L.7.2.2 Mountain-Front Recharge Head and Conductance

Natural recharges or influxes of water occur along the western boundary of the model domain. The locations and values of influx from these sources of model recharge have been studied extensively (Thorne et al. 2006). These recharge sources are modeled using the MODFLOW GHB package and are located in general locations as specified in prior work. The head and conductance values for these recharge sources were treated as calibration parameters, adjusted within reasonable ranges until the simulated head values reasonably matched the observed heads.

The *TC & WMEIS* groundwater flow model is sensitive to the GHB recharge head and conductance values. As expected, model-simulated head values increase across the model domain with increases in GHB recharge head values. The model-simulated head values were more sensitive to GHB recharge head values when conductance values were high.

The GHB head values derived during preliminary calibration for mountain-front recharge ranged from 128 meters (420 feet) amsl to 165 meters (541 feet) amsl. The GHB conductance values derived during preliminary calibration for mountain-front recharge ranged from 5.00×10^4 square meters (5.38×10^5 square feet) per year to 5.00×10^5 square meters (5.38×10^6 square feet) per year. Table L–12 details the GHB head and conductance ranges for each area of the model where the GHB boundary condition is encoded. Because model convergence and dry-cell behavior (particularly in the Gable Gap area) were extremely sensitive to the GHB parameters, these settings were adopted for the Base and Alternate Case models.

Table L–12. Summary of Encoded Generalized Head Boundary Head and Conductance Values

Model Domain Area	Minimum Head (meters)	Maximum Head (meters)	Minimum Conductance (square meters/year)	Maximum Conductance (square meters/year)
Rattlesnake Mountain Front	128	130	100,000	500,000
Dry Creek Area	165	165	50,000	100,000
Cold Creek Area	158	158	50,000	100,000

Note: To convert meters to feet, multiply by 3.281; square meters to square feet, by 10.7639.

L.7.2.3 Flow Storage Properties of Material Types

Specific yield is a flow storage parameter and is defined as the volume of water that an unconfined aquifer releases from storage per unit surface area per unit decline in the water table (WHI 2006). Specific yield values derived during preliminary calibration are listed in Table L–13. In general, preliminary calibration shows the groundwater flow model is not particularly sensitive to specific yield. The values listed in Table L–13 were not modified from their initial estimates. Later sensitivity analysis shows slightly better RMS error results can be achieved with a higher specific yield for Ringold Gravel. This result suggests that the specific yield of Ringold Gravel is higher than presented in Table L–13, a result more consistent with the specific yield of other gravels in the model.

Table L–13. Specific Yield Values Derived from the Preliminary Calibration

Material Type (Model Zone)	Specific Yield
Hanford mud (1)	0.2
Hanford silt (2)	0.18
Hanford sand (3)	0.26
Hanford gravel (4)	0.3
Ringold Sand (5)	0.26
Ringold Gravel (6)	0.15
Ringold Mud (7)	0.2
Ringold Silt (8)	0.18
Plio-Pleistocene sand (9)	0.26
Plio-Pleistocene silt (10)	0.18
Cold Creek sand (11)	0.26
Cold Creek gravel (12)	0.25
Highly conductive Hanford gravel (13)	Not encoded at preliminary calibration
Activated basalt (14)	Not encoded at preliminary calibration

L.7.2.4 Hydraulic Conductivity Properties of Material Types

The *TC & WM EIS* groundwater flow model is sensitive to hydraulic conductivity values for the various material types encoded in the model. The preliminary calibration found that the model is most sensitive to those material types occupying the largest volume of space within the model domain. As shown in Table L–6, the three material types that occupy the highest percentage of the model domain volume are Ringold Gravel (34.6 percent), Ringold Mud (19.4 percent), and Hanford gravel (16.5 percent). Hydraulic conductivity values derived during preliminary calibration are listed in Table L–14.

For comparison purposes, field and laboratory hydraulic conductivity from a limited data survey are summarized in Table L–15. Additional hydraulic conductivity data resulting from pump testing for the Hanford and Ringold Formations are included in Figure L–53.

Table L–14. Hydraulic Conductivity Values Derived from the Preliminary Calibration

Material Type (Model Zone)	Hydraulic Conductivity (K_x) ^a	Hydraulic Conductivity (K_y) ^b	Hydraulic Conductivity (K_z) ^c
Hanford mud (1)	0.5	0.5	0.05
Hanford silt (2)	15.0	15.0	1.5
Hanford sand (3)	175.0	175.0	17.5
Hanford gravel (4)	1,200.0	1,200.0	120.0
Ringold Sand (5)	15.0	15.0	1.5
Ringold Gravel (6)	25.0	25.0	2.5
Ringold Mud (7)	0.5	0.5	0.05
Ringold Silt (8)	1.1	1.1	0.11
Plio-Pleistocene sand (9)	75.0	75.0	7.5
Plio-Pleistocene silt (10)	10.0	10.0	1.0
Cold Creek sand (11)	125.0	125.0	12.5
Cold Creek gravel (12)	700	700	70
Highly conductive Hanford gravel (13)	Not encoded at preliminary calibration	Not encoded at preliminary calibration	Not encoded at preliminary calibration
Activated basalt (14)	Not encoded at preliminary calibration	Not encoded at preliminary calibration	Not encoded at preliminary calibration

^a Hydraulic conductivity with respect to the x axis, meters per day.

^b Hydraulic conductivity with respect to the y axis, meters per day.

^c Hydraulic conductivity with respect to the z axis, meters per day.

Note: To convert meters to feet, multiply by 3.281.

L.7.3 Selection of Calibration Parameters, Initial Estimates, and Target Ranges

The process of preliminary calibration produced a groundwater flow model framework that had examined all of the potential calibration parameters (see Table L–11). Of these parameters, the initial heads, natural recharge, anthropogenic recharge, river heads, riverbed conductances, and mountain-front recharge heads and conductances were fixed by consideration of technical guidance, field data constraints, calculation, and/or model stability and sensitivity. The remaining adjustable parameters were the material properties, specifically storage parameters and hydraulic conductivities.

Initial estimates for the gradient-based calibration were chosen from a literature review of site-specific data. The data were largely based on field tests and laboratory-scale measurements of the properties of Hanford suprabasalt sediments. These initial estimates and target ranges are shown in Table L–15. The preliminary calibration suggested that the groundwater flow model was most sensitive to the hydraulic conductivities of the Ringold Gravel, Ringold Mud, and Hanford gravel model units.

Table L-15. Initial Estimates for Material Properties

Stratigraphic Unit/ Lithologic Unit	Low Laboratory Hydraulic Conductivity $K_{h,sat}$ (m/day)	High Laboratory Hydraulic Conductivity $K_{h,sat}$ (m/day)	Low Field Hydraulic Conductivity $K_{h,sat}$ (m/day)	High Field Hydraulic Conductivity $K_{h,sat}$ (m/day)	Range in Hydraulic Conductivity $K_{h,sat}$ (m/day) ^a	MODFLOW Initial Estimate Hydraulic Conductivity $K_{h,sat}$ (m/day)	Comment
Alluvium (Qal)	No Data	No Data	No Data	No Data	No Data	1×10^2	Assume Qal=Hs
Hanford gravel (Hg)	1.7×10^{-2} , b, c	2.3×10^2 , b, c	1 ^d , e, f, g	3.35×10^3 , e, f, g	1×10^{-3} to 3×10^3	1×10^3	
Hanford sand (Hs)	3.0×10^{-3} , b, c	5×10^2 , b, c	1 ^d , e, f, g	2.41×10^2 , d, g	1×10^{-3} to 5×10^2 , d, g	1×10^2	
Hanford silt (Hss)	2.7×10^{-3} , b	1.49×10^2 , b	No Data	No Data	1×10^{-3} to 1.5×10^2	10	
Hanford mud (Hm)	No Data	No Data	No Data	No Data	No Data	1×10^{-3}	Assume Hm=Rm
Cold Creek gravel (CCg)	No Data	No Data	No Data	No Data	No Data	1×10^3	Assume CCg=Hg
Cold Creek sand (CCs)	No Data	No Data	No Data	No Data	No Data	1×10^2	Assume CCs=Hs
Plio-Pleistocene gravel (Pplg)	No Data	No Data	No Data	No Data	No Data	1×10^3	Assume Pplg=Hg
Plio-Pleistocene sand (Ppls)	No Data	No Data	No Data	No Data	No Data	1×10^2	Assume Ppls=Hs
Plio-Pleistocene silt (Pplss)	2.3×10^{-3} , b, h	5.88×10^2 , b, h	No Data	No Data	1×10^{-3} to 6×10^2	10	
Plio-Pleistocene cement (Pplc)	No Data	No Data	No Data	No Data	No Data	1	Assume Pplc=Ppls0.1
Ringold Gravel (RgE)	7.0×10^{-4} , c, i	6.7^c , i	5×10^{-2} , f, j, o	1.55×10^3 , f, j, o	1×10^{-3} to 1.55×10^3	1×10^2	
Ringold Gravel (RgA)	2.2×10^{-3} , c, i	1.6^c , i	1.7 ^m	2 ^m	1×10^{-3} to 2	1	
Ringold Sand (Rs)	No Data	No Data	9 ^g	12 ^g	9 to 12	10	
Ringold Silt (Rss)	No Data	No Data	No Data	No Data	No Data	1	Assume Rss=Hs*0.1
Ringold Mud (Rm)	8.6×10^{-5} , c, d, i	5.62×10^{-2} , c, d, i	No Data	No Data	8.64×10^{-5} to 5.6×10^{-2}	1×10^{-3}	

^a Textbook Ranges (Fetter 1988; Freeze and Cherry 1979) for these parameters in m/day are: gravel, mixed sand and gravel, 1 to 90000; sand, 0.1 to 900; silt, 0.01 to 90; and clay (mud), 0.0001 to 0.1.

^b Khaleel and Freeman 1995.

^c Connelly, Ford, and Borghese 1992.

^d Schalla et al. 1988.

^e Fruchter et al. 1996.

^f Spane, Thorne, and Newcomer 2001a.

^g DOE 1994.

^h Rohay et al. 1993.

ⁱ Byrnes and Miller 2006.

^j Rohay, Swett, and Last 1994.

^k Williams et al. 2000.

^l Spane and Thorne 2000.

^m Spane, Thorne, and Newcomer 2001b.

ⁿ Spane, Thorne, and Newcomer 2002.

^o Spane, Thorne and Newcomer 2003.

Note: To convert meters to feet, multiply by 3.281.

Key: $K_{h,sat}$ =saturated hydraulic conductivity; m/day=meters per day; MODFLOW=modular three-dimensional finite-difference groundwater flow model.

L.8 GRADIENT-BASED CALIBRATION

The gradient-based calibration of the transient model used PEST in conjunction with MODFLOW. The goal of PEST is to adjust the variable parameters in the model in a way that minimizes the difference between observed values of head (historic field measurements) and corresponding model simulations. The development of the calibration data sets and the objective function were described in Section L.6.

The fundamental assumption underlying gradient-based calibration is that there is a single set of adjustable parameters that, when inserted in the flow model, yield a minimum value for the objective function. The further away the parameters are from the optimal set, the larger the objective function (i.e., discrepancy between field observation of head and model simulations). The gradient-based method starts with initial estimates for the set of parameters and calculates the steepest downhill gradient (i.e., the set of adjustments to the parameters that yields the maximum decrease in objective function). The parameters are all moved in the steepest downhill direction, and the calculation is repeated until two subsequent iterations are within a specified tolerance or the maximum number of iterations is achieved.

Initial calculations using this method confirmed that the flow model was more sensitive to hydraulic conductivity values than to storage parameters. In particular, the model was most sensitive to the hydraulic conductivities of the Hanford gravel, Ringold Sand, Ringold Gravel, Cold Creek gravel, and the Highly conductive Hanford gravel. A variety of different PEST settings and initial estimates were investigated. The final production results for the three calibration data sets are typical (Table L-16).

Table L-16. Base Case PEST-Optimized Conductivity Values with Confidence Limits – Selected Material Types (meters per day)

Horizontal Hydraulic Conductivity (K_h)				
Material Type (Model Zone)	Initial Value	PEST-Optimized Value	95th Percentile Confidence Limits	
			Lower Limit	Upper Limit
Head Calibration Data Set 1				
Hanford gravel (4)	600	229.698	216.106	244.144
Ringold Sand (5)	15	3.89152	3.00041	5.04728
Ringold Gravel (6)	25	12.8691	12.3253	13.437
Cold Creek gravel (12)	700	140	127.235	154.046
Highly conductive Hanford gravel (13)	3,000	5162.08	4637.68	5745.77
Head Calibration Data Set 2				
Hanford gravel (4)	600	246.565	232.431	261.558
Ringold Sand (5)	15	3.64608	3.1234	4.25624
Ringold Gravel (6)	25	13.7969	13.3136	14.2979
Cold Creek gravel (12)	700	214.445	187.926	244.707
Highly conductive Hanford gravel (13)	3,000	5219.59	4569.74	5961.85
Head Calibration Data Set 3				
Hanford gravel (4)	600	207.281	205.684	208.89
Ringold Sand (5)	15	3	2.62202	3.43246
Ringold Gravel (6)	25	14.2736	13.9357	14.6197
Cold Creek gravel (12)	700	140	130.501	150.191
Highly conductive Hanford gravel (13)	3,000	7124.82	6456.74	7862.03

Notes: K_z (vertical hydraulic conductivity) is equal to $K_h/10$. To convert meters to feet, multiply by 3.281.

Key: PEST=parameter estimation.

The final sets of parameters for the gradient-based calibrations appeared to have reasonable values and acceptable consistency among the three independent head calibration data sets. The confidence ranges

(i.e., difference between the upper and lower confidence limits) were considered unreasonably narrow for a primary purpose of this *TC & WM EIS*: to adequately describe the uncertainty of the groundwater flow model with respect to the parameters. The results suggested that the assumption of the gradient-based method that the objective function varied smoothly with the distance of the parameter set from their optimal values and that there was one unique set of optimal parameters may not be valid for this groundwater flow model.

To test this assumption, a number of MODFLOW calculations were performed in which all of the parameters were held at their optimal, PEST-derived values, except for one. The selected parameter was varied over a range greater than the PEST-derived confidence limit, and the objective function was calculated. This process was completed five times, each time varying only one of the hydraulic conductivity parameters. Figure L-9 shows one such result. The x axis shows the value of the hydraulic conductivity for Hanford gravel that was used in the specific calculation. All other hydraulic conductivities were kept at their optimal values. The y axis shows the resulting value of the objective function. If the gradient-based assumption was correct, this process should have resulted in a curve that was approximately parabolic in shape, with a single minimum. These calculations demonstrate that the objective function does not vary smoothly with parameter variations over a single range and suggest that the objective function contains many local minima. Although the gradient-based parameter values themselves are likely to be reasonable representations of the hydraulic conductivities for the flow model, the description of the uncertainties in these parameters did not meet the data quality objective for the calibration process.

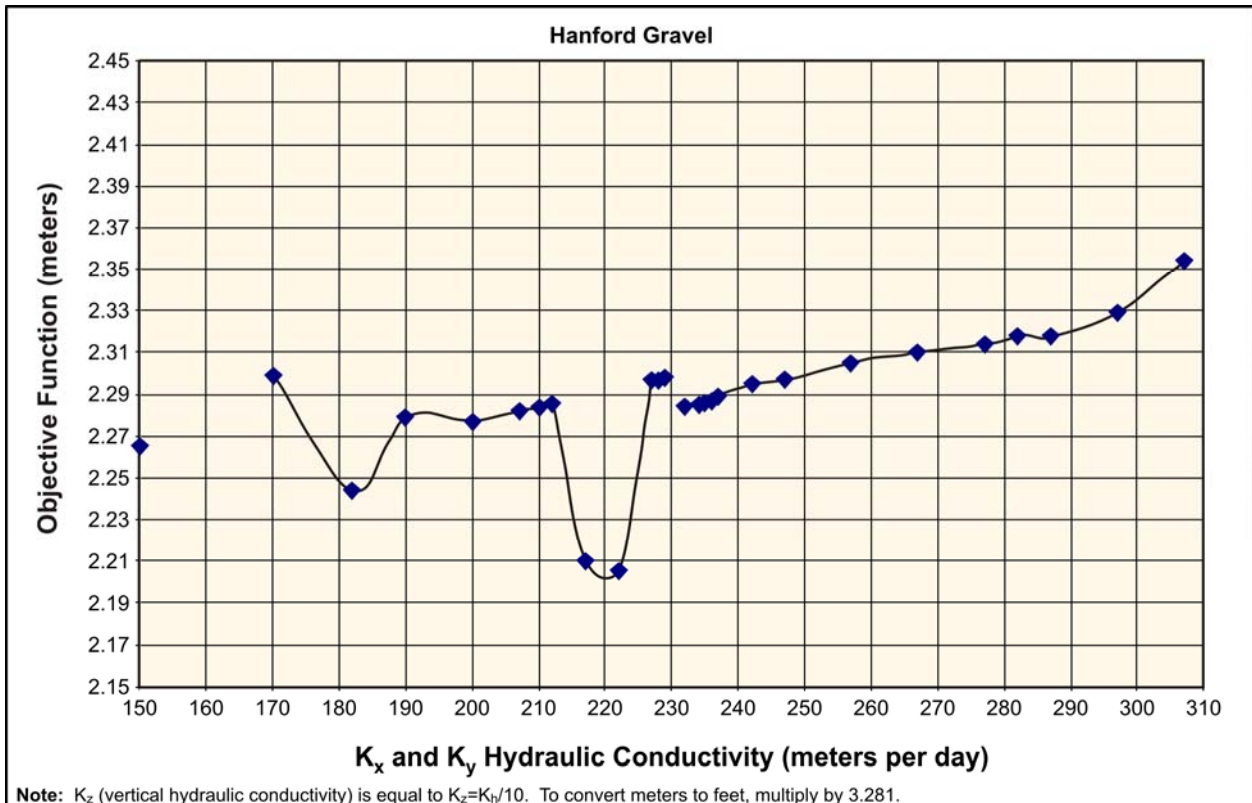


Figure L-9. Objective Function Variations as a Function of Hydraulic Conductivity Changes

L.9 MONTE CARLO OPTIMIZATION AND UNCERTAINTY ANALYSIS

The preliminary and gradient-based calibration processes demonstrated the following:

- The flow model is more sensitive to hydraulic conductivity variations than variations in storage parameters.
- The flow model requires a highly conductive zone of Hanford gravel across the center of the model through the Gable Gap area to satisfy the extremely flat water table conditions measured across this region over a large variation in operational recharge.
- Ringold Gravel, which is at the water table underneath the 200-West Area, is at least two orders of magnitude less conductive than the highly conductive zone of Hanford gravel, and at least 30 times less conductive than regular Hanford gravel.
- The flow model is sensitive to relatively small changes in hydraulic conductivities in the three primary units, with nonlinear responses in objective function.

At the end of these two processes, reasonable values for the hydraulic conductivities of the primary hydrostratigraphic units were obtained, but the uncertainty in these values was not well estimated. To further understand the behavior of the flow model to changes in the hydraulic conductivity parameters, a Monte Carlo optimization and uncertainty analysis was conducted on the groundwater flow model.

L.9.1 Design of the Analysis

The objective function (difference between field observations of water table elevation and model simulations) responds non-linearly to changes in the hydraulic conductivity parameters. Small changes in the sensitive parameters can lead to large changes in the quality of model agreement with historic water-level measurements. Further, an analysis of the topology of the objective function shows that there are many individual, discrete local minima. Because of this behavior, the problem of describing uncertainty with respect to the hydraulic conductivities changes from a description of the shape of a single nearly parabolic curve in parameter space (i.e., the conceptualization behind gradient-based methods) to a description of the locations of a collection of a large number of discrete local minima.

To solve this problem, three searches were conducted in the 13-dimensional hydraulic conductivity parameter space, one search for each calibration data set (see Section L.6). Each search was composed of a number of realizations: 6,660 Base Case realizations for Calibration Data Set 1, 6,400 Base Case realizations for Calibration Data Set 2, and 6,400 Base Case realizations for Calibration Data Set 3. Each realization was independent from all others. Each realization was created by randomly selecting hydraulic conductivity values for the 13 stratigraphic units with a linear probability distribution over a range of several orders of magnitude around the values listed in Table L-15. These randomly selected parameters were used to create a MODFLOW run over the calibration period of the model (1948–2006). The objective function was calculated for each run and tabulated. The process was repeated as computer resources permitted.

L.9.2 Base Case – Results of the Analysis

The cumulative density of the objective function for each of the three data sets are shown in Figures L-10 through L-12. The *x* axis of each plot is the RMS difference between the field-measured and modeled water table elevations for all wells in the calibration data set for all measurement times. The *y* axis shows the fraction of realizations that were lower than or equal to the corresponding RMS value. Note that the three curves have reasonably similar sigmoidally shaped cumulative distributions that vary over a similar RMS range.

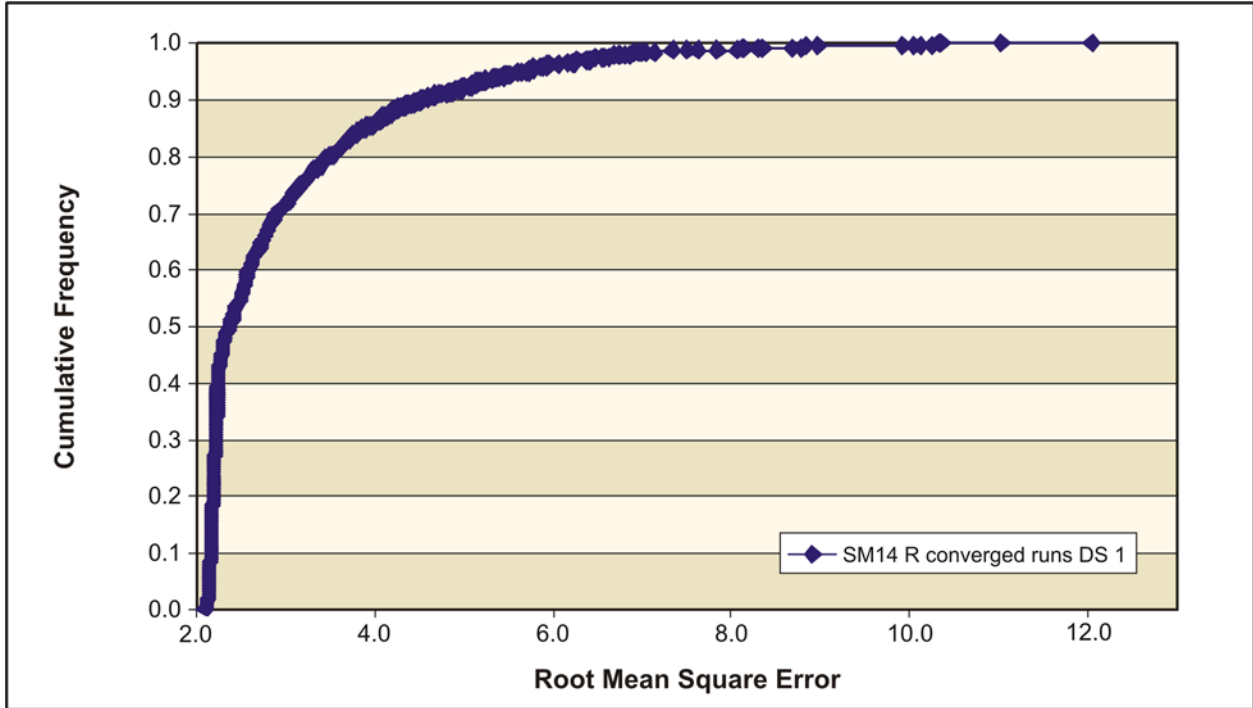


Figure L-10. Cumulative Density of the Objective Function – Base Case Model, Calibration Data Set 1

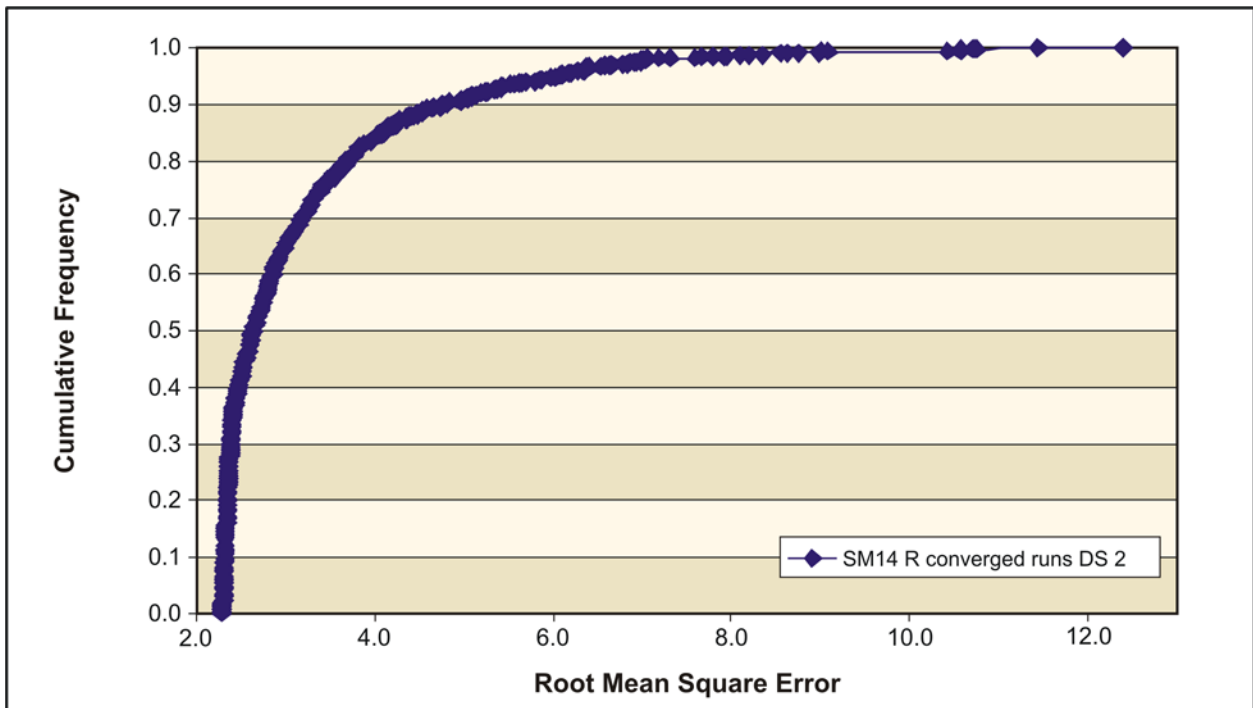


Figure L-11. Cumulative Density of the Objective Function – Base Case Model, Calibration Data Set 2

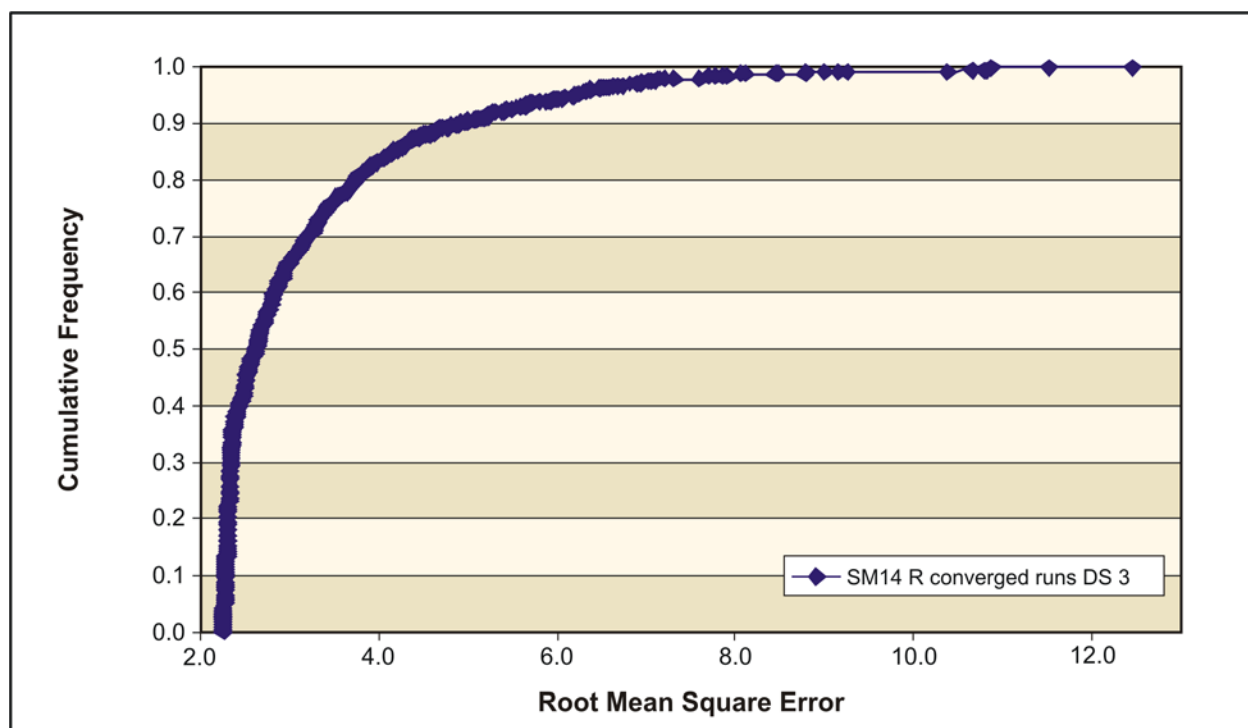


Figure L-12. Cumulative Density of the Objective Function – Base Case Model, Calibration Data Set 3

For each data set, the best realizations were chosen according to two criteria. The first criterion was that the RMS value for that realization was among the lowest (at least in the lowest 1 percent). The second criterion was that MODPATH (MODFLOW particle-tracking postprocessing package), particle tracks from sources in the 200-East Area showed reasonable qualitative agreement with the observed shape of the tritium plume originating near the Plutonium-Uranium Extraction (PUREX) Plant in the 200-East Area. In fact, as the RMS value decreased, the qualitative agreement of the MODPATH particle tracks with the PUREX Plant plume shape became increasing better. Section L.10.1.3.1 discusses the Base Case tritium plume delineations in more detail.

Finally, the distributions of the hydraulic conductivity values for the best realizations were compared to the distributions of the hydraulic conductivity values for all realizations. Figures L-13 through L-25 show these comparisons for the Base Case model, Calibration Data Set 1, for the 13 hydrostratigraphic units. (The comparisons for the other two calibration data sets are similar.) Each figure shows two cumulative densities. The x axis of each plot is the hydraulic conductivity (meters per day) for the hydrostratigraphic unit. The y axis shows the fraction of realizations that were lower than or equal to the corresponding hydraulic conductivity value. Two curves are plotted for each hydrostratigraphic unit. The curve plotted with the red symbols shows the cumulative distribution for all realizations. It is used to show the portion of parameter space that was searched. For example, for Hanford gravel (see Figure L-16) realizations were generated that covered the range of hydraulic conductivity from about 0.05 meters per day (0.16 feet per day) up to about 1,000,000 meters per day (3,281,000 feet per day), roughly a variation over eight orders of magnitude. The curve plotted with the green symbols shows the portion of parameter space that was covered by the best set of realizations. For example, the best realizations for Hanford gravel were restricted to a relatively narrow range – from about 110 meters per day (361 feet per day) to about 175 meters per day (574 feet per day). The steepness of the green curve relative to the red curve shows the degree of sensitivity the flow model shows to a particular hydraulic conductivity. When the green curve is steep, as it is for Hanford gravel (see Figure L-16), Ringold Gravel (see Figure L-18), and Highly conductive Hanford gravel (see Figure L-25), the flow model is

sensitive to those hydraulic conductivities and the best RMS values can only be obtained across a narrow range of values. For the units where the green curve is not as steep, and covers more of the range represented by the red curve, the flow model is less sensitive to those parameters, and good agreement between measured and modeled water table elevations can be obtained over a much broader range of hydraulic conductivities. Note that there is no particular ordering or correspondence in terms of RMS on either the green or red curves. Slight changes in hydraulic conductivity values can lead to higher or lower RMS error. The relationship between RMS and hydraulic conductivity is not linear. This analysis shows where (in hydraulic conductivity parameter space) the best realizations were found, but not that a particular hydraulic conductivity leads to a good result.

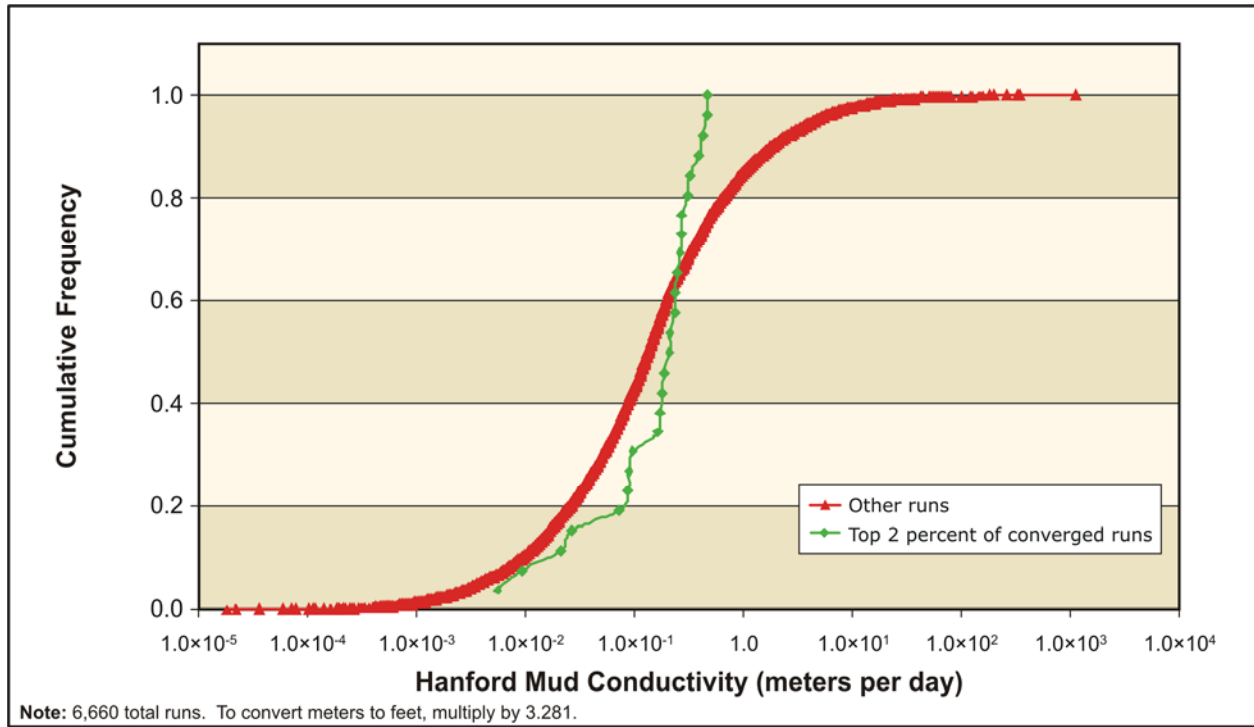


Figure L-13. Distribution of Hydraulic Conductivity Values – Hanford Mud

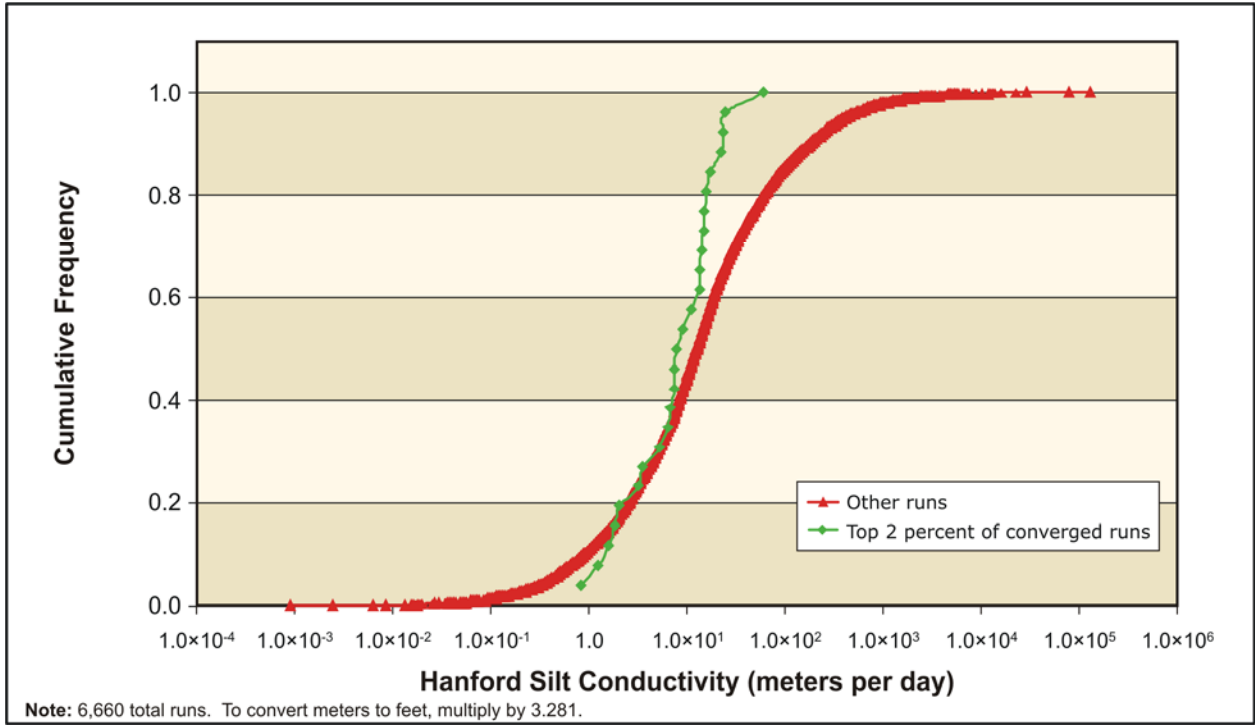


Figure L-14. Distribution of Hydraulic Conductivity Values – Hanford Silt

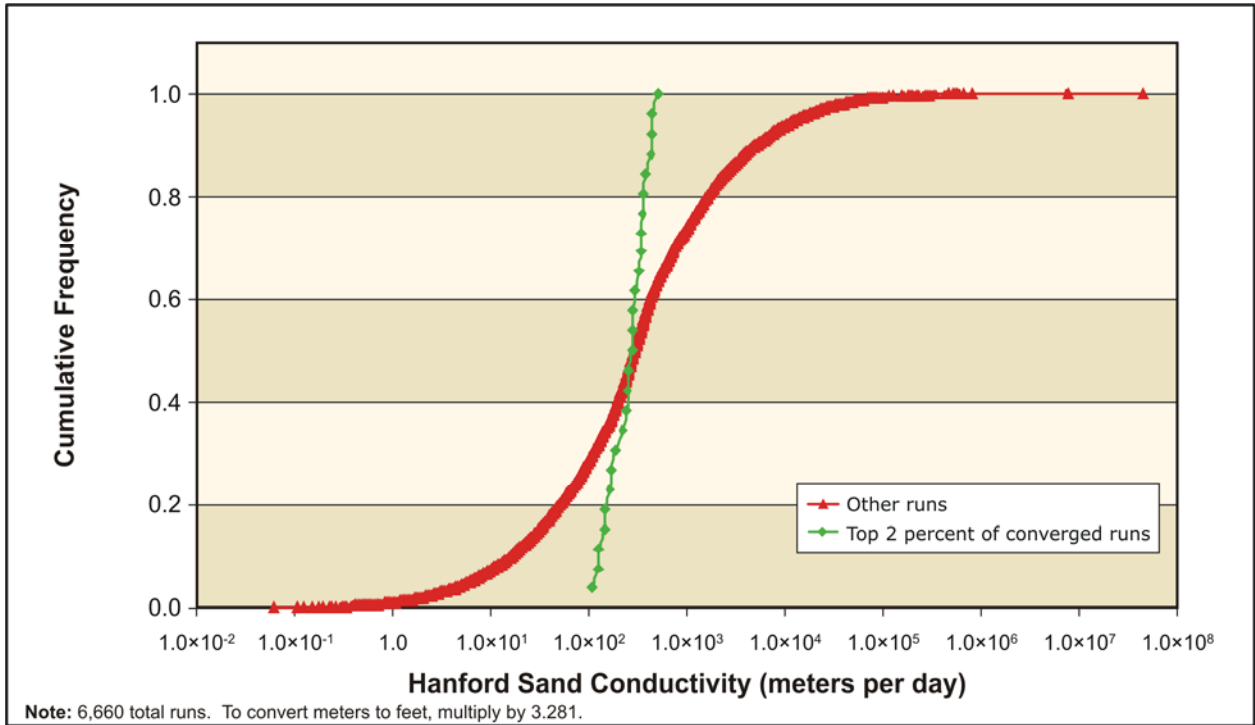


Figure L-15. Distribution of Hydraulic Conductivity Values – Hanford Sand

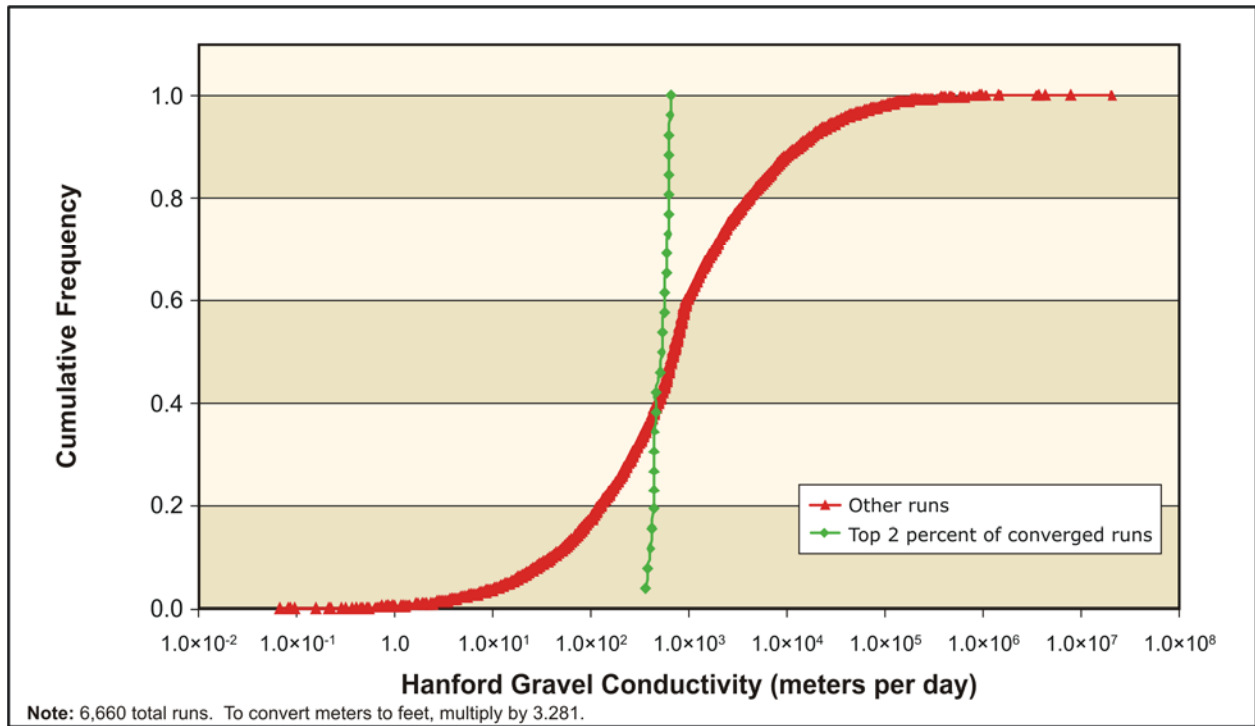


Figure L-16. Distribution of Hydraulic Conductivity Values – Hanford Gravel

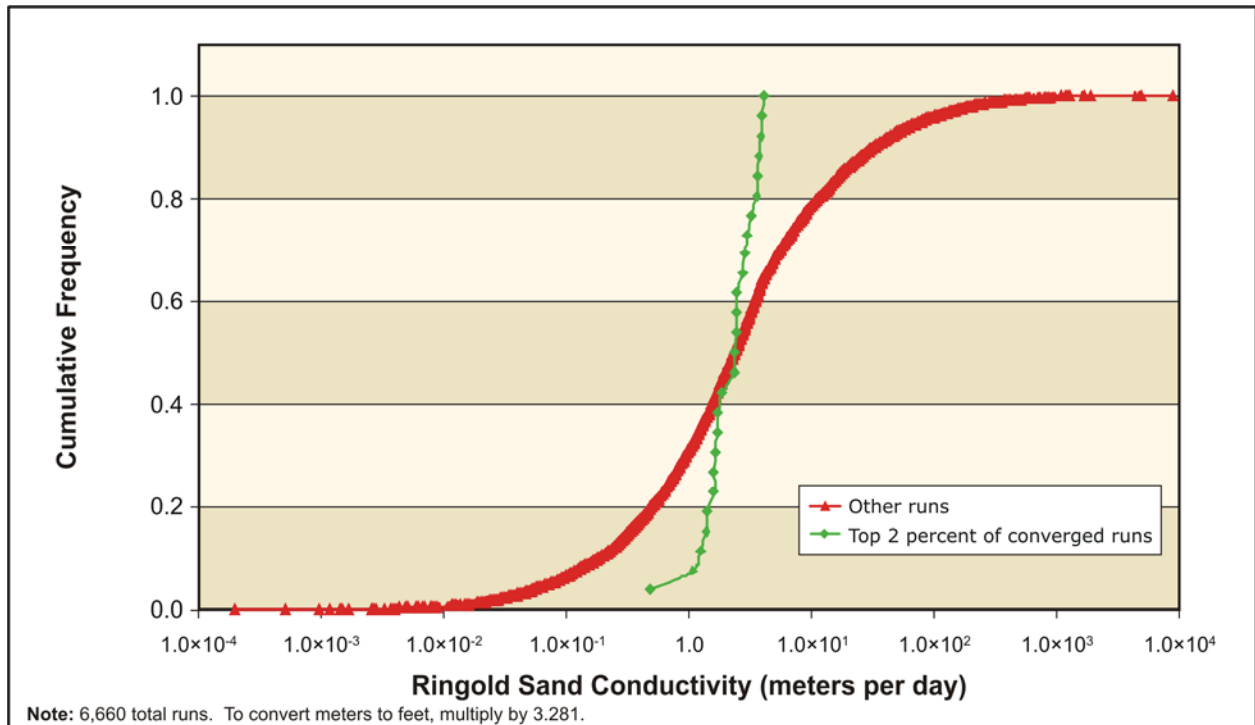


Figure L-17. Distribution of Hydraulic Conductivity Values – Ringold Sand

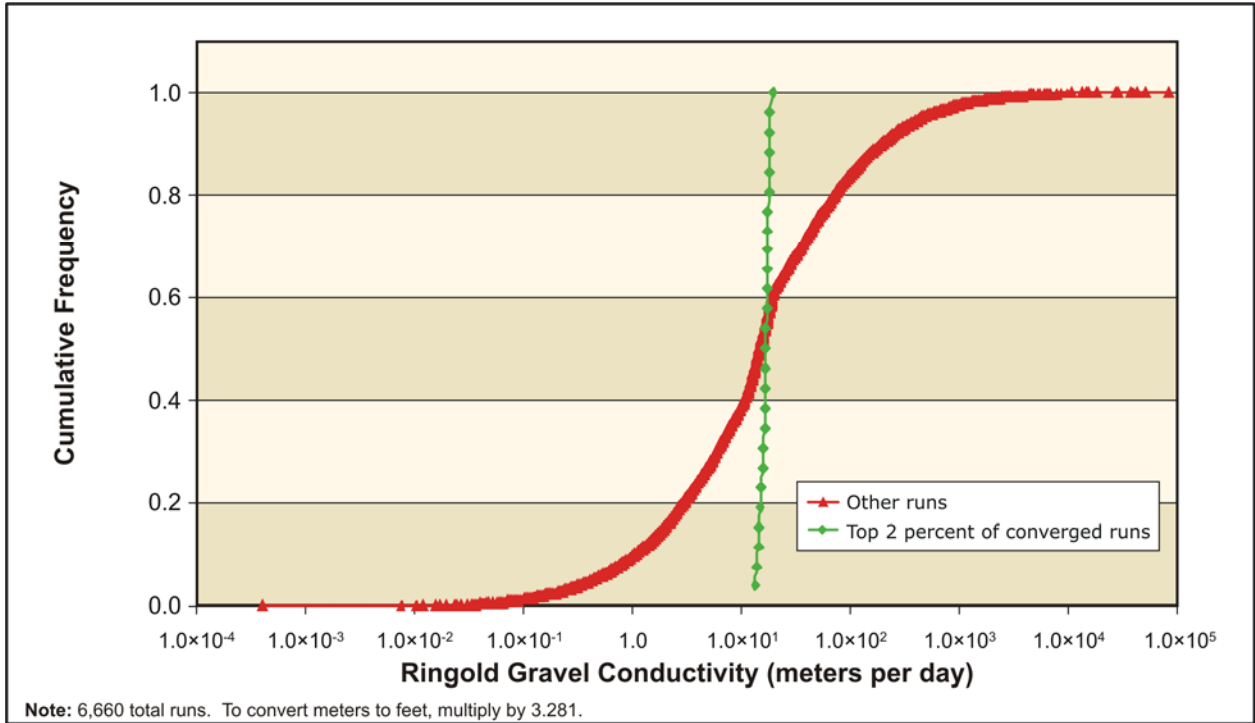


Figure L-18. Distribution of Hydraulic Conductivity Values – Ringold Gravel

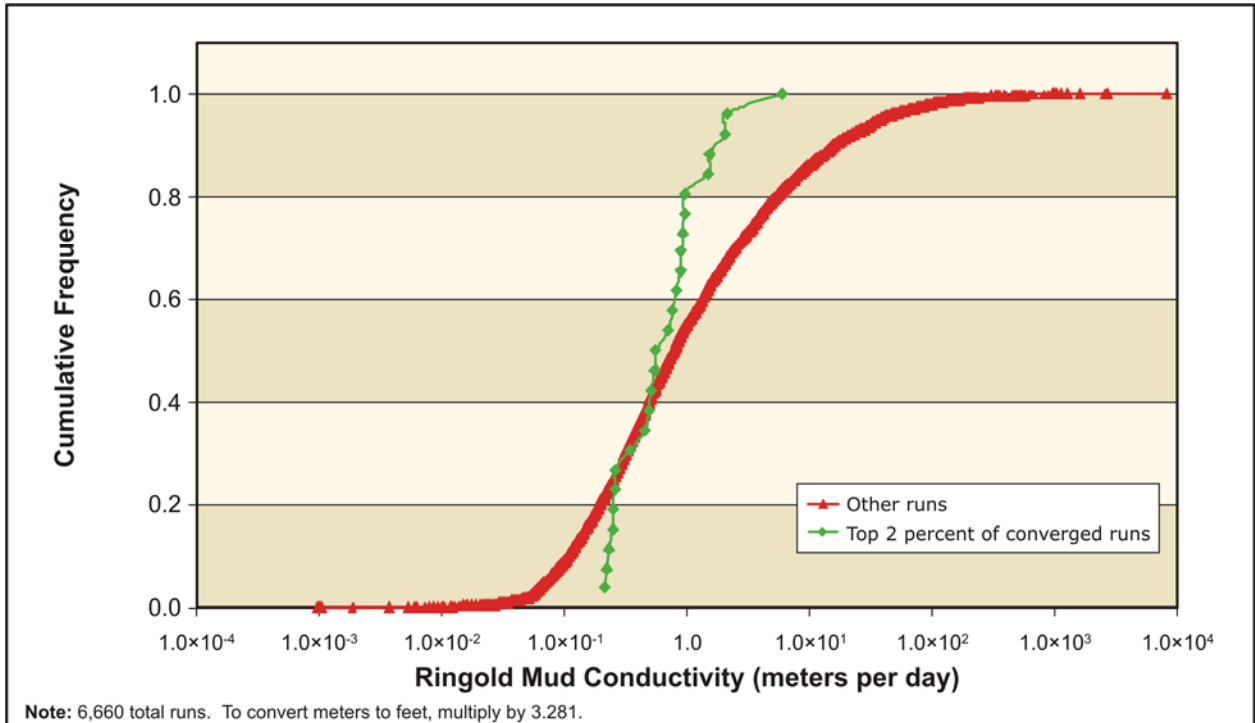


Figure L-19. Distribution of Hydraulic Conductivity Values – Ringold Mud

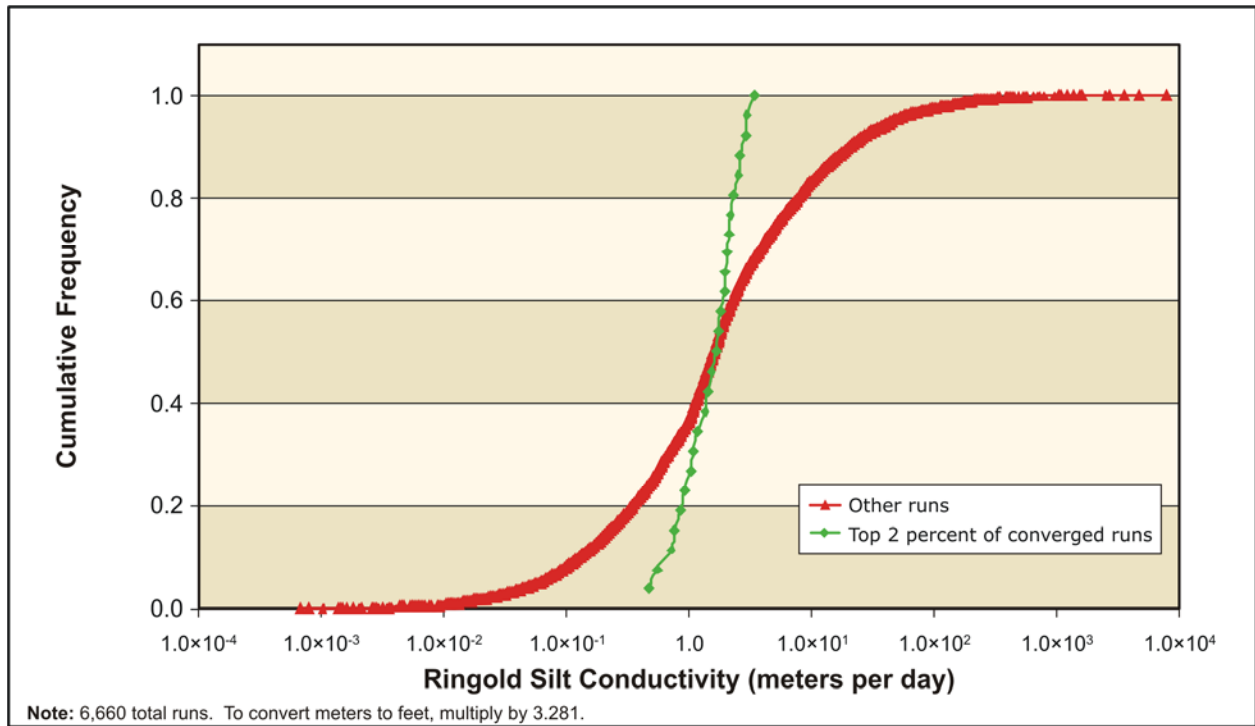


Figure L-20. Distribution of Hydraulic Conductivity Values – Ringold Silt

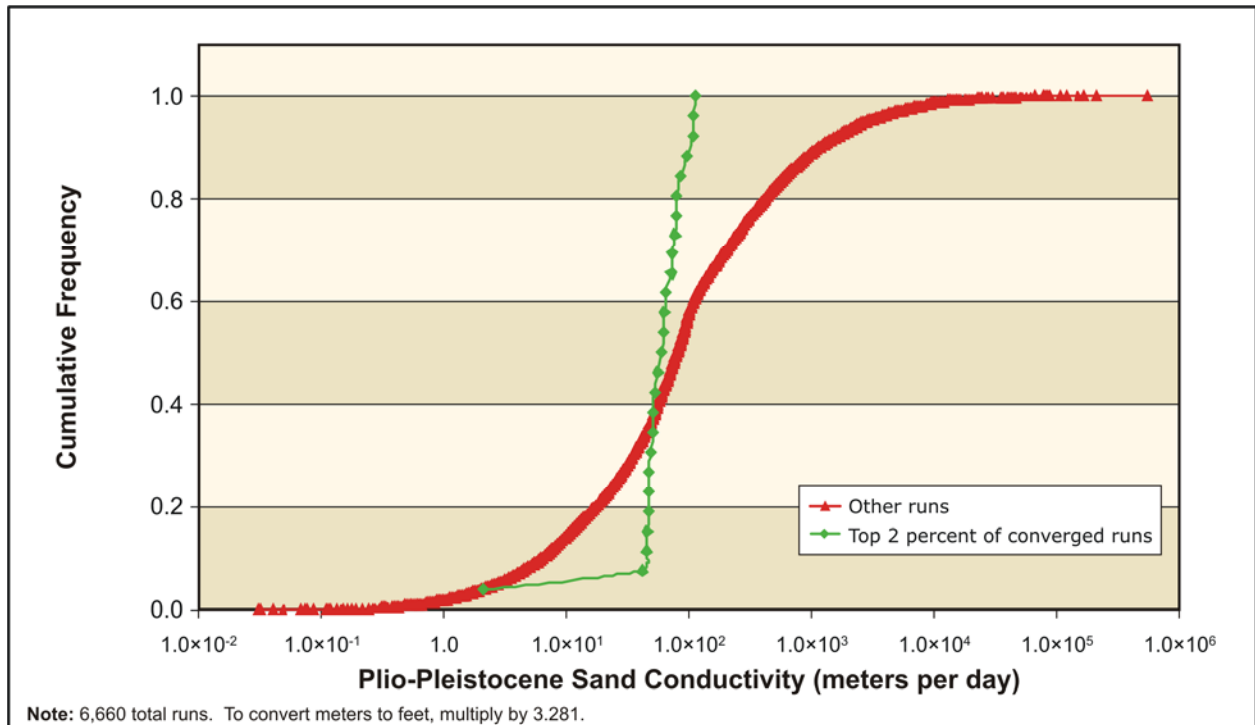


Figure L-21. Distribution of Hydraulic Conductivity Values – Plio-Pleistocene Sand

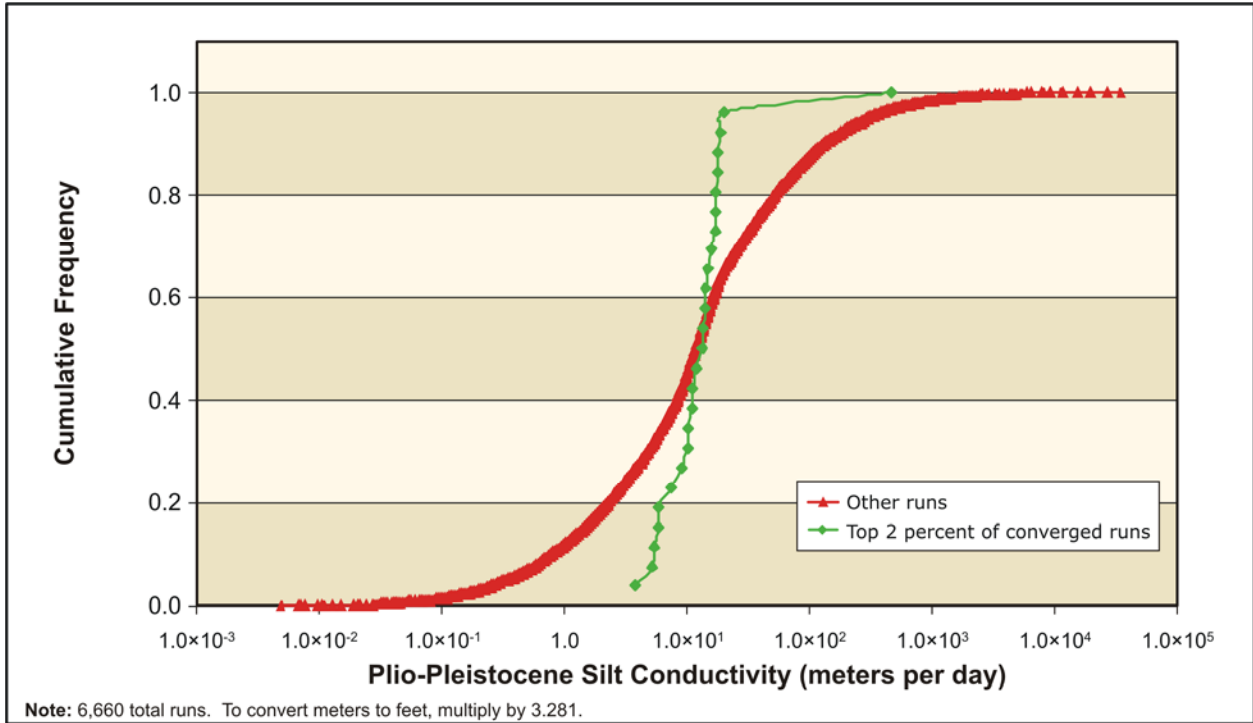


Figure L-22. Distribution of Hydraulic Conductivity Values – Plio-Pleistocene Silt

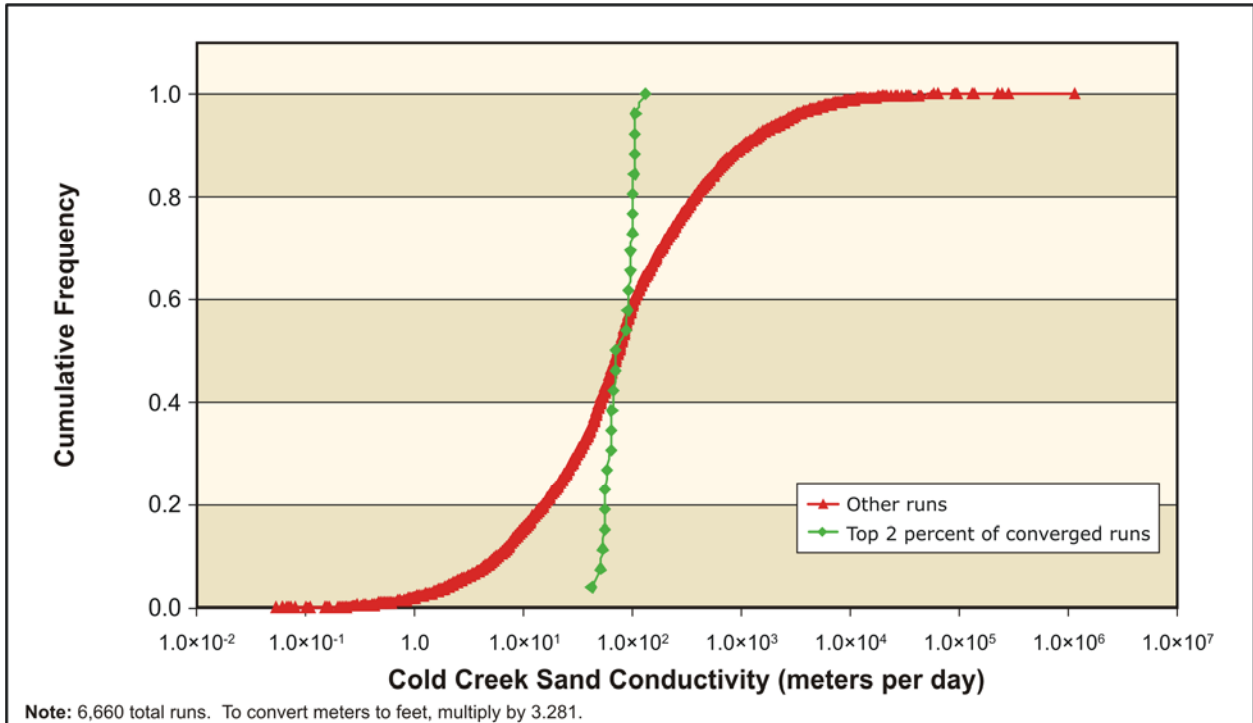


Figure L-23. Distribution of Hydraulic Conductivity Values – Cold Creek Sand

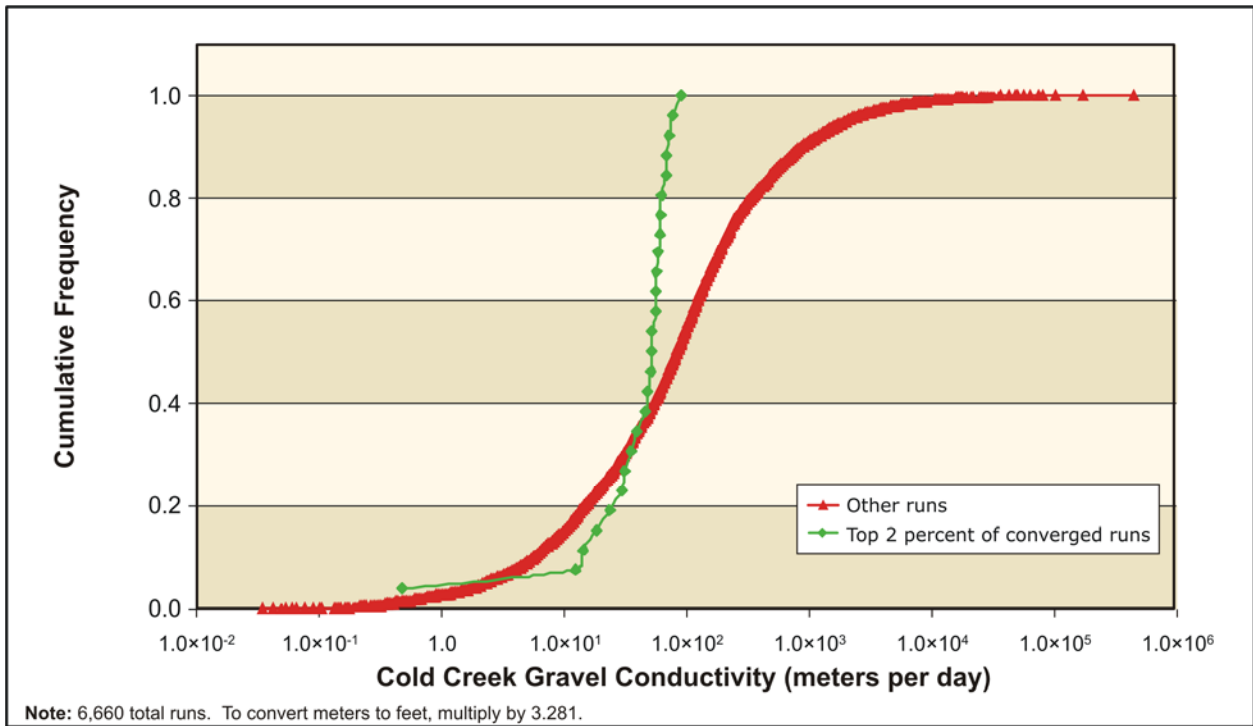


Figure L-24. Distribution of Hydraulic Conductivity Values – Cold Creek Gravel

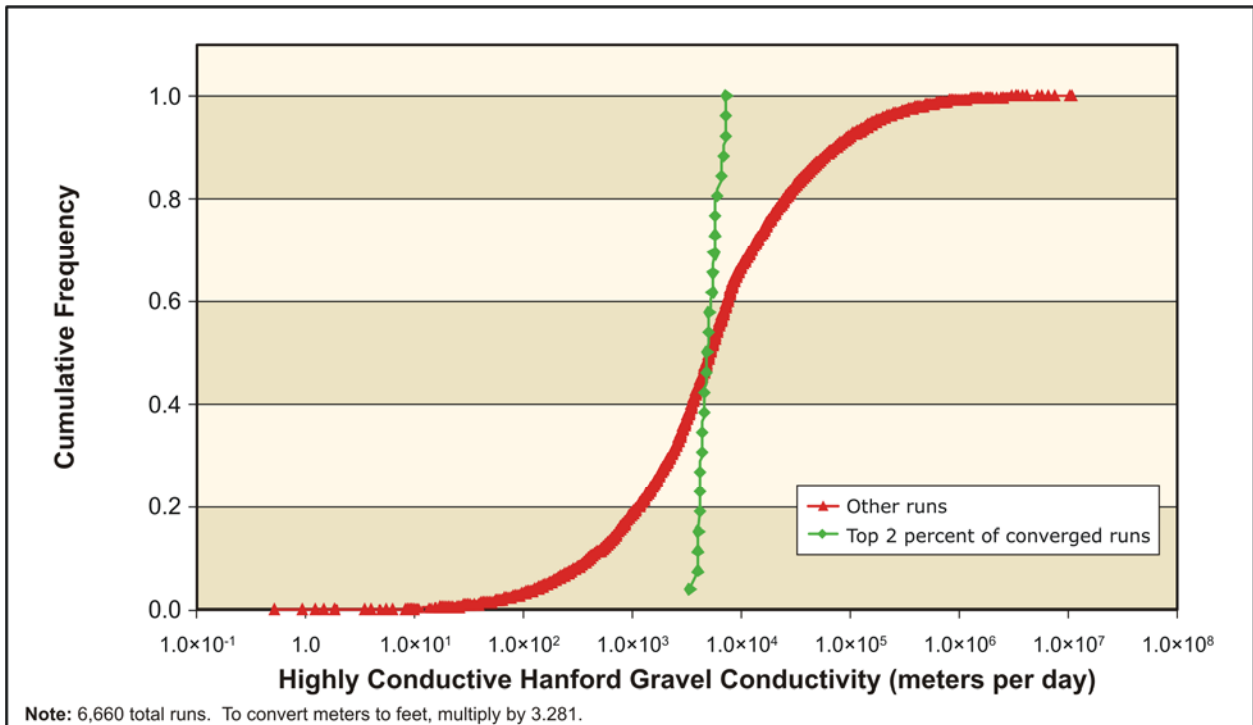


Figure L-25. Distribution of Hydraulic Conductivity Values – Highly Conductive Hanford Gravel

Table L–17 summarizes the results of the Base Case Monte Carlo Optimization and Uncertainty Analysis. For each of the three data sets, the thirteen hydrostratigraphic units are listed. For each unit, the range of hydraulic conductivity values found in the best realizations are listed. Note that the hydraulic conductivities found in the best realizations are similar to those found in the gradient-based search. However, the degree of sensitivity of the flow model to each parameter, and the range of acceptable values is much more reasonable from this analysis than from the gradient-based confidence intervals.

Table L–17. Summary of Base Case Monte Carlo Optimization and Uncertainty Analysis

Base Case Hydraulic Conductivity Distribution (meters per day)						
Material Type	Data Set 1		Data Set 2		Data Set 3	
	Minimum	Maximum	Minimum	Maximum	Minimum	Maximum
Hanford mud	5.4×10^{-3}	4.7×10^{-1}	5.4×10^{-3}	4.7×10^{-1}	2.0×10^{-2}	5.0×10^{-1}
Hanford silt	8.0×10^{-1}	6.1×10^1	5.0×10^{-1}	6.1×10^1	2.3	1.8×10^2
Hanford sand	4.2×10^1	1.7×10^2	3.7×10^1	1.8×10^2	3.1×10^1	1.6×10^2
Hanford gravel	1.3×10^2	2.2×10^2	1.3×10^2	2.1×10^2	1.5×10^2	2.4×10^2
Ringold Sand	4.9×10^{-1}	4.2	2.7×10^{-1}	4.2	2.4×10^{-1}	4.1
Ringold Gravel	1.3×10^1	1.9×10^1	1.2×10^1	1.7×10^1	1.3×10^1	1.7×10^1
Ringold Mud	2.1×10^{-1}	6.0	2.9×10^{-1}	6.0	2.7×10^{-1}	2.1
Ringold Silt	4.6×10^{-1}	3.4	4.6×10^{-1}	3.3	5.1×10^{-1}	2.0×10^1
Plio-Pleistocene sand	2.1	1.1×10^2	2.1	1.2×10^2	2.6×10^1	1.2×10^2
Plio-Pleistocene silt	3.8	4.5×10^2	1.8×10^{-1}	4.5×10^2	1.0×10^{-2}	3.0×10^1
Cold Creek sand	4.2×10^1	1.3×10^2	3.0×10^1	1.3×10^2	3.0×10^1	1.0×10^2
Cold Creek gravel	5.0×10^{-1}	9.3×10^1	4.0	1.2×10^2	2.0×10^1	1.2×10^2
Highly conductive Hanford gravel	3.3×10^3	7.2×10^3	3.8×10^3	7.9×10^3	4.5×10^3	4.8×10^3

Note: To convert meters to feet, multiply by 3.281.

Approximately 400 model runs were completed, targeting head observation data set 4 (the validation data set), and RMS error values were calculated. Results concluded that the hydraulic conductivity values producing the lowest RMS error using validation data set 4 reasonably correlate to the hydraulic conductivity values that produced the lowest RMS error using calibration data sets 1, 2, and 3.

L.9.3 Alternate Case – Results of the Analysis

The cumulative density of the objective function for each of the three data sets are shown in Figures L–26 through L–28. The x axis of each plot is the RMS difference between the field-measured and modeled water table elevations for all wells in the calibration data set for all measurement times. The y axis shows the fraction of realizations that were lower than or equal to the corresponding RMS value. Note that the three curves have reasonably similar sigmoidally shaped cumulative distributions that vary over a similar RMS range.

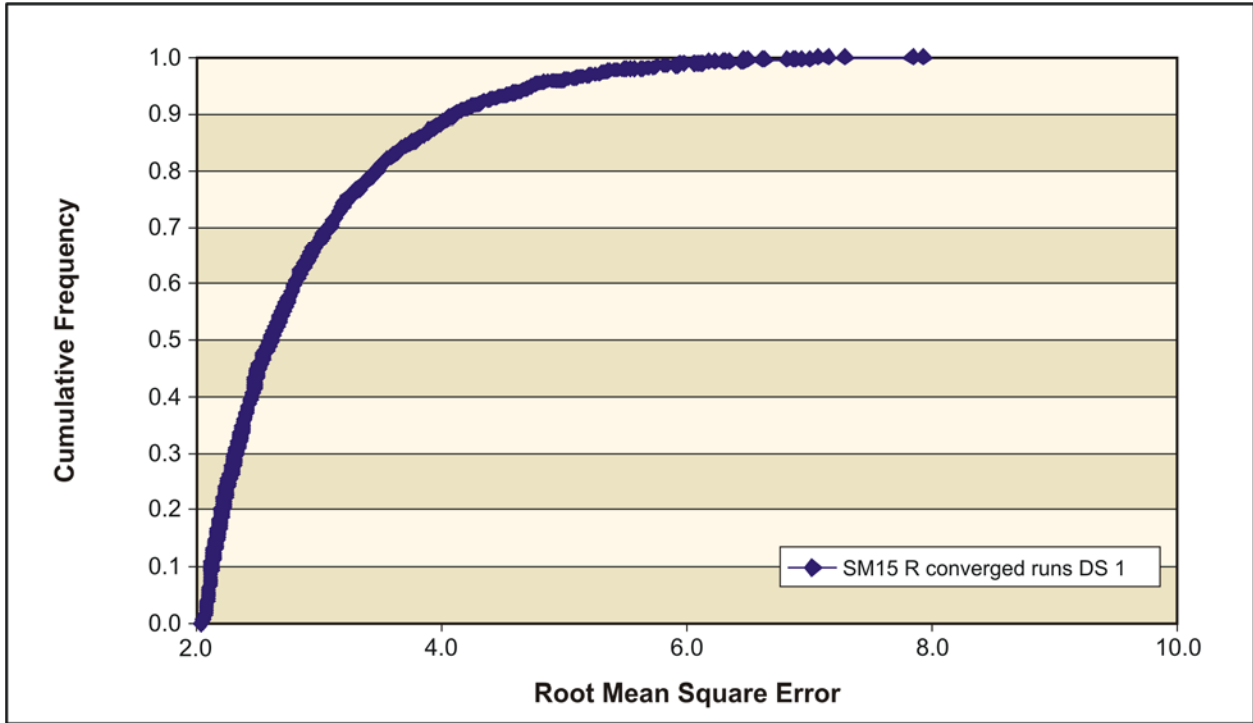


Figure L-26. Cumulative Density of the Objective Function – Alternate Case Model – Calibration Data Set 1

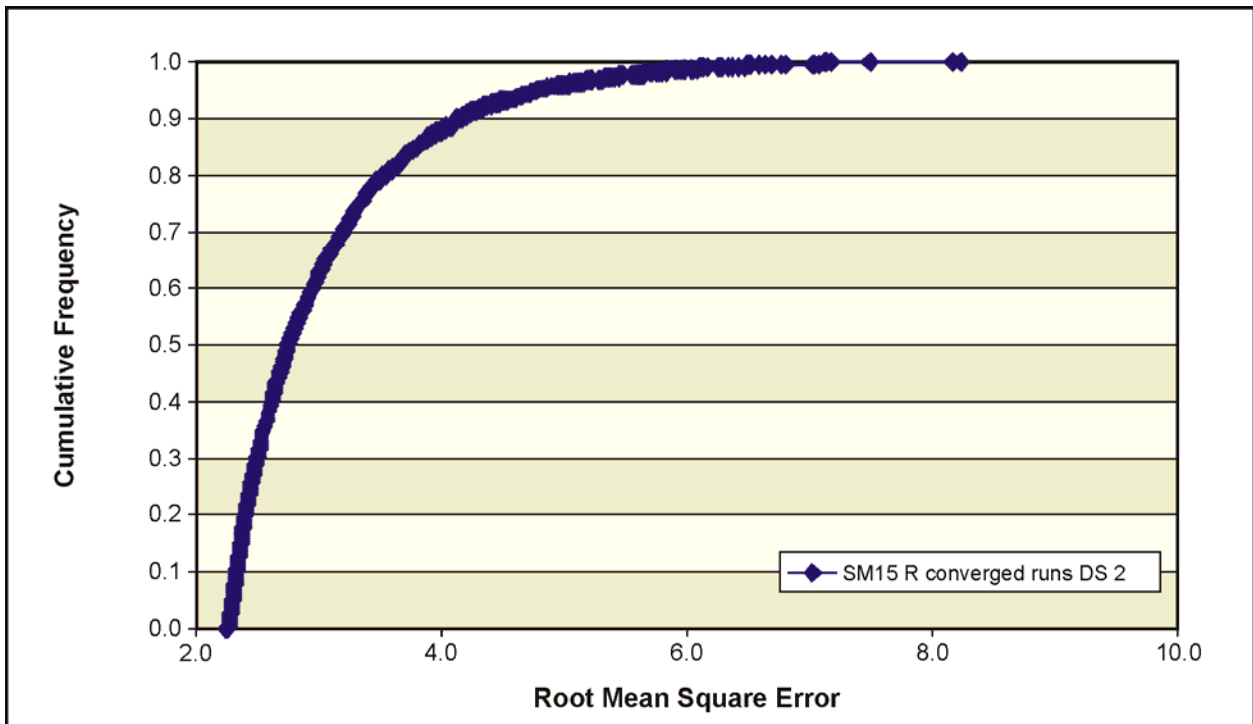


Figure L-27. Cumulative Density of the Objective Function – Alternate Case Model – Calibration Data Set 2

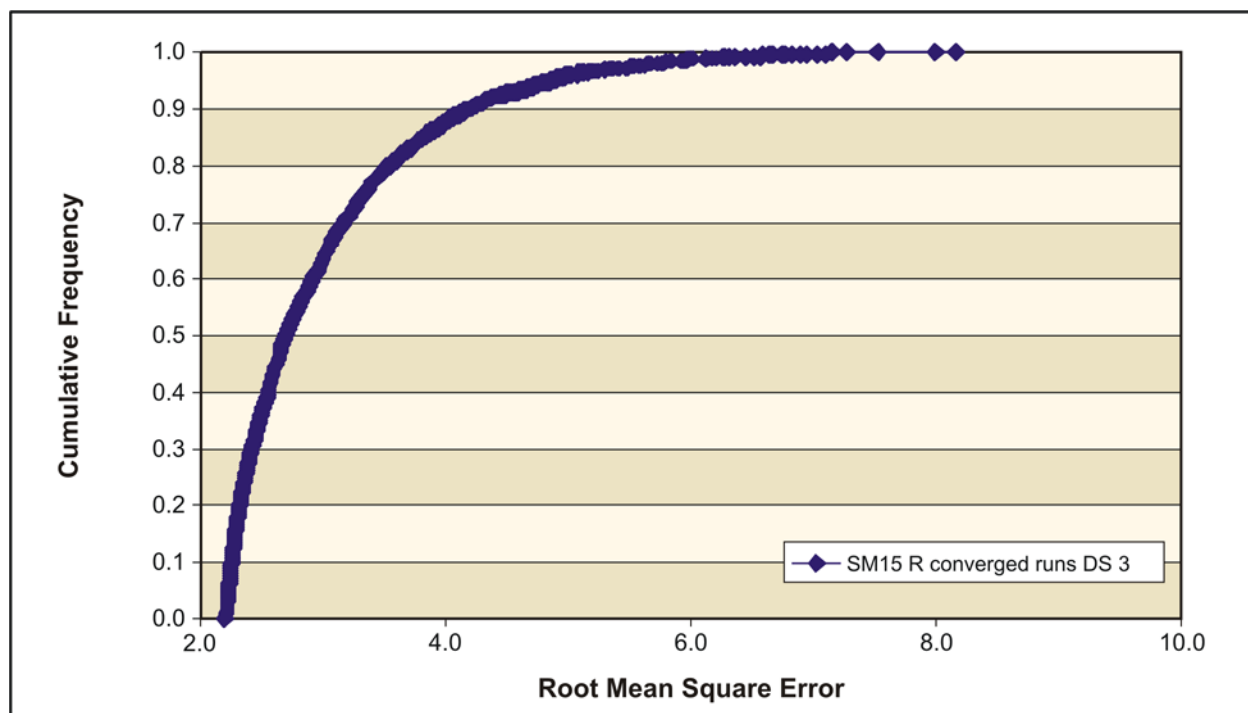


Figure L-28. Cumulative Density of the Objective Function – Alternate Case Model – Calibration Data Set 3

For each data set, the best realizations were chosen according to two criteria. The first criterion was that the RMS value for that realization was among the lowest (at least in the lowest 1 percent). The second criterion was that MODPATH particle tracks from sources in the 200-East Area showed reasonable qualitative agreement with the observed shape of the tritium plume originating near the PUREX plant in the 200-East Area. In fact, as the RMS value decreased, the qualitative agreement of the MODPATH particle tracks with the shape of the PUREX Plant plume became increasingly better. Section L.10.2.3.1 discusses the Alternate Case tritium plume delineations in more detail.

Finally, the distributions of the hydraulic conductivity values for the best realizations were compared to the distributions of the hydraulic conductivity values for all realizations. Figures L-29 through L-41 show these comparisons for the Alternate Case model, Calibration Data Set 1, for the 13 hydrostratigraphic units. (The comparisons for the other two calibration data sets are similar.) Each figure shows two cumulative densities. The x axis of each plot is the hydraulic conductivity (meters per day) for the hydrostratigraphic unit. The y axis shows the fraction of realizations that were lower than or equal to the corresponding hydraulic conductivity value. Two curves are plotted for each hydrostratigraphic unit. The curve plotted with the red symbols shows the cumulative distribution for all realizations. It is used to show the portion of parameter space that was searched. For example, for Hanford gravel (see Figure L-32), realizations were generated that covered the range of hydraulic conductivities from about 5 meters per day (16.4 feet per day) up to about 10,000 meters per day (32,810 feet per day), roughly a variation over three orders of magnitude. The curve plotted with the green symbols shows the portion of parameter space that was covered by the best set of realizations. For example, the best realizations for Hanford gravel were restricted to a relatively narrow range—from about 110 meters per day (361 feet per day) to about 175 meters per day (574 feet per day). The steepness of the green curve relative to the red curve shows the degree of sensitivity the groundwater flow model shows to a particular hydraulic conductivity. When the green curve is steep, as it is for Hanford gravel (see Figure L-32), Ringold Gravel (see Figure L-34), and Highly conductive Hanford gravel (see Figure L-41), the flow model is sensitive to those hydraulic conductivities, and the best RMS values can only be obtained across a narrow range of values. For the units where the green curve is not as steep

and covers more of the range represented by the red curve, the flow model is less sensitive to those parameters, and good agreement between measured and modeled water table elevations can be obtained over a much broader range of hydraulic conductivities. Note that there is no particular ordering or correspondence in terms of RMS on either the green or red curves. Realizations with low or high RMSs can (and are) plotted next to realizations with high or low RMSs. This analysis shows where (in hydraulic conductivity parameter space) the best realizations were found, but not that a particular hydraulic conductivity leads to a good result.

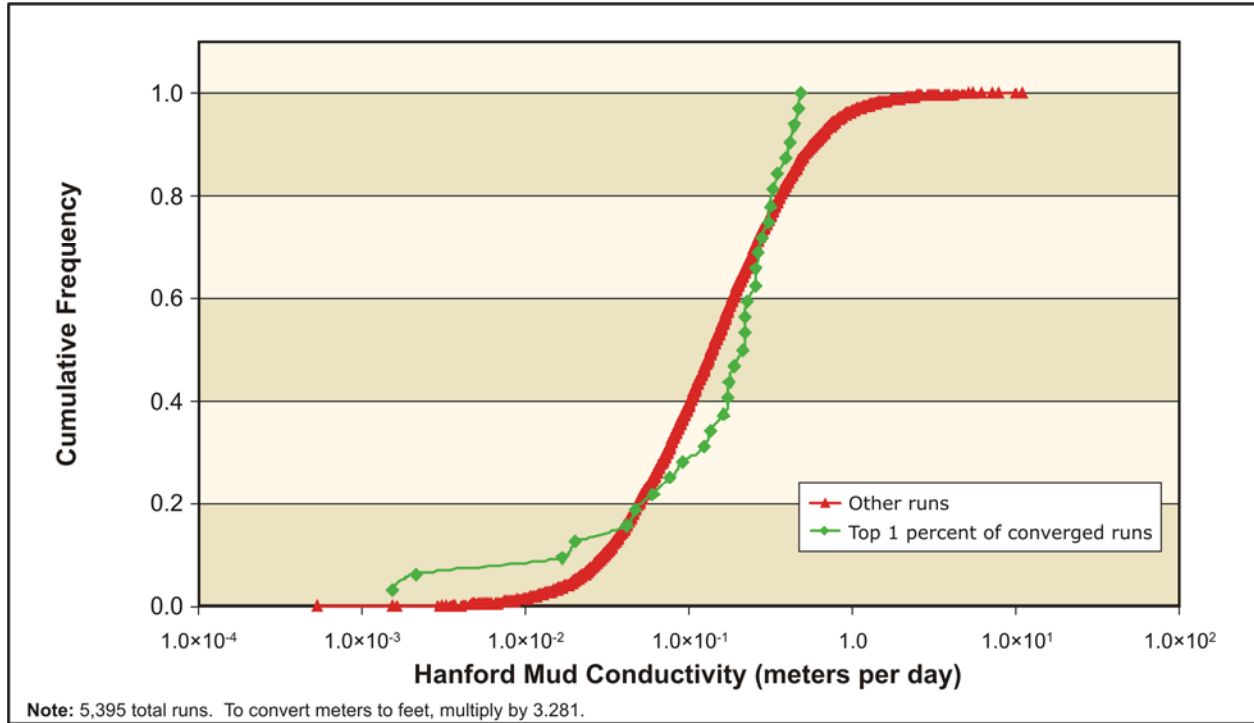


Figure L-29. Distribution of Hydraulic Conductivity Values – Hanford Mud

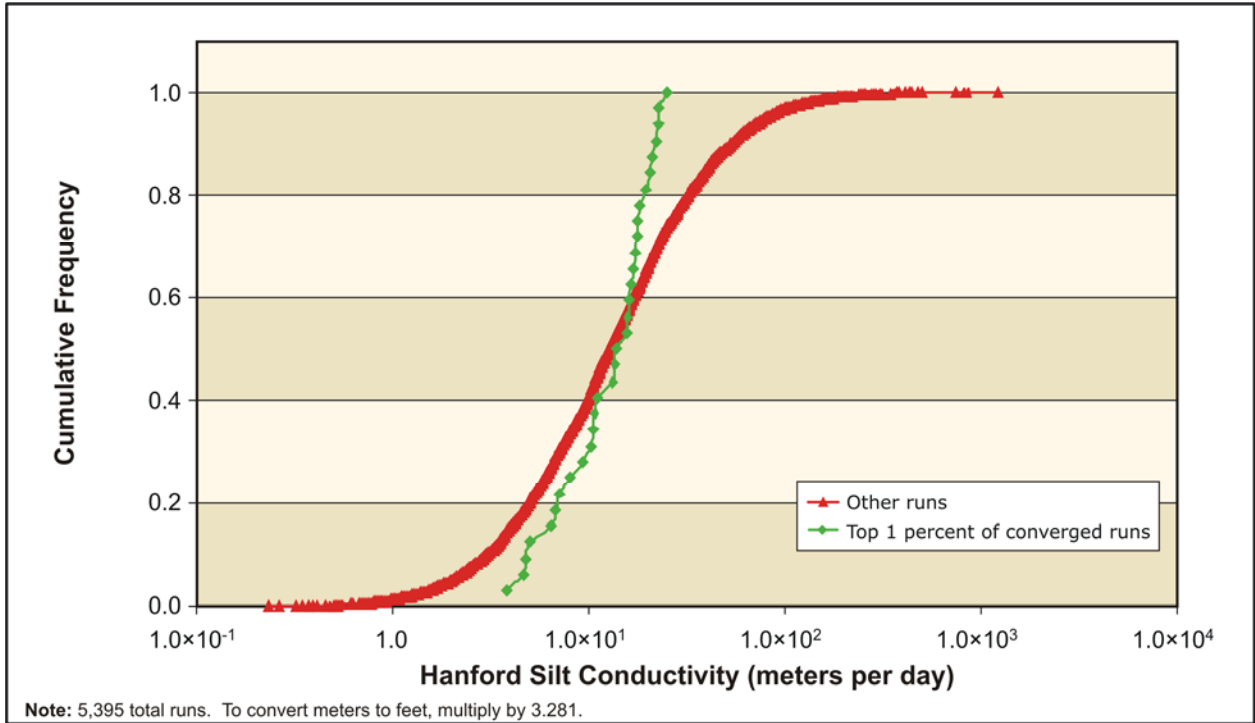


Figure L-30. Distribution of Hydraulic Conductivity Values – Hanford Silt

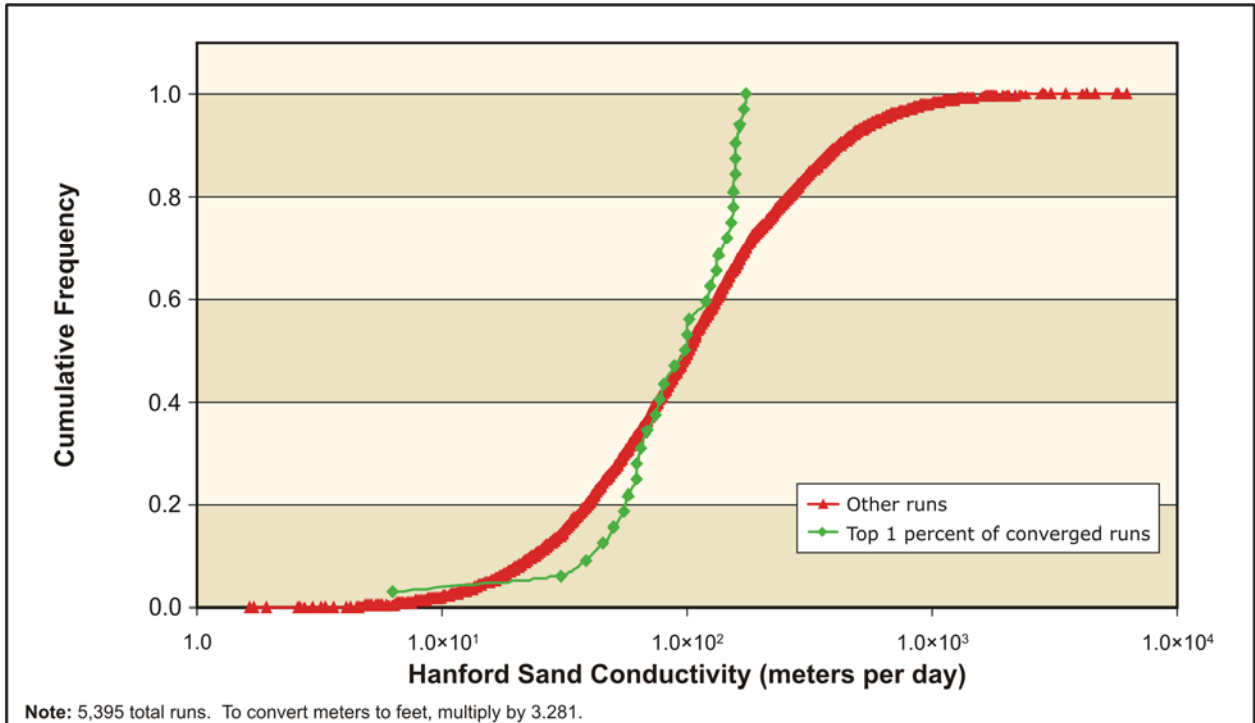


Figure L-31. Distribution of Hydraulic Conductivity Values – Hanford Sand

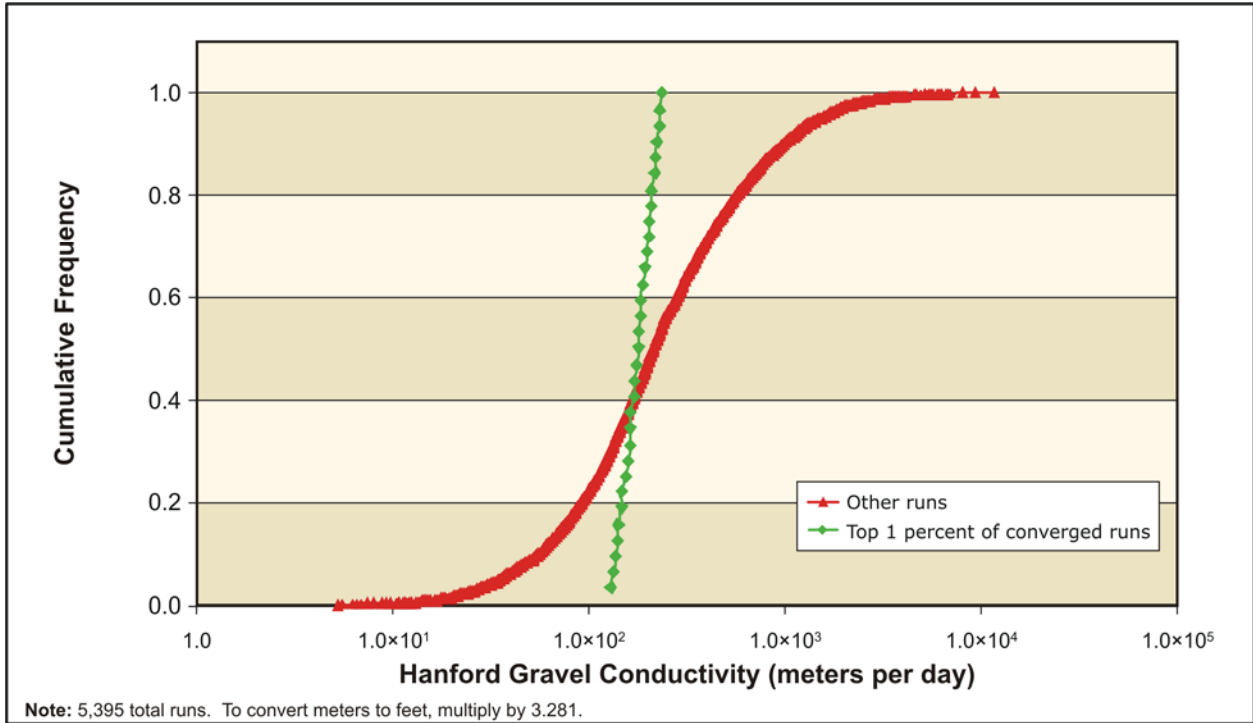


Figure L-32. Distribution of Hydraulic Conductivity Values – Hanford Gravel

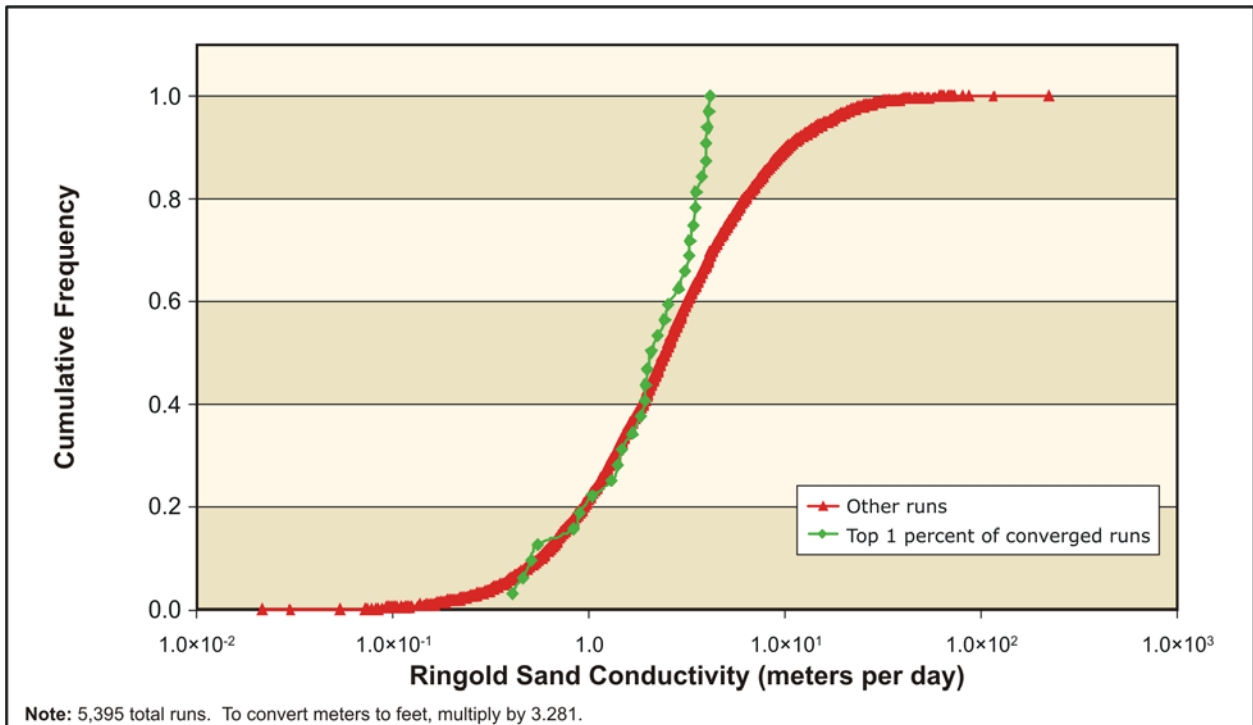


Figure L-33. Distribution of Hydraulic Conductivity Values – Ringold Sand

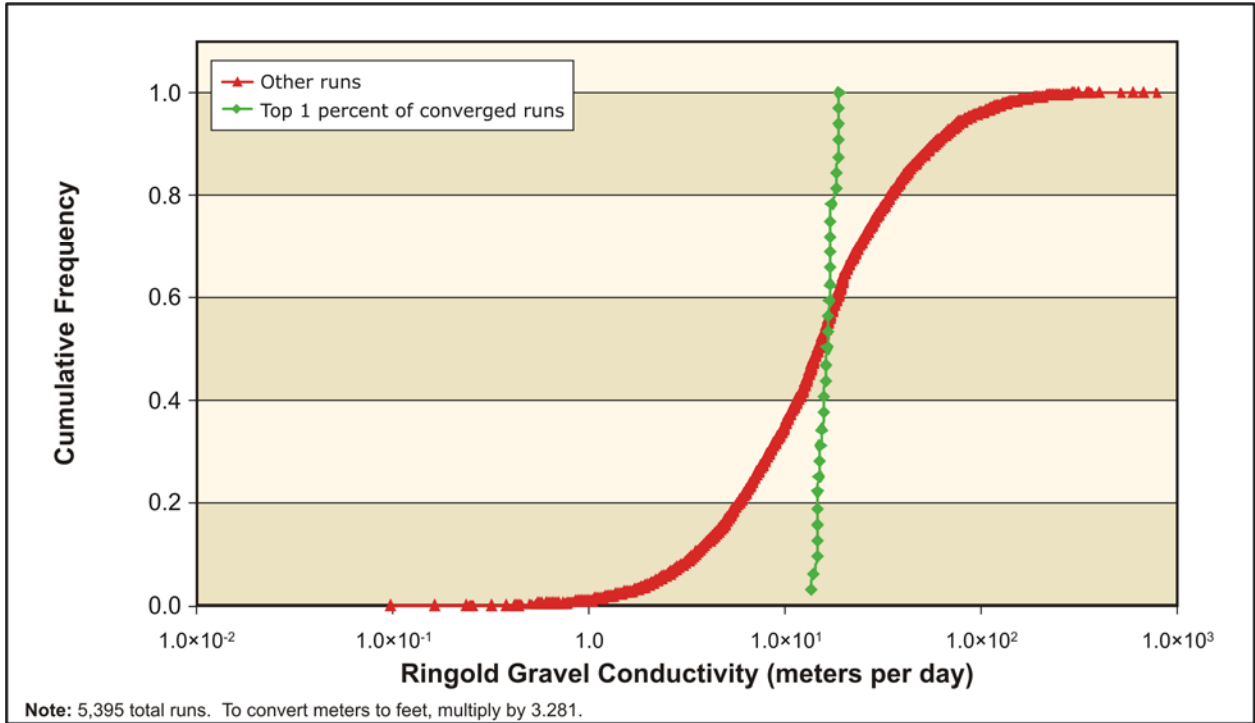


Figure L-34. Distribution of Hydraulic Conductivity Values – Ringold Gravel

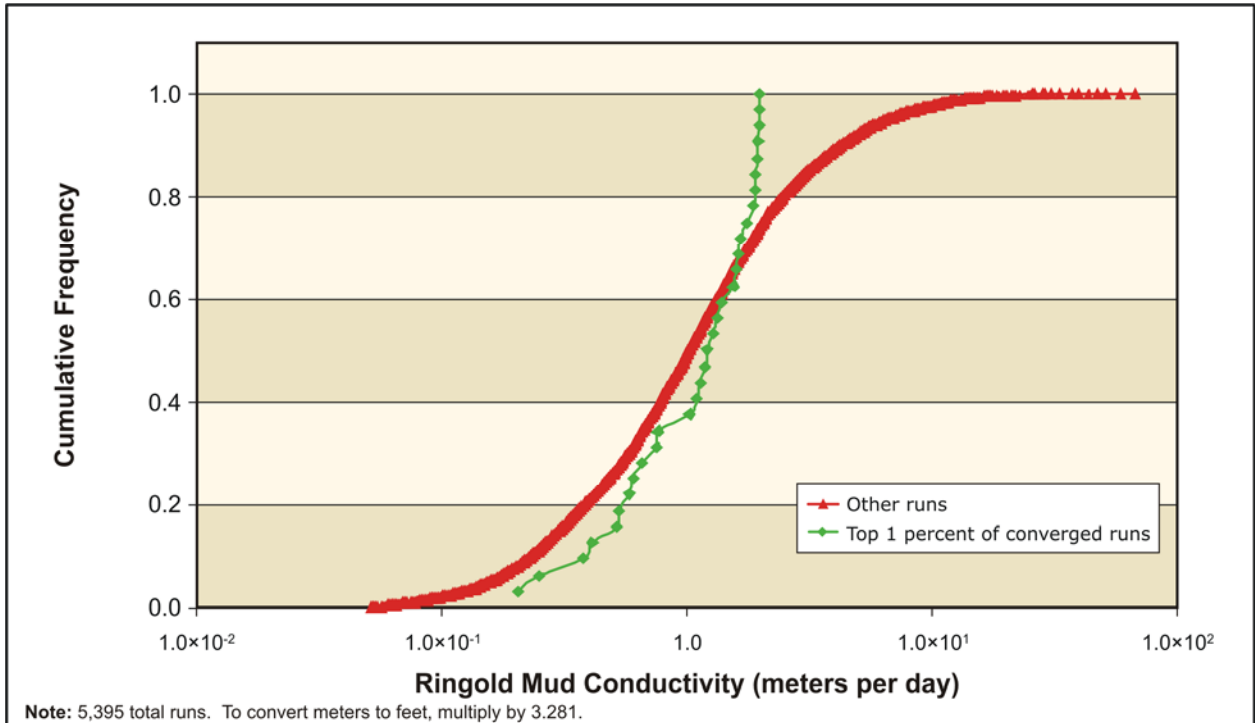


Figure L-35. Distribution of Hydraulic Conductivity Values – Ringold Mud

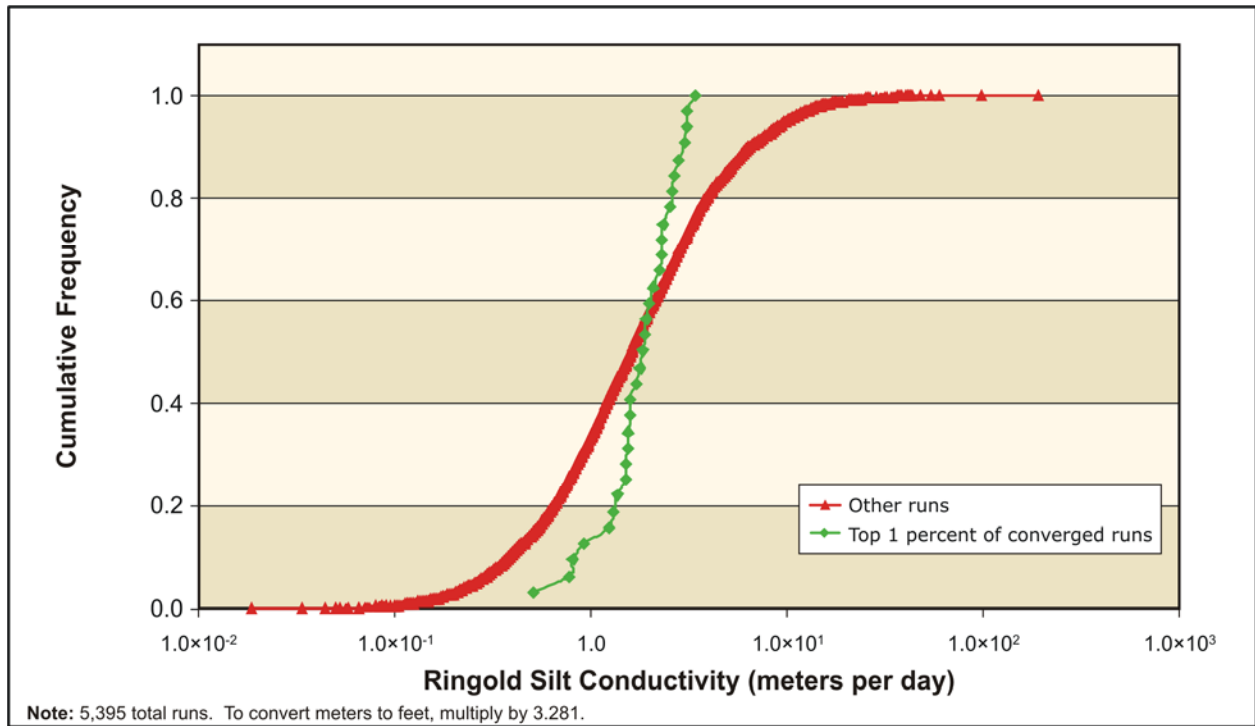


Figure L-36. Distribution of Hydraulic Conductivity Values – Ringold Silt

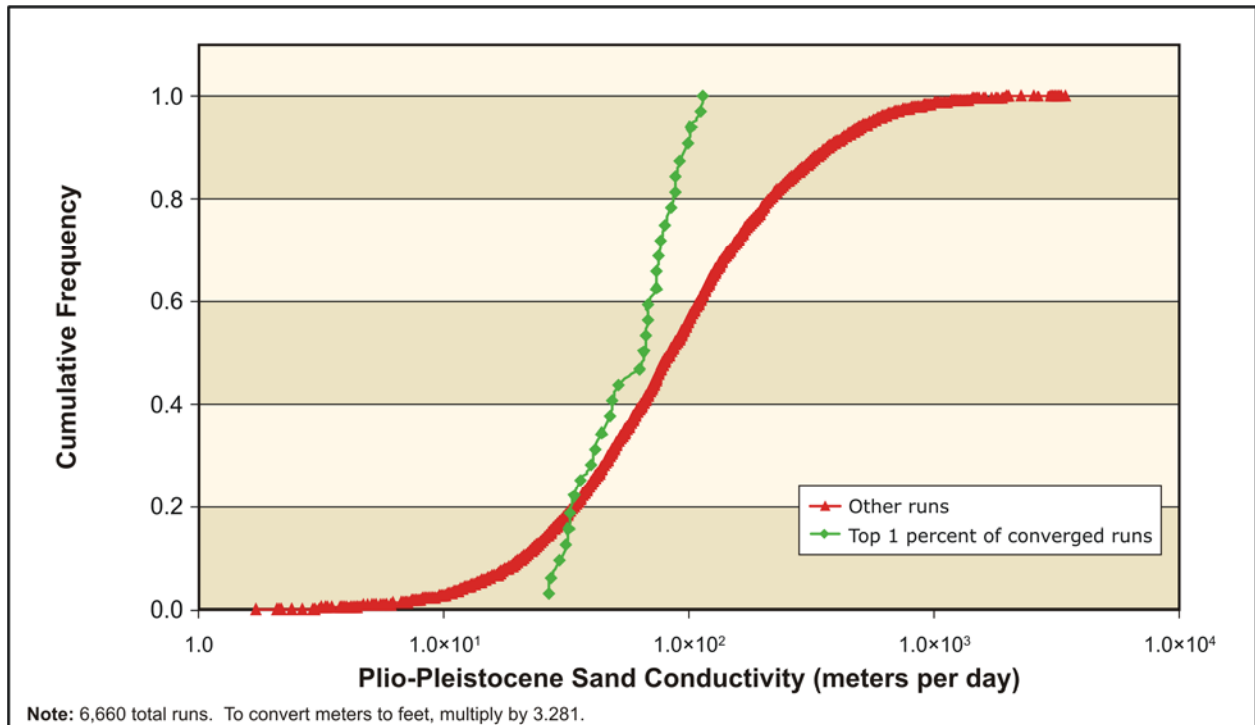


Figure L-37. Distribution of Hydraulic Conductivity Values – Plio-Pleistocene Sand

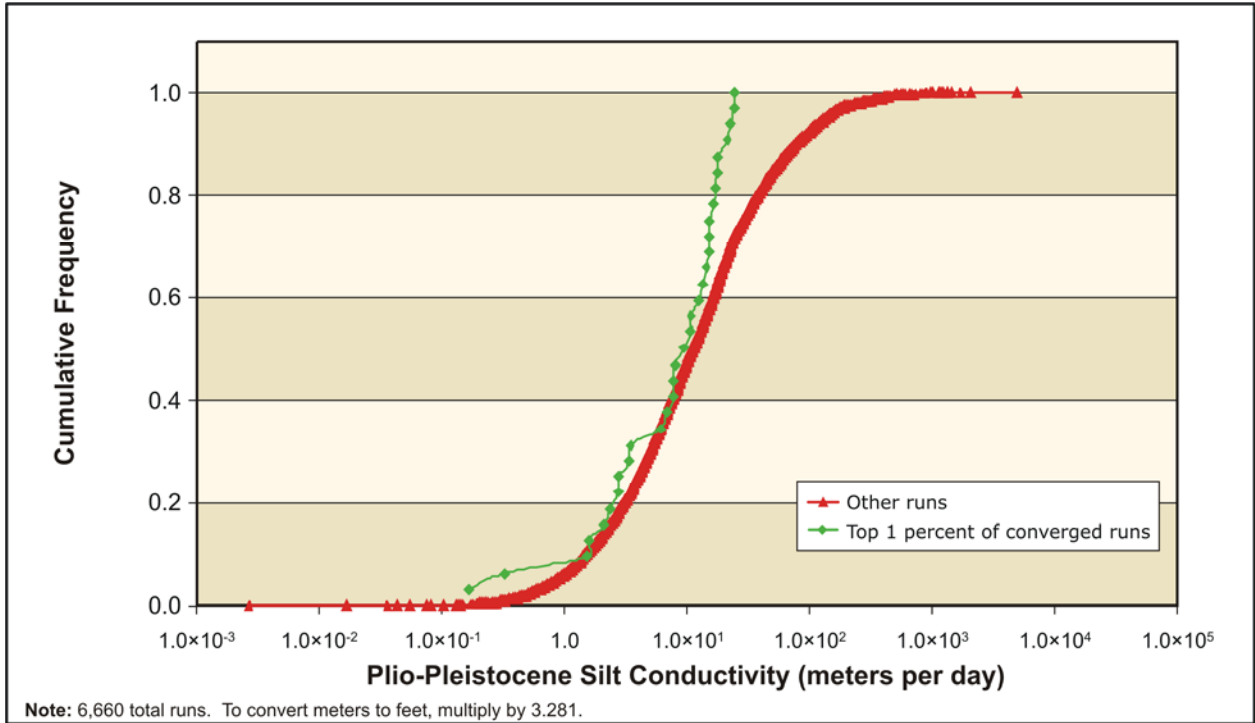


Figure L-38. Distribution of Hydraulic Conductivity Values – Plio-Pleistocene Silt

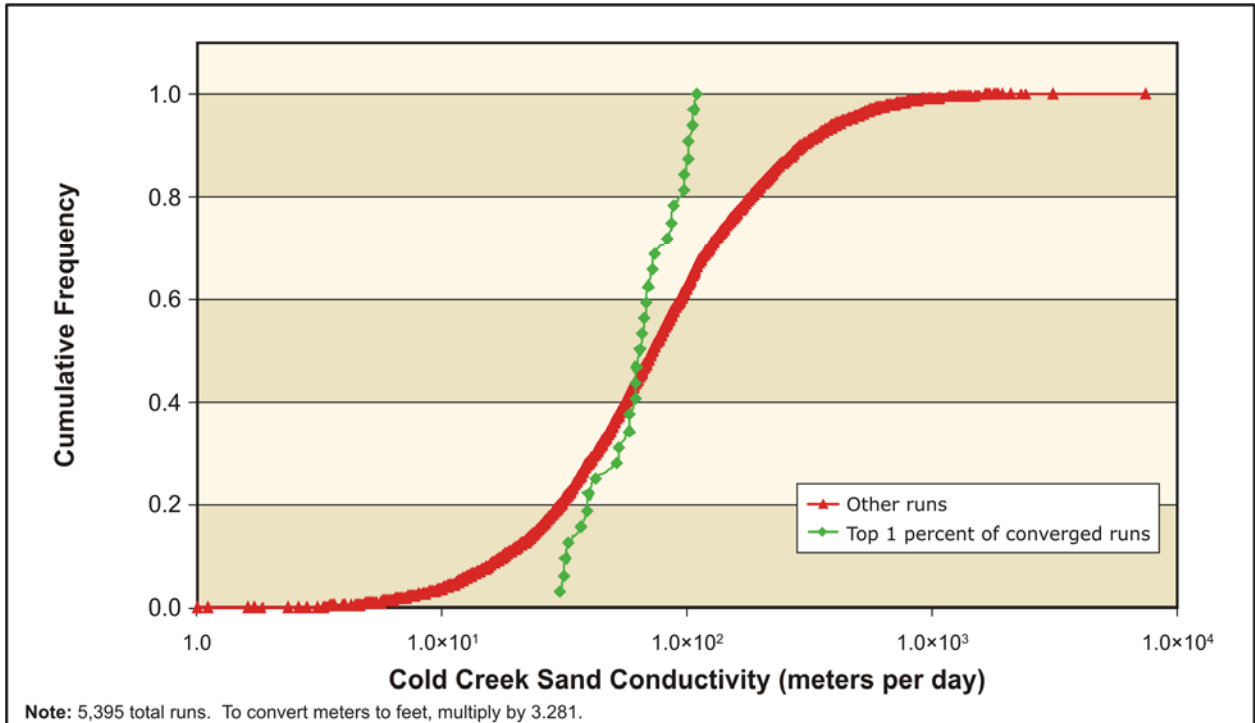


Figure L-39. Distribution of Hydraulic Conductivity Values – Cold Creek Sand

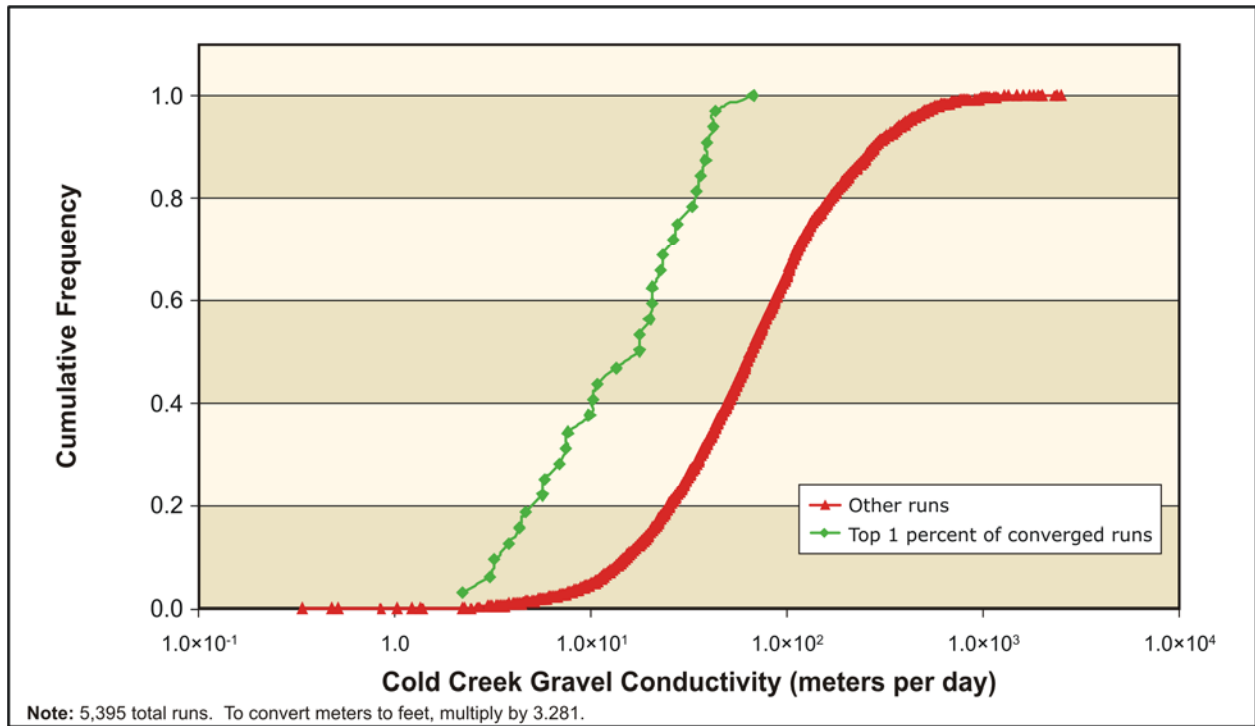


Figure L-40. Distribution of Hydraulic Conductivity Values – Cold Creek Gravel

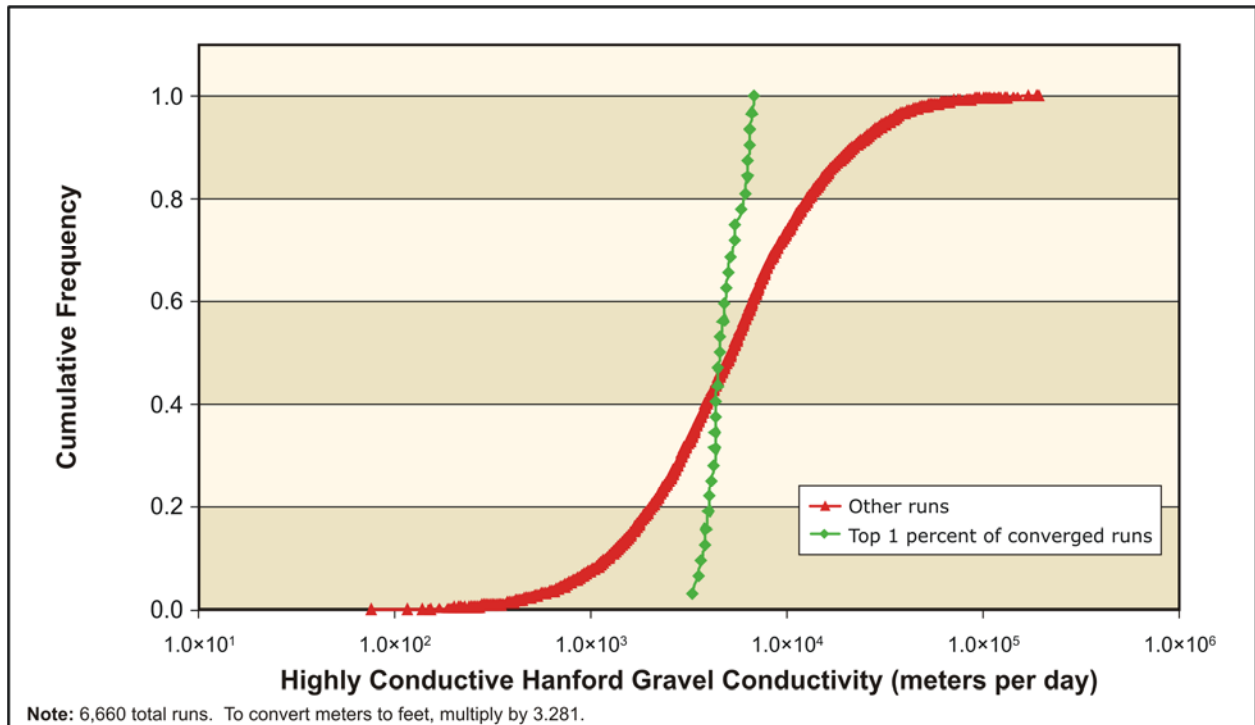


Figure L-41. Distribution of Hydraulic Conductivity Values – Highly Conductive Hanford Gravel

Table L–18 summarizes the results of the Alternate Case Monte Carlo optimization and uncertainty analysis. For each of the three data sets, the 13 hydrostratigraphic units is listed. For each unit, the range of hydraulic conductivity values found in the best realizations is listed. Note that the hydraulic conductivities found in the best realizations are not all that different than those found in the gradient-based search. However, this analysis yields a much more reasonable degree of sensitivity of the groundwater flow model to each parameter and range of acceptable values than the gradient-based confidence intervals.

Table L–18. Summary of Alternate Case Monte Carlo Optimization and Uncertainty Analysis

Alternate Case Hydraulic Conductivity Distribution (meters per day)						
Material Type	Data Set 1		Data Set 2		Data Set 3	
	Minimum	Maximum	Minimum	Maximum	Minimum	Maximum
Hanford mud	2×10^{-3}	4.8×10^{-1}	8.4×10^{-3}	5×10^{-1}	1.4×10^{-2}	4.9×10^{-1}
Hanford silt	3.8	2.5×10^1	8.5×10^{-1}	3.5×10^2	8.0×10^{-1}	2.3×10^1
Hanford sand	6.2	1.7×10^2	3.7×10^1	2.1×10^2	3.1×10^1	1.6×10^2
Hanford gravel	1.3×10^2	2.3×10^2	1.4×10^2	2.3×10^2	1.5×10^2	2.4×10^2
Ringold Sand	4×10^{-1}	4.2	3.4×10^{-1}	1.1×10^1	2×10^{-1}	4.2
Ringold Gravel	1.3×10^1	1.9×10^1	9.7	1.7×10^1	1.3×10^1	1.6×10^1
Ringold Mud	2×10^{-1}	2	2.8×10^{-1}	9.5	3.9×10^{-1}	2.5
Ringold Silt	5×10^{-1}	3.4	2.9×10^{-1}	3.7	5.1×10^{-1}	3.3
Plio-Pleistocene sand	2.7×10^1	1.1×10^2	2.2×10^1	3.4×10^2	2.1×10^1	1.9×10^2
Plio-Pleistocene silt	4.6×10^{-1}	2×10^1	2.3×10^{-1}	1.1×10^2	3.1×10^{-1}	2×10^1
Cold Creek sand	3×10^1	1.1×10^2	4×10^1	5.6×10^2	3.8×10^1	5.6×10^2
Cold Creek gravel	2.2	6.7×10^1	5×10^{-1}	9.1×10^1	3×10^{-1}	1.1×10^2
Highly conductive Hanford gravel	3.3×10^3	6.7×10^3	3.7×10^3	7.4×10^3	4.1×10^3	7.9×10^3

Note: To convert meters to feet, multiply by 3.281.

Approximately 400 model runs were completed, targeting head observation data set 4 (the validation data set), and RMS error values were calculated. Results concluded that the hydraulic conductivity values producing the lowest RMS error using validation data set 4 reasonably correlate to the hydraulic conductivity values that produced the lowest RMS error using calibration data sets 1, 2, and 3.

L.10 RESULTS FOR DESIGN VARIANTS

L.10.1 Base Case

The Monte Carlo optimization described in Section L.9 focused on identifying sets of hydraulic conductivity values that result in model-simulated head values that reasonably match observed heads over time and across the model domain. For the Base Case flow model, the Monte Carlo optimization identified 26 model runs, each with different sets of hydraulic conductivity values, where model simulations of head values reasonably match observed heads. These 26 model runs were evaluated further to determine which one best met the following additional selection criteria:

- The majority of the particles released to the water table within the Core Zone Boundary (200 Area Central Plateau of Hanford) move to the east toward the Columbia River rather than to the north through Gable Gap.

- Particles released to the water table in the 200 Areas (representing a historical tritium release) result in particle pathlines that qualitatively match the observed 200-East and 200-West Area tritium plumes, without considering the effects of dispersion.

After this additional evaluation, the Base Case flow model was selected. The selected model must meet the calibration acceptance criteria described in Section L.6.2. Table L–19 summarizes the calibration acceptance criteria along with the Base Case flow model’s performance for each criterion. Table L–20 lists calibrated hydraulic conductivity values for the Base Case flow model by material type. Table L–21 provides the hydraulic conductivity parameter correlation coefficient matrix for the Base Case flow model.

Table L–19. Summary of Base Case Flow Model Performance Compared to Calibration Acceptance Criteria

Flow Model Calibration Acceptance Criteria	Base Case Flow Model Performance
Residual distribution should be reasonably normal.	Residual distribution is reasonably normal (see Figure L–42).
The mean residual should be approximately 0.	Residual Mean = -0.164 meters (-0.538 feet).
The number of positive residuals should approximate the number of negative residuals.	Positive residuals approximately equal negative residuals (see Figure L–42).
The correlation coefficient (calculated versus observed) should be greater than 0.9.	Correlation coefficient = 0.979 (see Figure L–43).
The root mean square (RMS) error (calculated versus observed) should be less than 5 meters (16.4 feet), approximately 10 percent of the gradient in the water table elevation.	RMS error = 2.118 meters (6.948 feet) (see Figure L–43).
Residuals in the 200-East Area should be distributed similarly to those in the 200-West Area.	Residuals in the 200-East and 200-West Areas are distributed similarly (see Figures L–44 and L–45).
The residuals should be evenly distributed over time.	Residuals are approximately evenly distributed over time (see Figures L–46, L–47, L–48, and L–49).
The residuals should be evenly distributed across the site.	Residuals are approximately evenly distributed across the site (see Figures L–50, L–51, and L–52).
The calibrated parameters should compare reasonably well with field-measured values.	Calibrated hydraulic conductivity values are listed in Table L–20 and compare reasonably with field-measured values for material types to which the model is sensitive (i.e., Hanford formation and Ringold Formation material types). Figure L–53 provides field-measured values from aquifer pumping tests (Cole et al. 2001).
Parameters should be reasonably uncorrelated.	Hydraulic conductivity parameters are reasonably uncorrelated (see Table L–20 for the key to model material type zones and Table L–21 for the correlation coefficient matrix).

Table L–20. Base Case Flow Model Calibrated Hydraulic Conductivity Values

Material Type (Model Zone)	Hydraulic Conductivity (K _x) ^a	Hydraulic Conductivity (K _y) ^b	Hydraulic Conductivity (K _z) ^c
Hanford mud (1)	0.171	0.171	0.0171
Hanford silt (2)	6.8	6.8	0.68
Hanford sand (3)	123.6	123.6	12.36
Hanford gravel (4)	156.0	156.0	15.6
Ringold Sand (5)	3.57	3.57	0.357
Ringold Gravel (6)	19.2	19.2	1.92
Ringold Mud (7)	1.514	1.514	0.1514
Ringold Silt (8)	1.51	1.51	0.151
Plio-Pleistocene sand (9)	96.8	96.8	9.68
Plio-Pleistocene silt (10)	5.81	5.81	0.581
Cold Creek sand (11)	99.13	99.13	9.913
Cold Creek gravel (12)	62.7	62.7	6.27
Highly conductive Hanford gravel (13)	3982.0	3982.0	398.2
Activated basalt (14)	0.001	0.001	0.0001

^a Hydraulic conductivity with respect to the *x* axis, meters per day.

^b Hydraulic conductivity with respect to the *y* axis, meters per day.

^c Hydraulic conductivity with respect to the *z* axis, meters per day.

Note: To convert meters to feet, multiply by 3.281.

Table L–21. Base Case Hydraulic Conductivity Parameter Correlation Coefficient Matrix

Model Zone	1	2	3	4	5	6	7	8	9	10	11	12	13
1	1.00	-0.14	0.00	0.01	-0.04	-0.09	0.12	-0.08	-0.07	0.00	0.13	-0.14	0.07
2	-0.14	1.00	-0.11	-0.20	0.12	-0.05	-0.18	0.04	0.88	-0.06	-0.10	-0.09	-0.12
3	0.00	-0.11	1.00	0.08	0.08	0.15	0.02	-0.09	-0.04	-0.03	0.04	-0.11	-0.02
4	0.01	-0.20	0.08	1.00	0.05	-0.39	0.11	0.04	-0.17	-0.12	0.04	-0.09	0.24
5	-0.04	0.12	0.08	0.05	1.00	-0.22	0.07	-0.07	0.09	-0.12	-0.28	-0.13	-0.12
6	-0.09	-0.05	0.15	-0.39	-0.22	1.00	-0.35	-0.15	0.03	0.06	0.14	-0.03	-0.15
7	0.12	-0.18	0.02	0.11	0.07	-0.35	1.00	0.03	-0.11	-0.10	-0.01	-0.02	0.01
8	-0.08	0.04	-0.09	0.04	-0.07	-0.15	0.03	1.00	-0.06	-0.04	0.46	-0.13	0.06
9	-0.07	0.88	-0.04	-0.17	0.09	0.03	-0.11	-0.06	1.00	0.00	-0.07	-0.08	-0.12
10	0.00	-0.06	-0.03	-0.12	-0.12	0.06	-0.10	-0.04	0.00	1.00	0.09	-0.04	0.13
11	0.13	-0.10	0.04	0.04	-0.28	0.14	-0.01	0.46	-0.07	0.09	1.00	-0.22	0.30
12	-0.14	-0.09	-0.11	-0.09	-0.13	-0.03	-0.02	-0.13	-0.08	-0.04	-0.22	1.00	-0.27
13	0.07	-0.12	-0.02	0.24	-0.12	-0.15	0.01	0.06	-0.12	0.13	0.30	-0.27	1.00

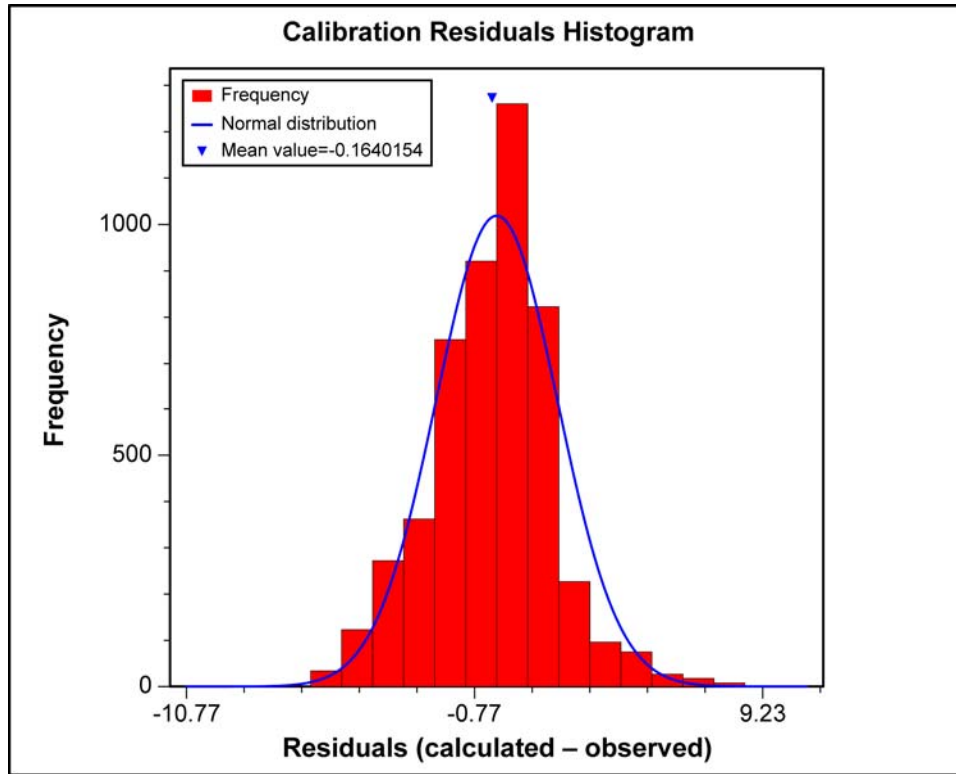


Figure L-42. Base Case Flow Model Residual Distribution

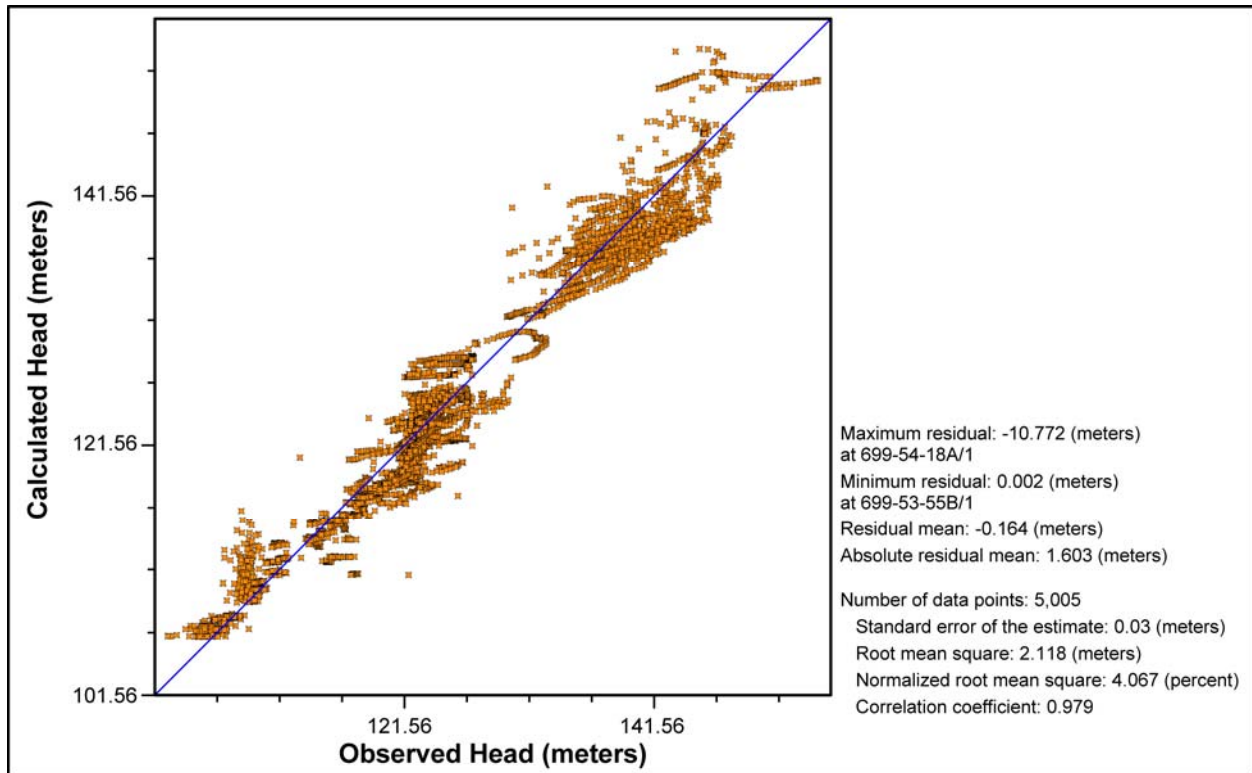


Figure L-43. Base Case Flow Model Calibration Graph and Statistics

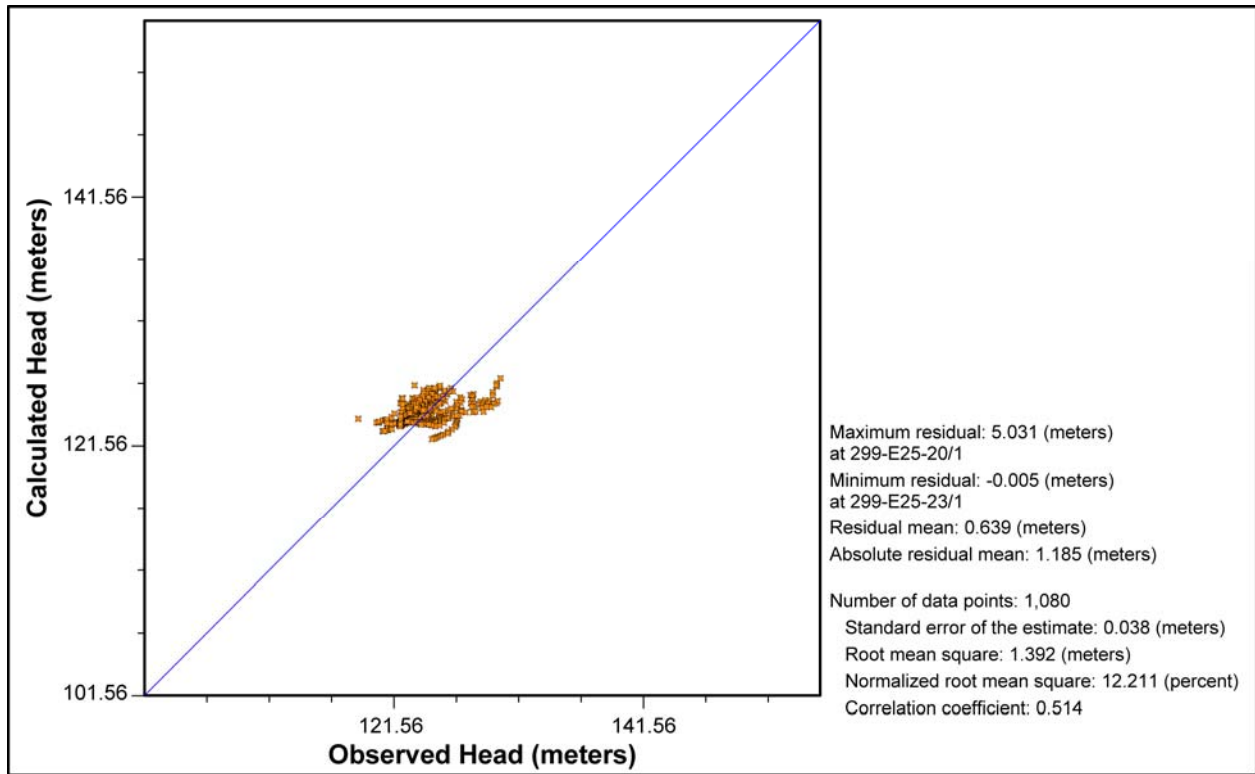


Figure L-44. Base Case Flow Model Residuals – 200-East Area

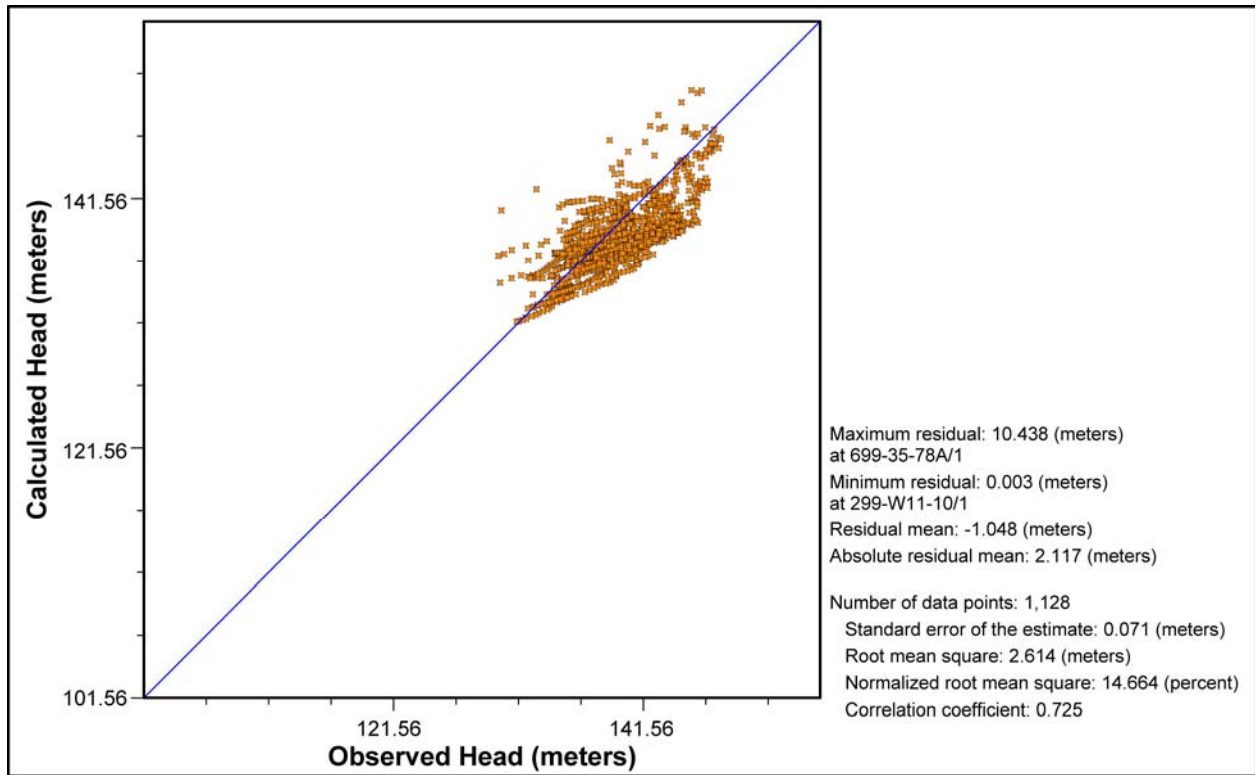


Figure L-45. Base Case Flow Model Residuals – 200-West Area

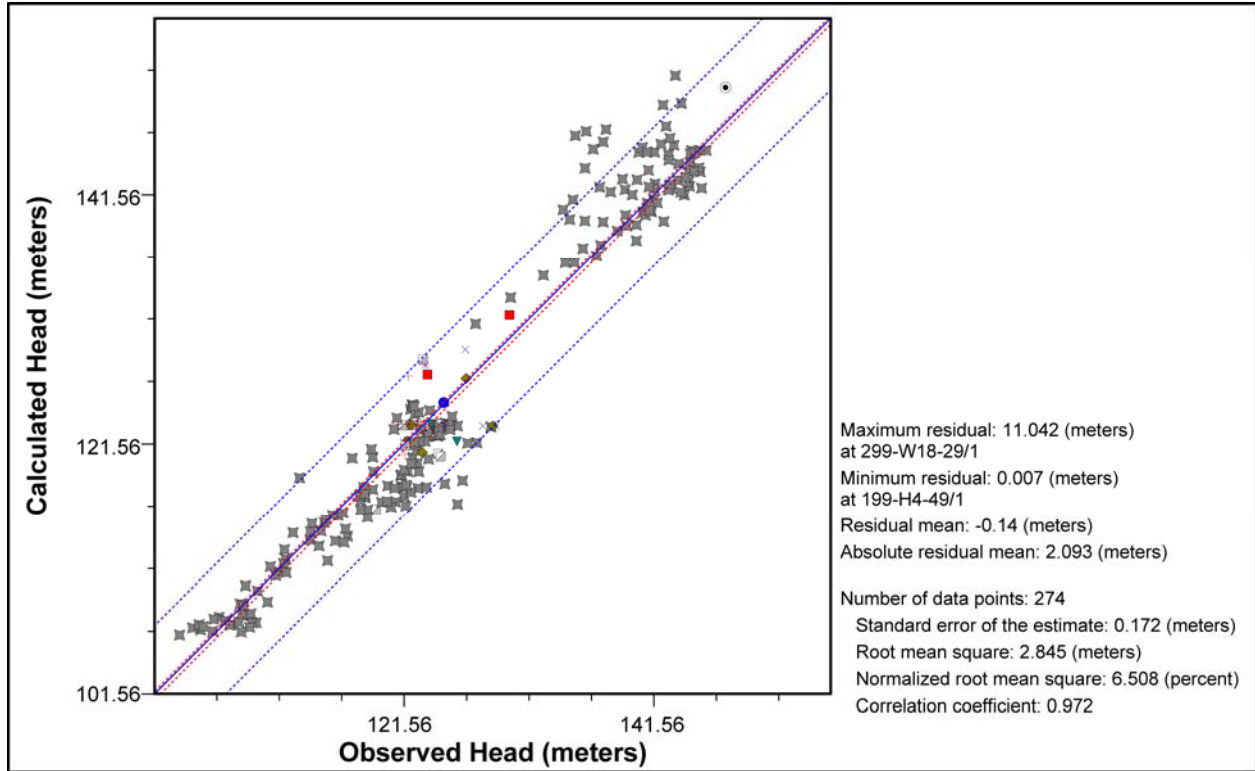


Figure L-46. Base Case Flow Model Residuals – Calendar Year 1955

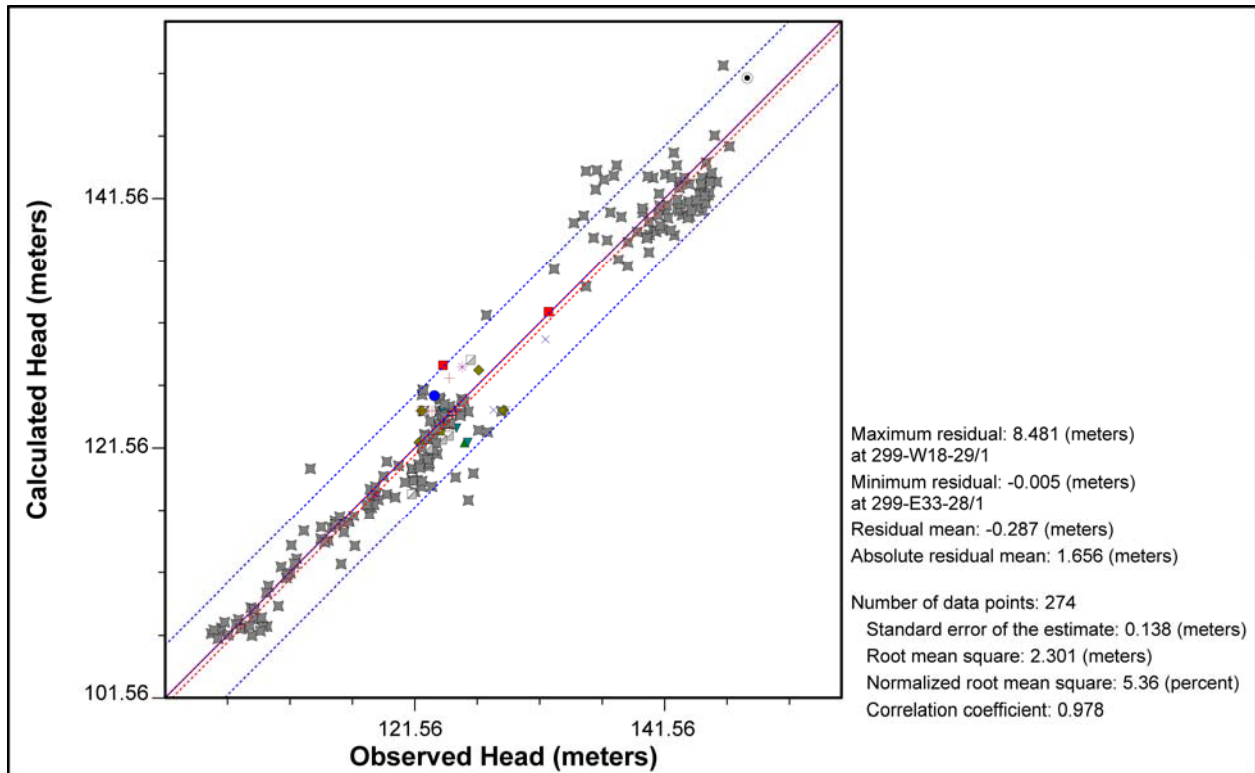


Figure L-47. Base Case Flow Model Residuals – Calendar Year 1975

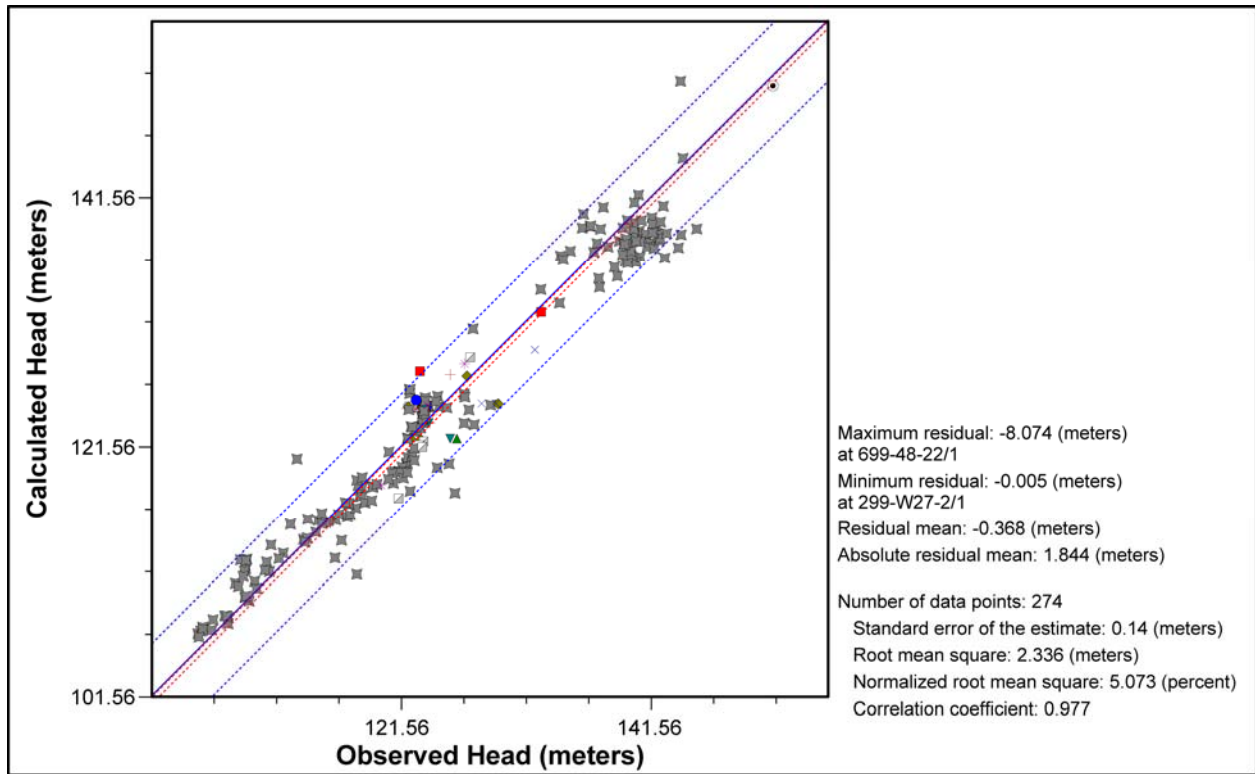


Figure L-48. Base Case Flow Model Residuals – Calendar Year 1995

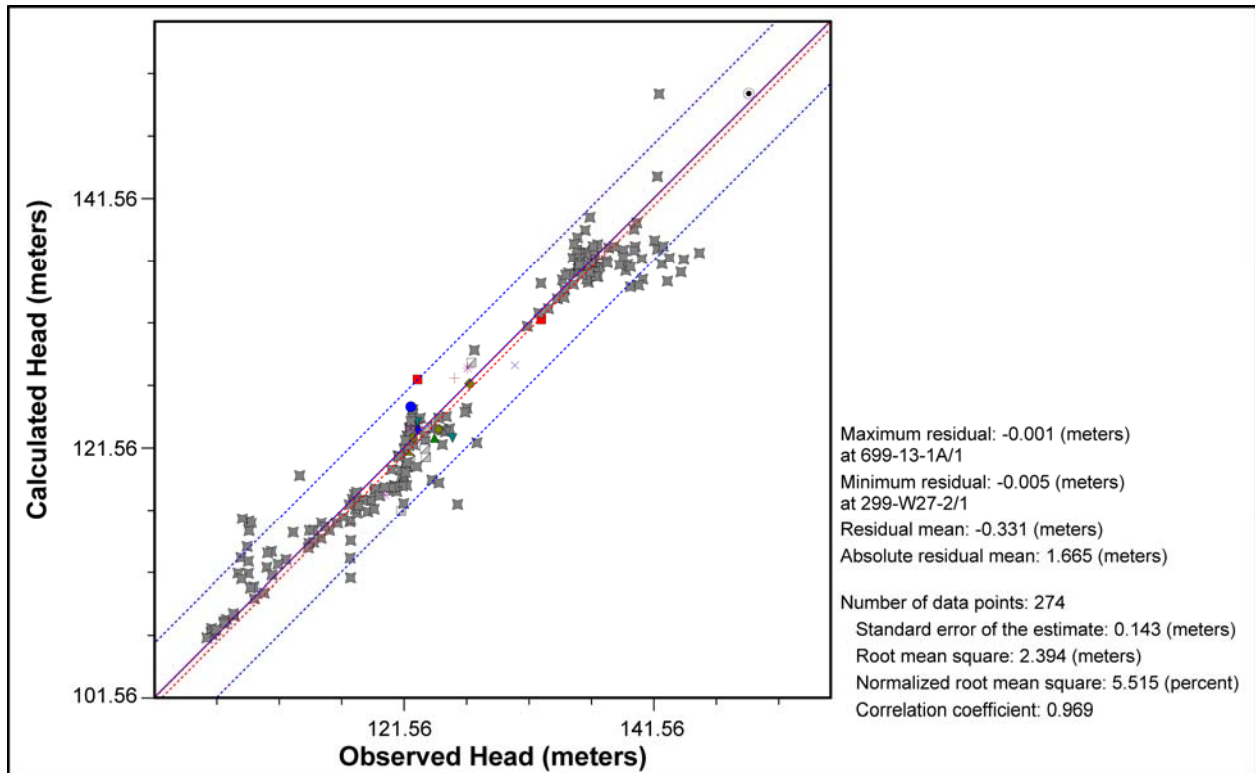


Figure L-49. Base Case Flow Model Residuals – Calendar Year 2015

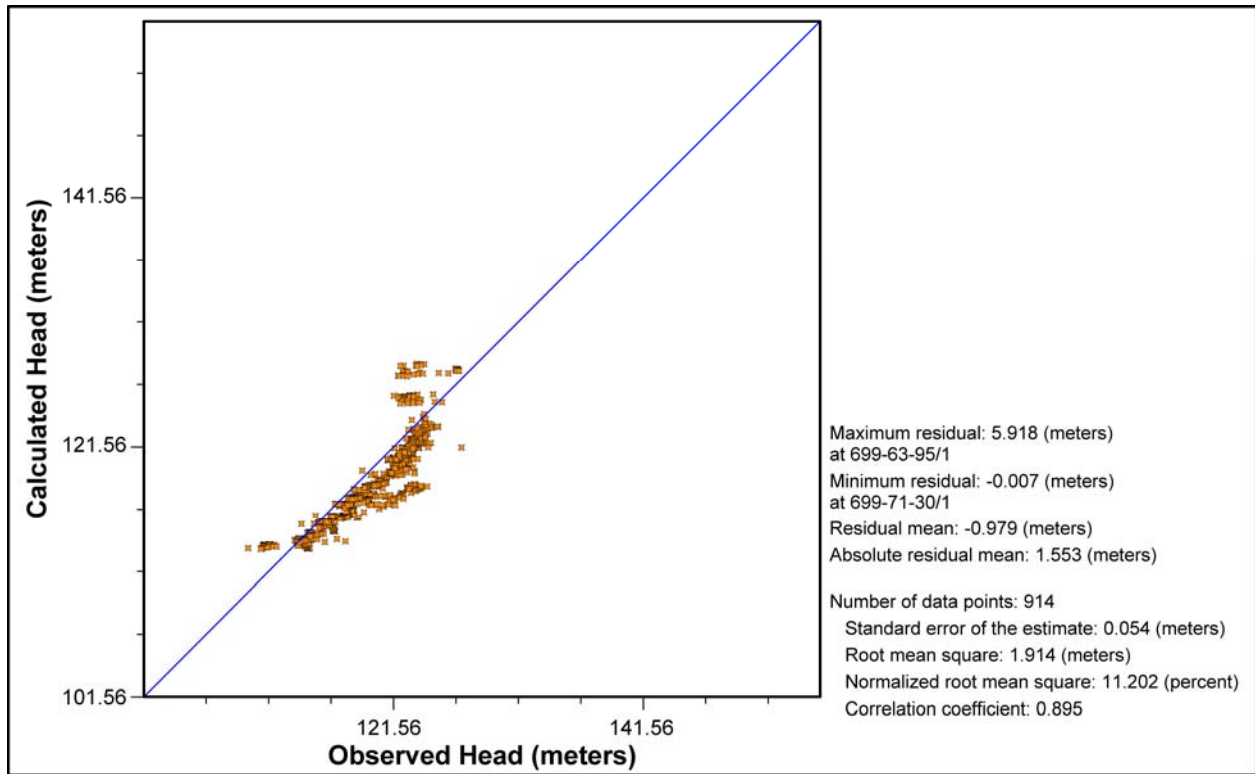


Figure L-50. Base Case Flow Model Residuals in Northern Region of Model

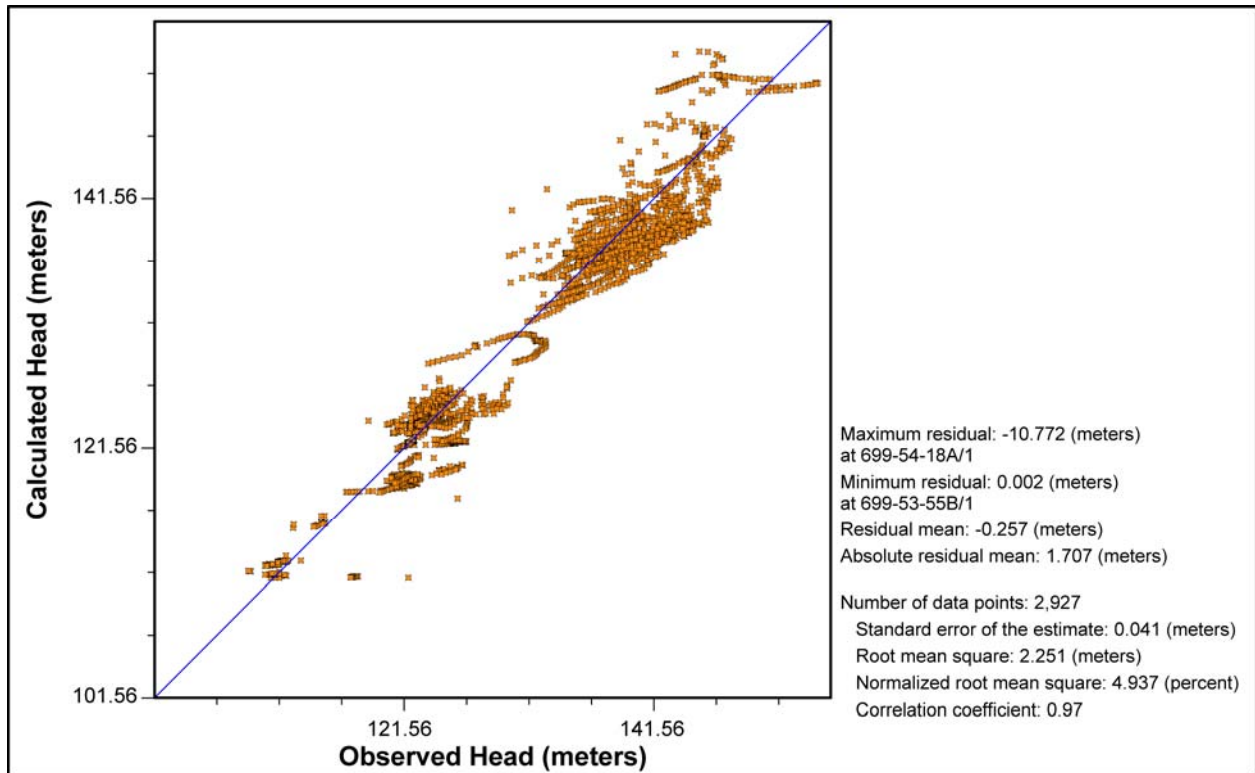


Figure L-51. Base Case Flow Model Residuals in Central Region of Model

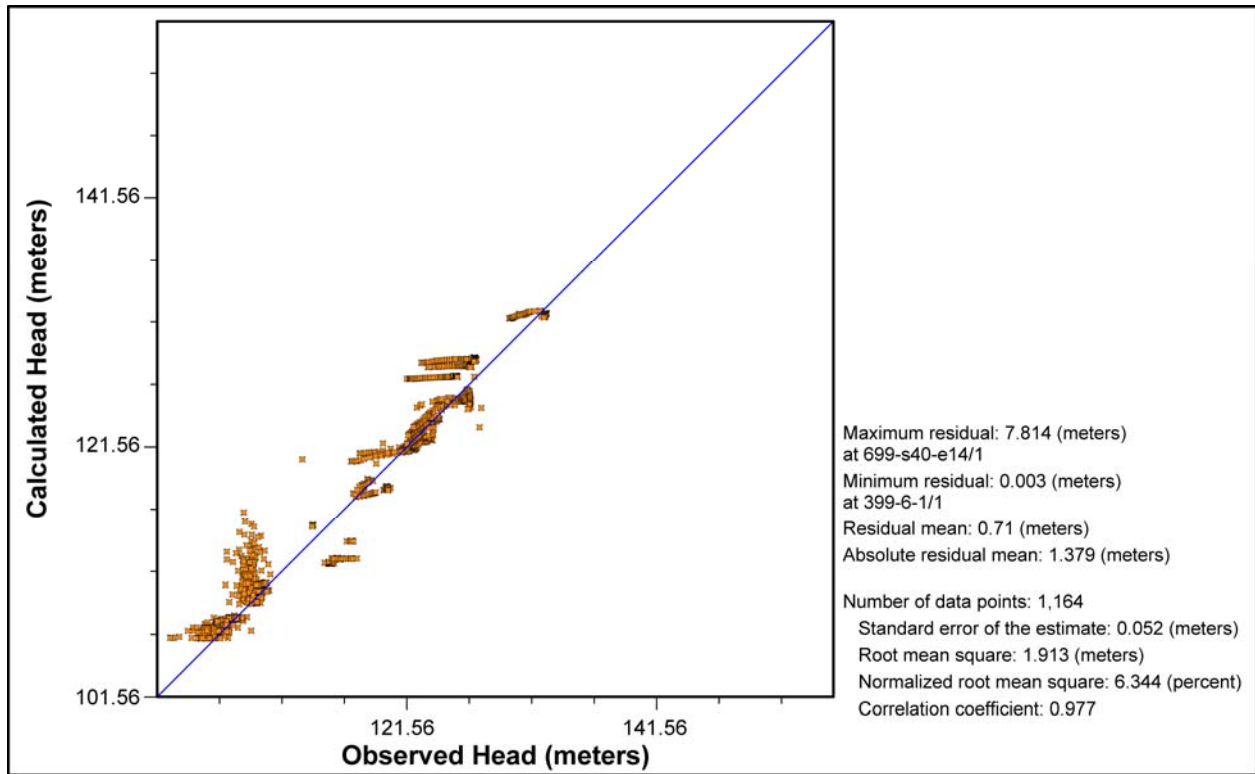


Figure L-52. Base Case Flow Model Residuals in Southern Region of Model

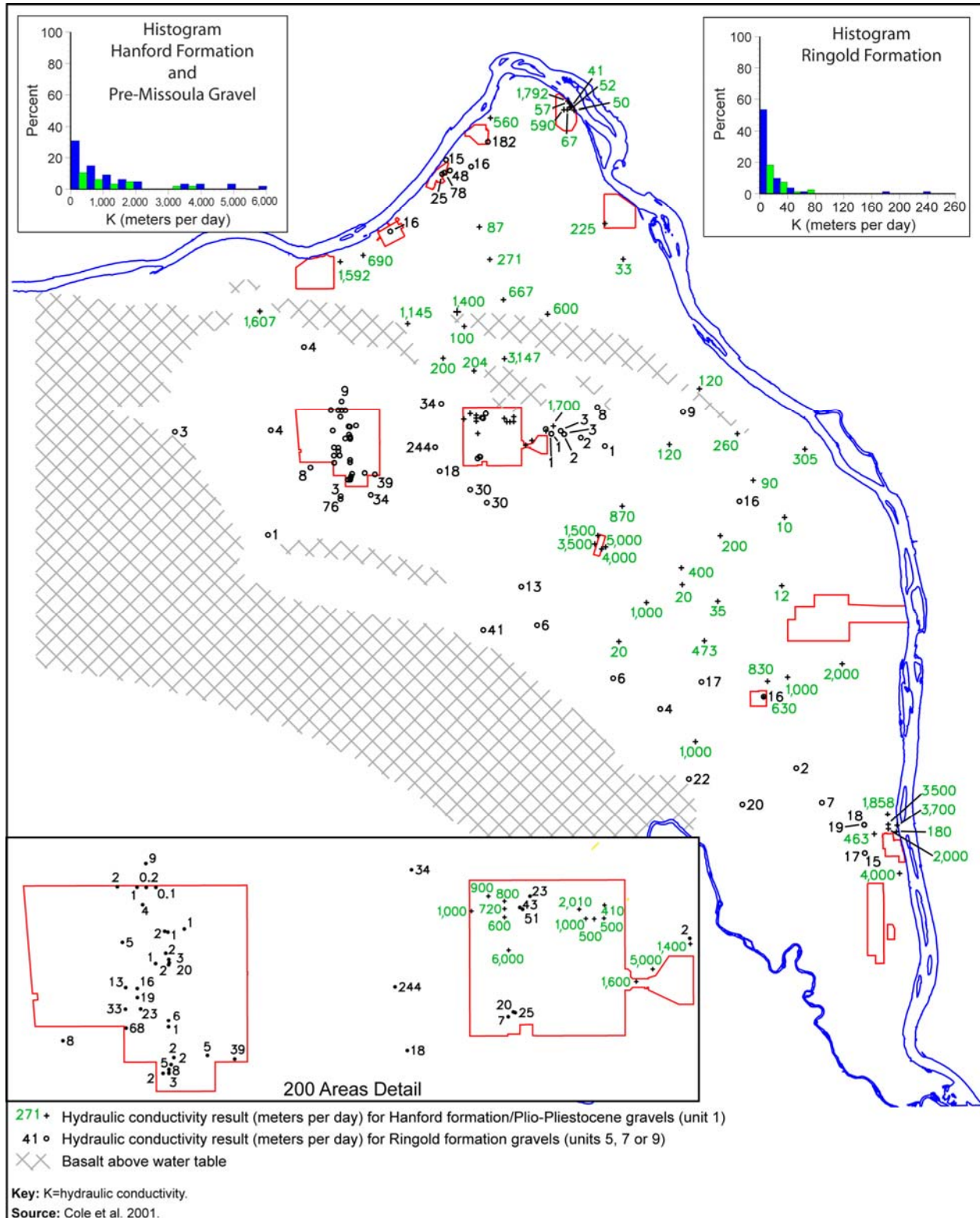


Figure L-53. Distribution of Wells with Hydraulic Conductivity Determined from Aquifer Pumping Tests

The Base Case flow model is most sensitive to the hydraulic conductivity values of the Ringold Gravel, the Hanford gravel, and the highly conductive Hanford gravel. The Base Case hydraulic conductivity of Ringold Gravel is about 20 meters per day (65.6 feet per day) (see Table L-20). The histogram of hydraulic conductivity distribution for the Ringold Formation as measured in aquifer pump tests is shown in the upper right-hand corner of Figure L-53. The majority of the field measured hydraulic conductivities are between 10 and 30 meters per day (between 32.8 and 98.4 feet per day), in reasonable agreement with the Base Case value. Base Case hydraulic conductivities for the Hanford gravel and the highly conductive Hanford gravel are about 125 meters per day (410 feet per day) and about 4,000 meters per day (13,124 feet per day), respectively (see Table L-20). The histogram of hydraulic conductivity for the Hanford Formation as measured in aquifer pump tests is shown in the upper left-hand corner of Figure L-53. Note that the range of measured hydraulic conductivities for the Hanford Formation is much broader than the Ringold Formation. Measured hydraulic conductivities for the Hanford Formation show a maximum of about 300 meters per day (984 feet per day), with a secondary occurrence between 3,000 and 5,000 meters per day (between 9,843 and 16,405 feet per day). This suggests that the inclusion of the highly conductive Hanford gravel in the conceptual model reflects an important component of the hydraulic conductivity distribution at the site.

In addition to the calibration acceptance criteria, water (or mass) balance and a long-term steady state condition must be achieved in the calibrated flow model. Cumulative mass water balance data are shown in Figure L-54, indicating a cumulative mass balance error of approximately -1.4 percent. Total water balance and storage data as a function of time are shown in Figure L-55. These data show storage values relative to the total water balance and indicate that storage-in is approximately equal to storage-out in model year 140 (calendar year 2080). This confirms that a long-term steady state condition is achieved. Note that, in Figure L-55, there is a spike in “Total Storage In” and “Total In” at model year 82. This spike is the result of a stress period change to the final long-term stress period. As a result, the model is moving from a relatively long time step at the end of the previous stress period to a relatively short time step at the beginning of the final stress period.

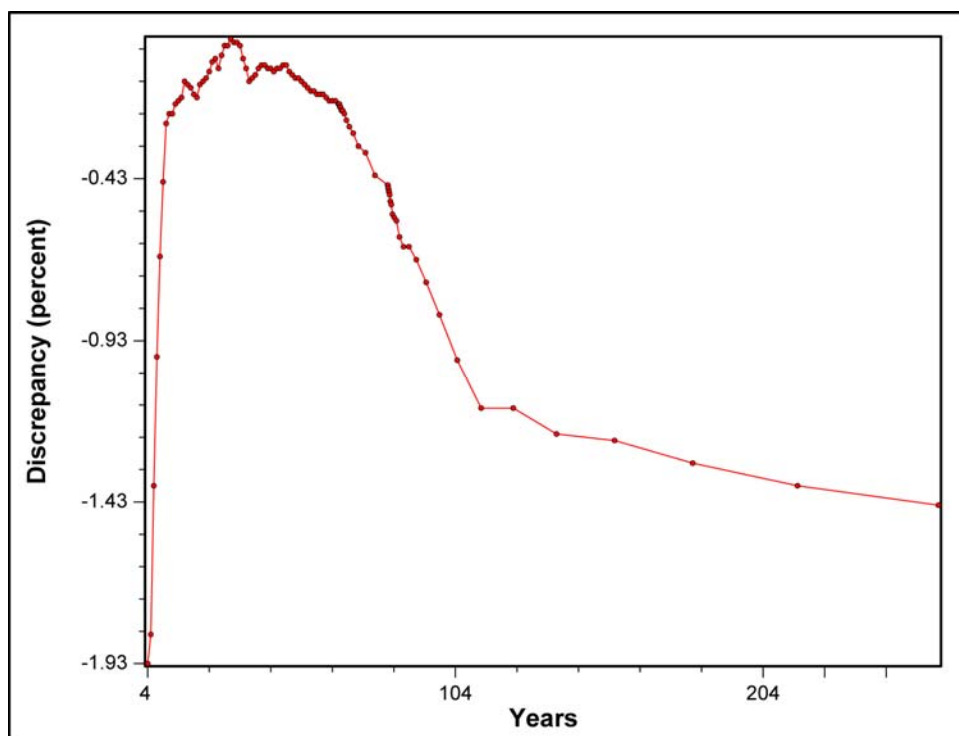


Figure L-54. Base Case Flow Model Cumulative Water Balance Discrepancy – Year 0 (Calendar Year 1940)

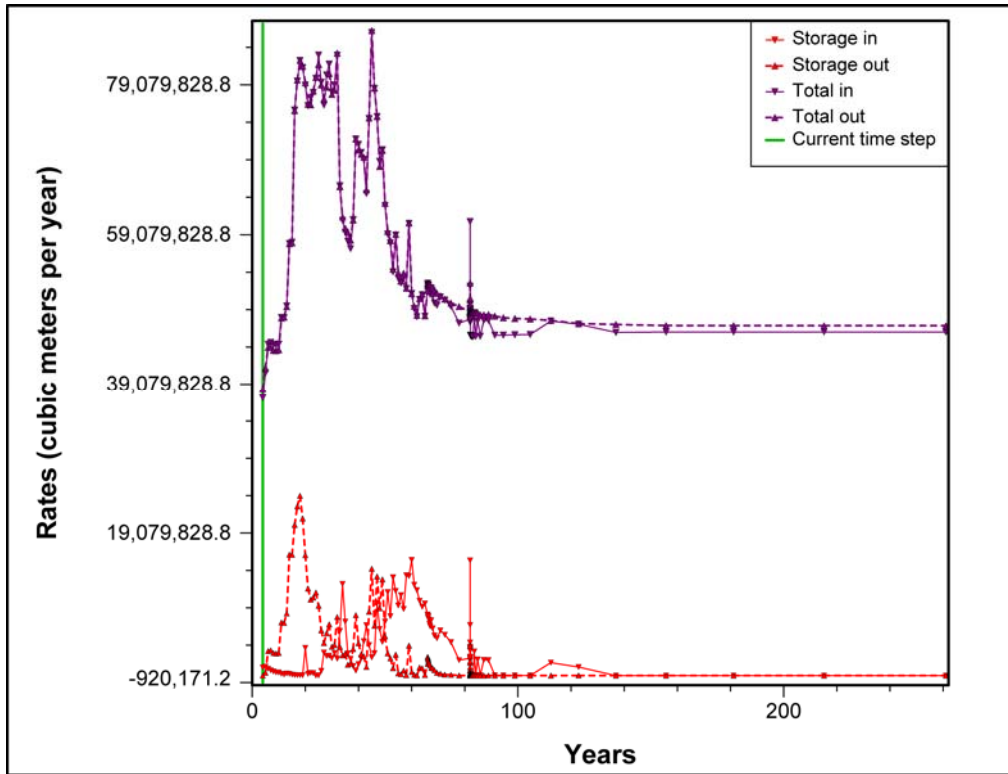
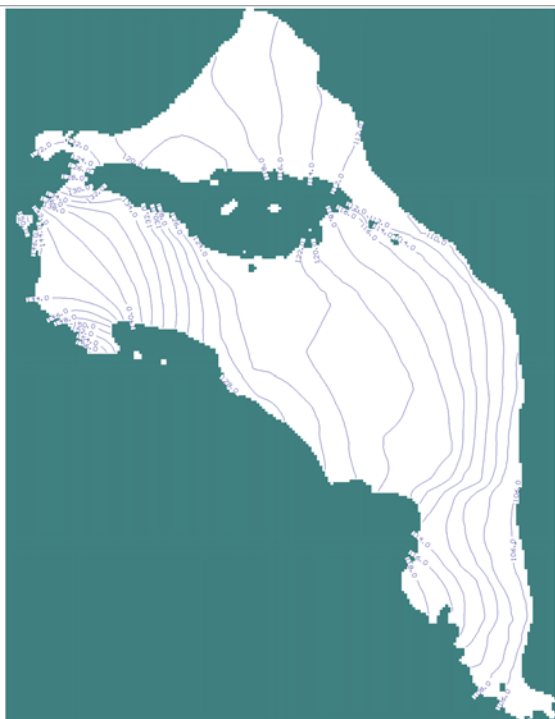


Figure L-55. Base Case Flow Model Total Water and Storage Rates Over Time – Year 0 (Calendar Year 1940)

L.10.1.1 Potentiometric Distribution

A goal for the Base Case flow model is to produce a potentiometric distribution of heads that shows a steep water table in the 200-West Area due to the low-conductivity material types in that area and a relatively flat water table in the 200-East Area where high-conductivity material types are present. The pre-Hanford potentiometric surface is assumed to be approximately the same as the post-Hanford long-term steady state condition, with water table mounding occurring below areas where and at times when Hanford operational discharges were released at the ground surface. Figures L-56, L-57, and L-58 are Base Case flow model simulations of the potentiometric surface in calendar years 1944 (pre-Hanford), 1975 (Hanford operations), and 2200 (post-Hanford), respectively.



**Figure L-56. Base Case Flow Model
Potentiometric Head Distribution –
Calendar Year 1944**

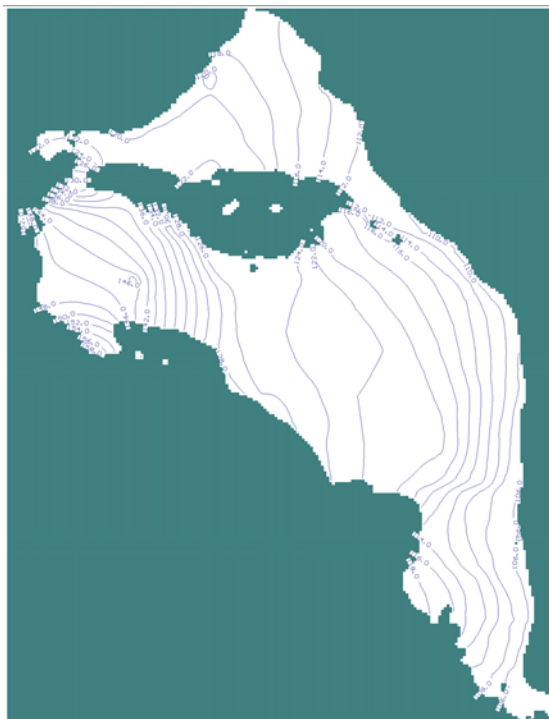


**Figure L-57. Base Case Flow Model
Potentiometric Head Distribution –
Calendar Year 1975**

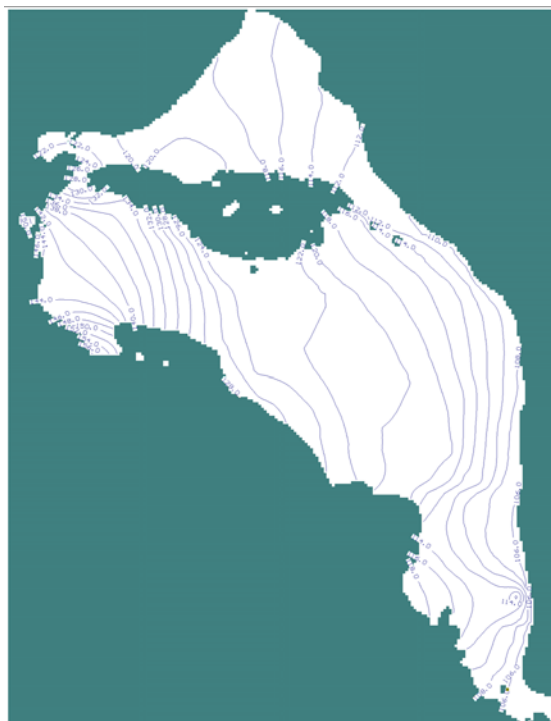


**Figure L-58. Base Case Flow Model
Potentiometric Head Distribution –
Calendar Year 2200**

L.10.1.2 Velocity Field

The Base Case flow model velocity field is variable in both magnitude and direction over time and across the model domain. This variability at selected locations within the model is shown in Figures L-59 through L-64. As expected, the velocities simulated in 200-West Area are generally lower than those simulated in the 200-East Area. An additional observation is that the velocity directions are highly variable during the Hanford operational period, particularly at BY Cribs in the 200-East Area, where the velocity directions change by approximately 180 degrees due to water table mounding, coupled with this source's proximity to Gable Gap, where water table velocity and direction are sensitive to water table elevation.

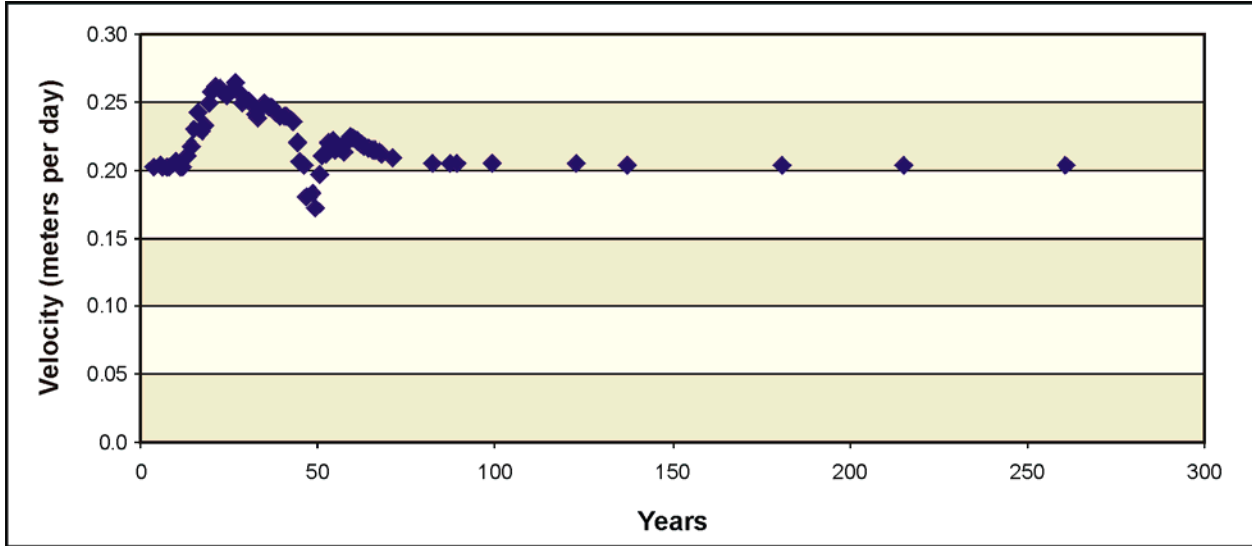


Figure L-59. Base Case Flow Model Velocity Magnitude at 216-B-26 (BC Cribs in 200-East Area) – Year 0 (Calendar Year 1940)

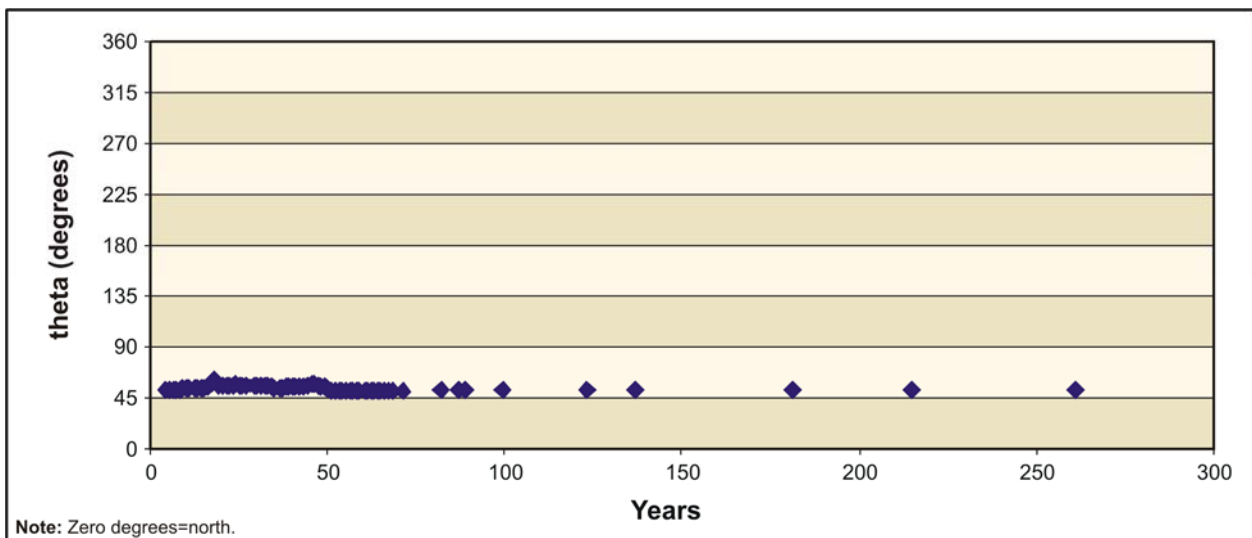


Figure L-60. Base Case Flow Model Velocity Direction at 216-B-26 (BC Cribs in 200-East Area) – Year 0 (Calendar Year 1940)

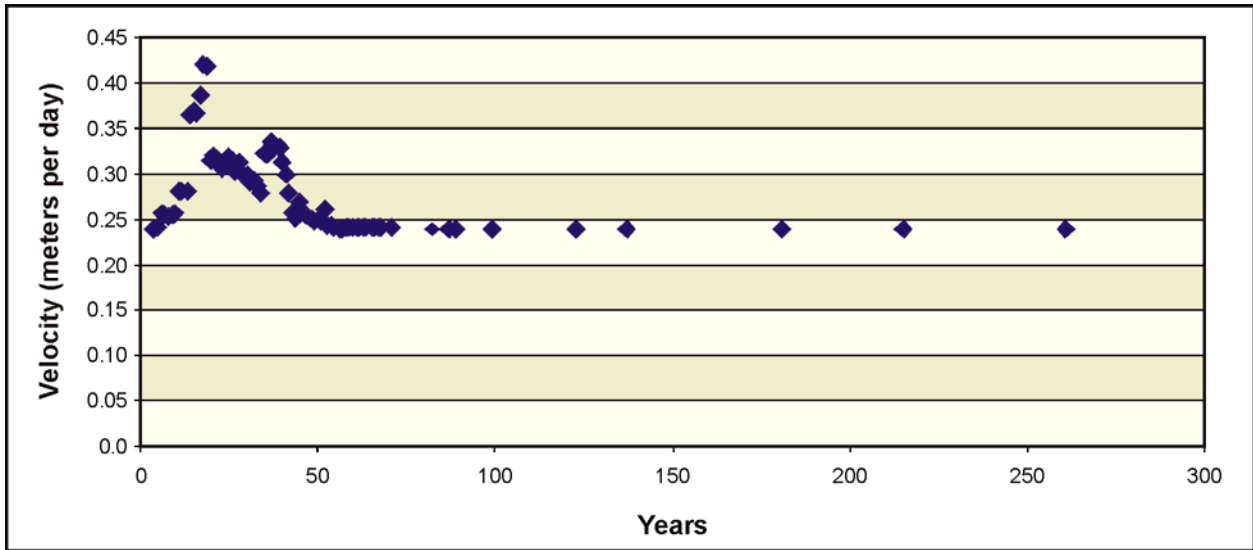
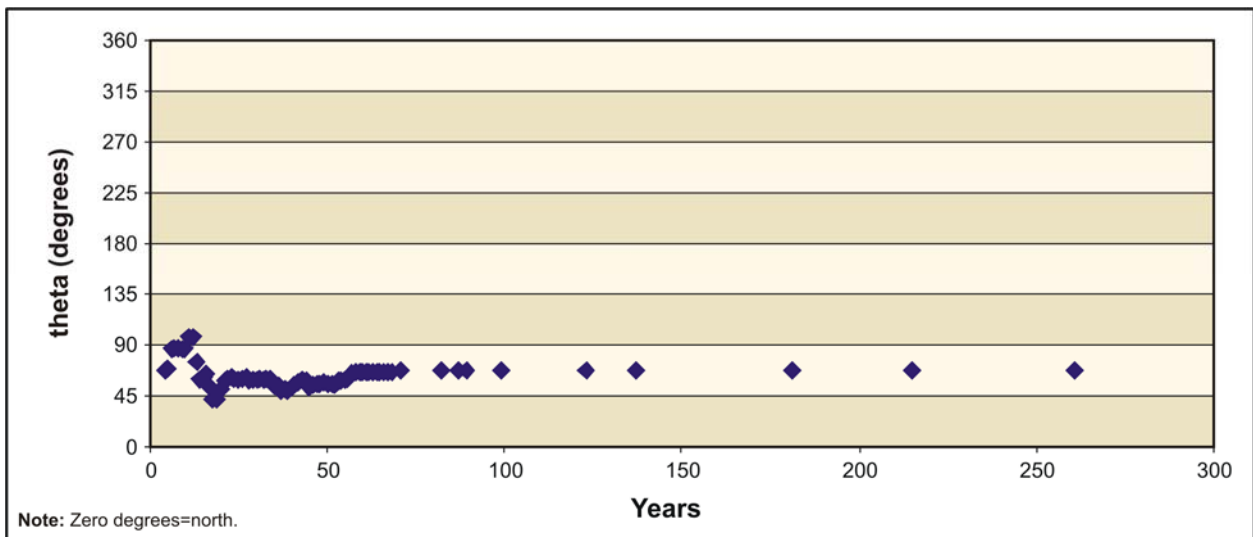


Figure L-61. Base Case Flow Model Velocity Magnitude at 216-T-28 Crib (200-West Area) –Year 0 (Calendar Year 1940)



Note: Zero degrees=north.

Figure L-62. Base Case Flow Model Velocity Direction at 216-T-28 Crib (200-West Area) –Year 0 (Calendar Year 1940)

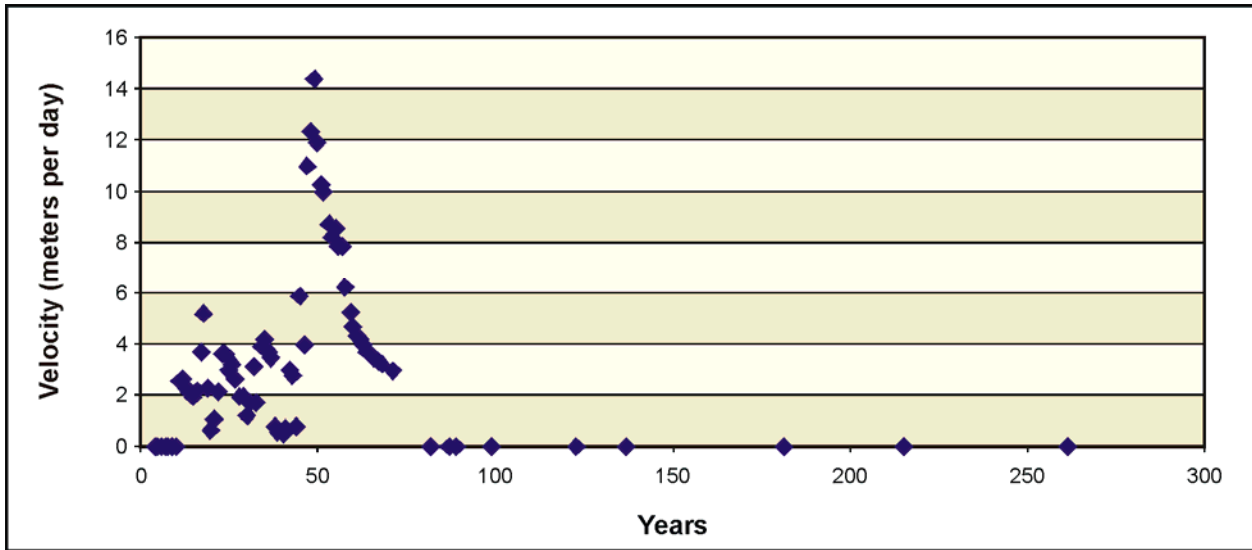


Figure L-63. Base Case Flow Model Velocity Magnitude at BY Cribs (200-East Area) – Year 0 (Calendar Year 1940)

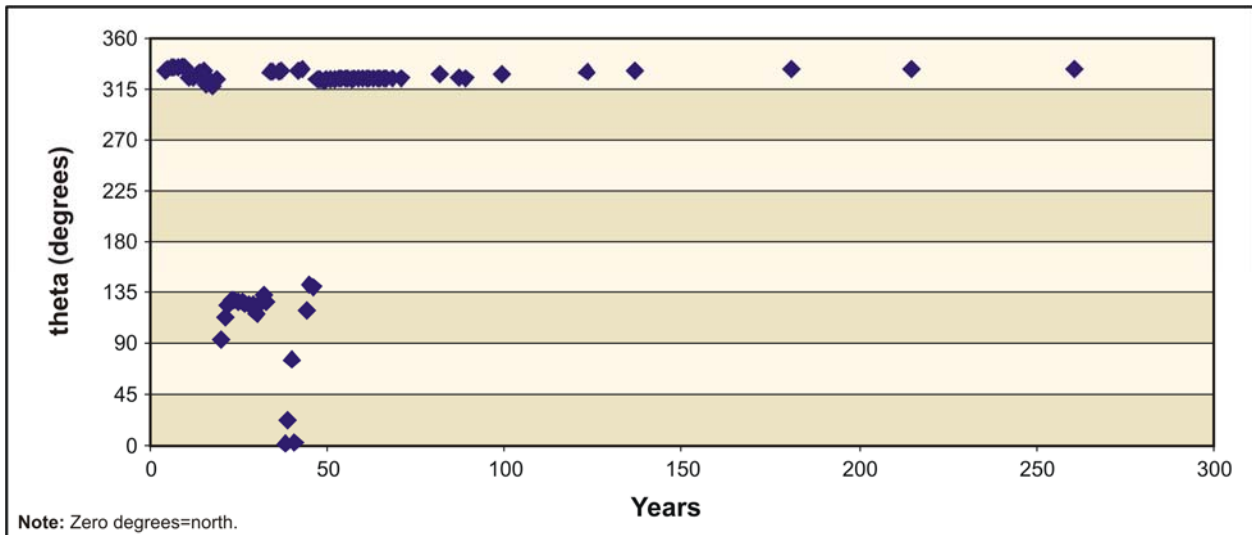


Figure L-64. Base Case Flow Model Velocity Direction at BY Cribs (200-East Area) – Year 0 (Calendar Year 1940)

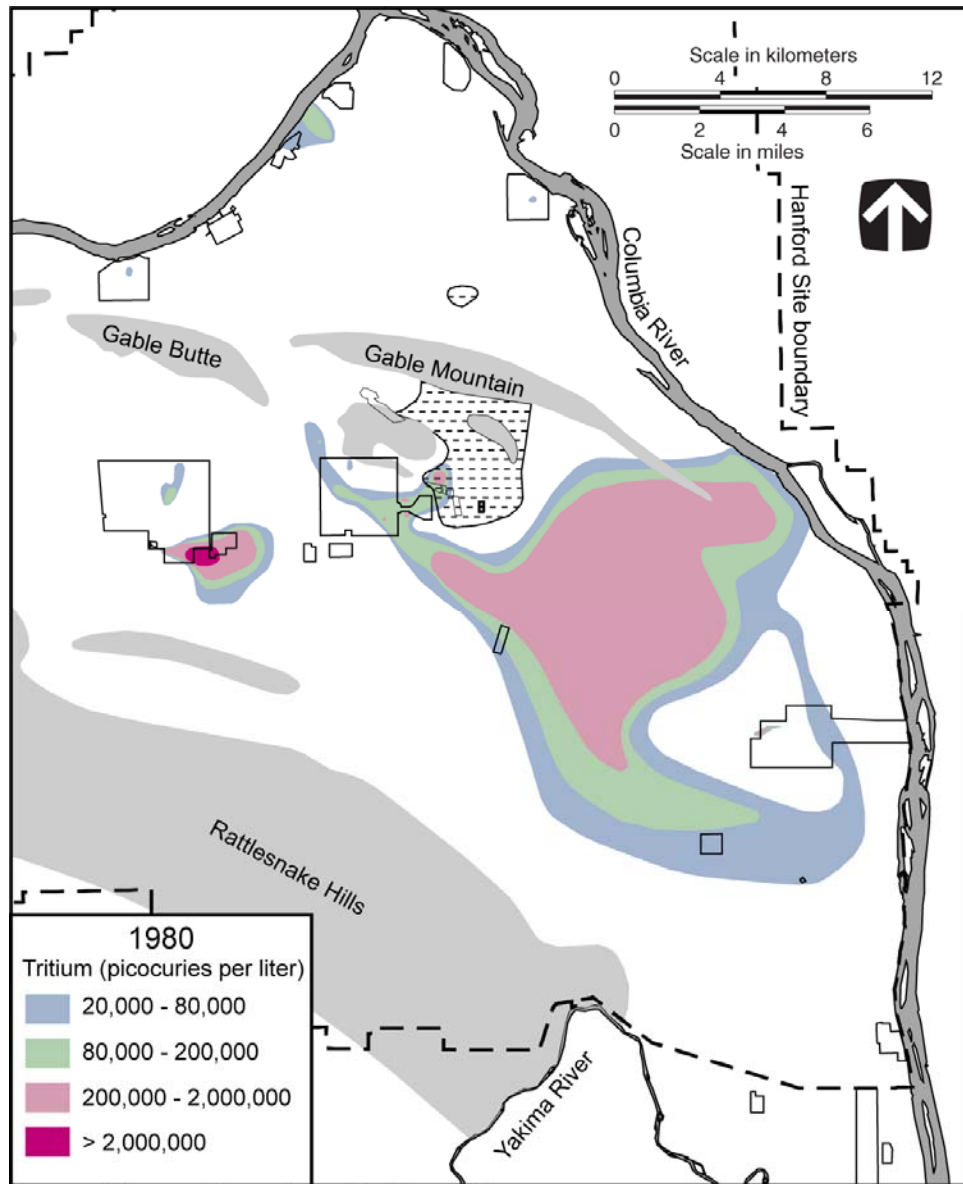
L.10.1.3 Pathline Analyses

Pathline analysis was performed on the top 26 model runs (see Section L.10.1) to narrow this field of models that performed well relative to the RMS error to a single Base Case flow model. Two pathline analyses, the tritium plume pathline analysis and the Central Plateau delineation pathline analysis, were performed on each of the top 26 models.

L.10.1.3.1 Hydrogen-3 (Tritium) Plume Pathline Analysis

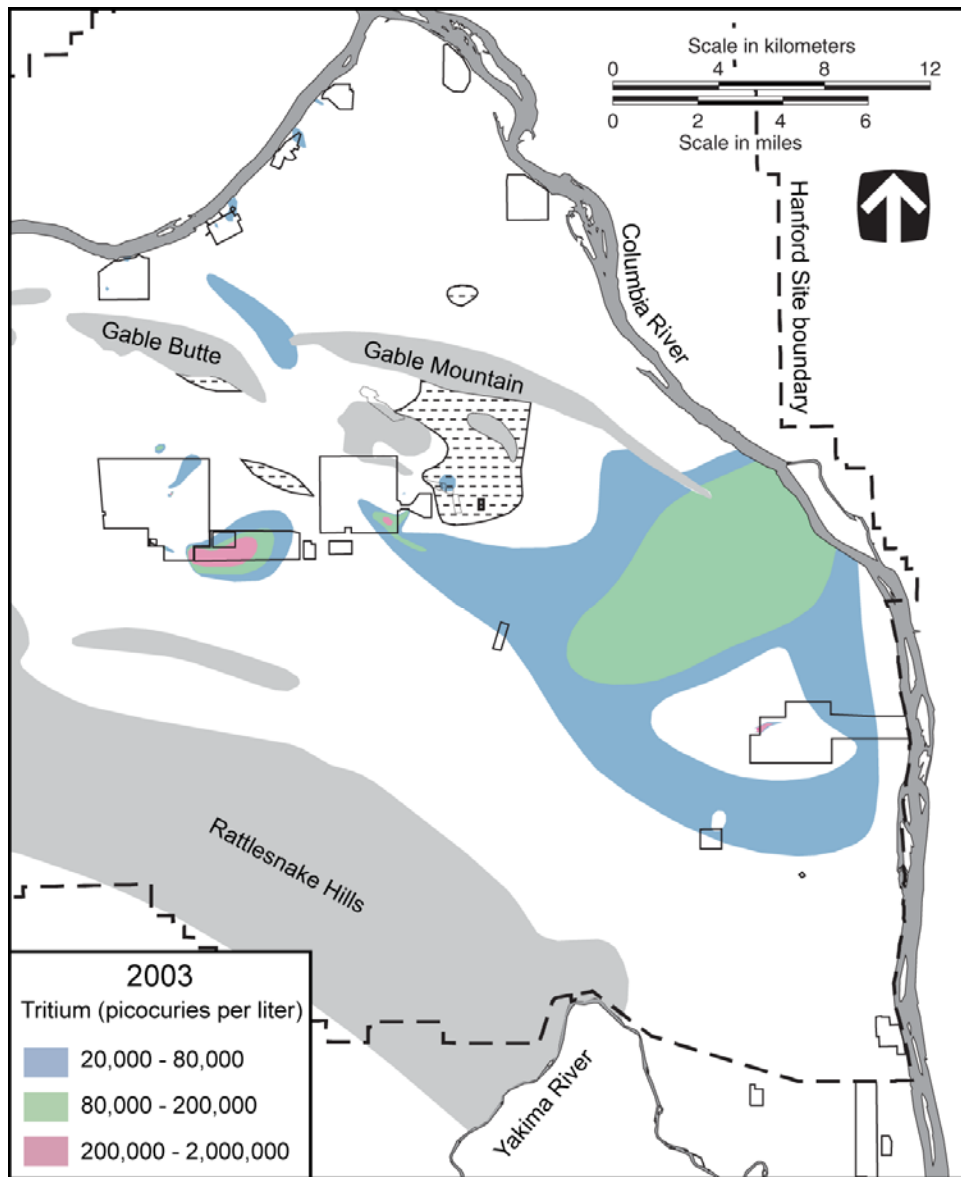
Tritium plume pathline analysis included a MODFLOW and MODPATH model run for each of the top 26 model cases, releasing particles in the 200-East and 200-West Areas representing an actual tritium release and comparing the particle pathlines to the general shape of the observed tritium plumes. This analysis is somewhat limited because no dispersion is applied to the particle pathlines so that spreading of the plume to its actual extents is constrained. This analysis does provide a qualitative means to compare

this final set of possible models to one another and aid in selecting the Base Case flow model. Figures L-65 and L-66 provide an interpretation of the field-observed tritium plume (Hartman, Morasch, and Webber 2004) to which the model-simulated pathlines were compared. Figures L-67 through L-70 provide the MODFLOW/MODPATH results of 4 of the 26 model runs, including the model run selected as the Base Case flow model. This analysis concluded that many of the top 26 model runs could be selected as the Base Case flow model if the selection were based only on the tritium plume pathline analysis.



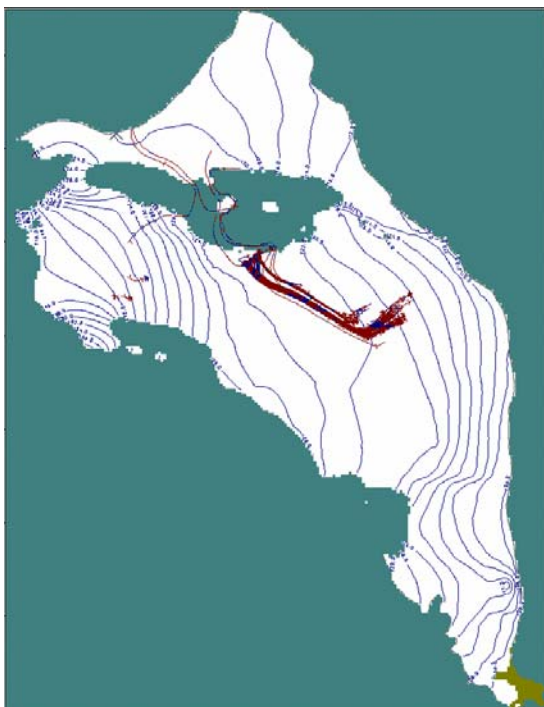
Source: Hartman, Morasch, and Webber 2004.

Figure L-65. Sitewide Hydrogen-3 (Tritium) Plumes – Calendar Year 1980

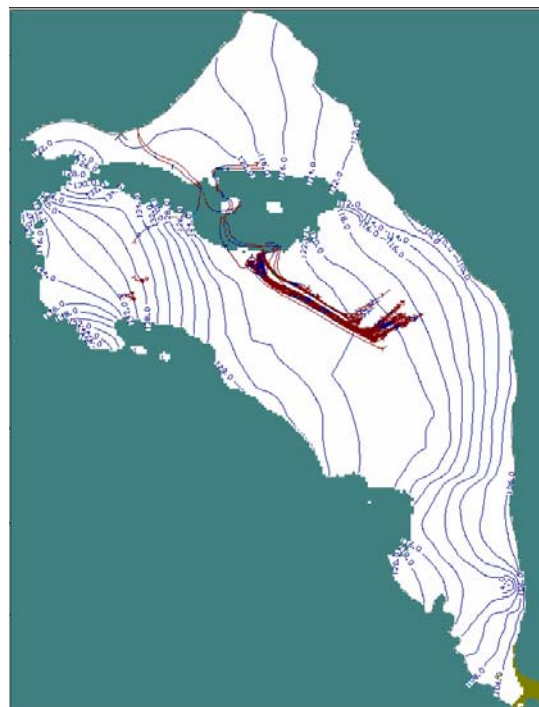


Source: Hartman, Morasch, and Webber 2004.

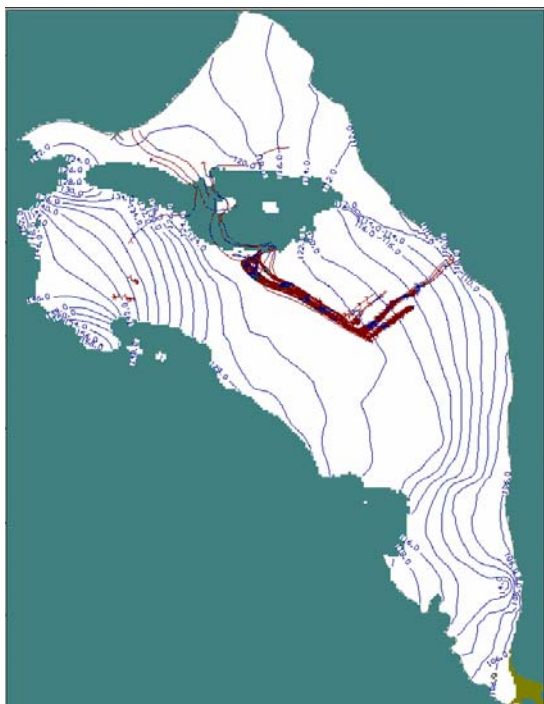
Figure L-66. Sitewide Hydrogen-3 (Tritium) Plumes – Calendar Year 2003



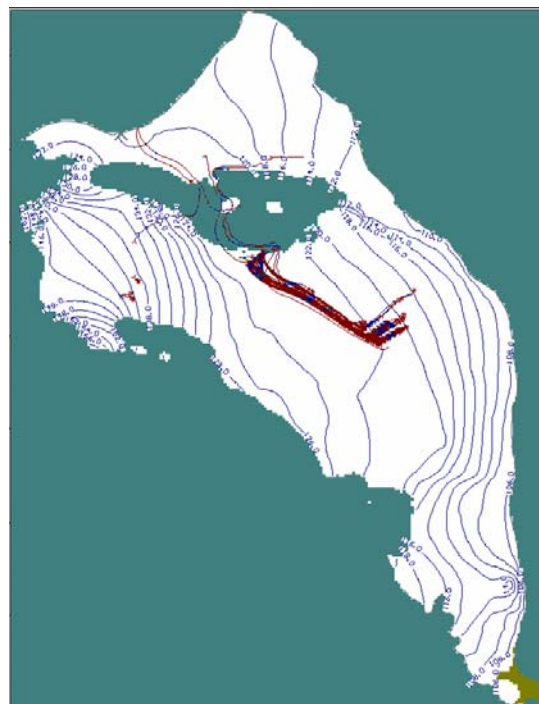
Note: To convert meters to feet, multiply by 3.281.
Figure L-67. Hydrogen-3 (Tritium) Plume Pathline Analysis Run 483
(root mean square error = 2.122 meters)



Note: To convert meters to feet, multiply by 3.281.
Figure L-68. Hydrogen-3 (Tritium) Plume Pathline Analysis Run 710
(root mean square error = 2.116 meters)
– Selected as Base Case Flow Model



Note: To convert meters to feet, multiply by 3.281.
Figure L-69. Hydrogen-3 (Tritium) Plume Pathline Analysis Run 716
(root mean square error = 2.110 meters)



Note: To convert meters to feet, multiply by 3.281.
Figure L-70. Hydrogen-3 (Tritium) Plume Pathline Analysis Run 723
(root mean square error = 2.090 meters)

L.10.1.3.2 Central Plateau Delineation Pathline Analysis

The *Technical Guidance Document* (DOE 2005) directed that the Base Case flow model would flow predominantly eastward from the 200 Areas of Hanford. The purpose of the central plateau delineation pathline analysis was to determine for each of the top 26 model runs the amount of particles released in the 200 Areas that would move to the north through Gable Gap and the amount of particles that would move to the east toward the Columbia River. This analysis included a MODFLOW and MODPATH model run for each of the top 26 model cases, releasing a uniformly distributed set of particles across the area across the central plateau. The central plateau is depicted as a rectangular-shaped boundary that includes all of the 200-East and 200-West Areas as well as other areas between and outside of the 200 Areas. This analysis provides a quantitative means to compare this final set of possible models to one another and aid in selecting a single Base Case flow model. Figures L-71 through L-74 provide the MODFLOW/MODPATH results of 4 of the 26 model runs, including the model run selected as the Base Case flow model (see Figure L-72).

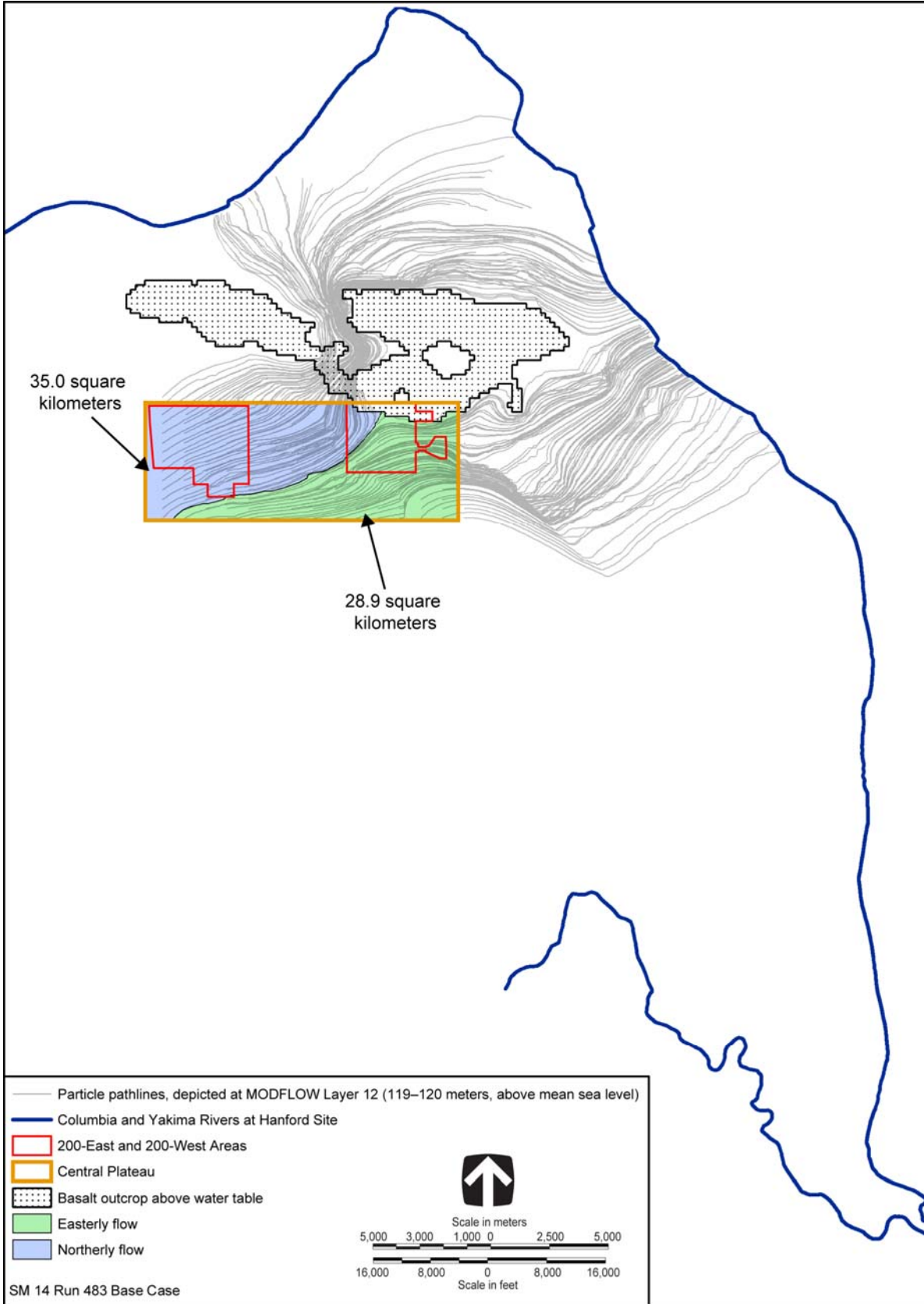


**Figure L-71. Central Plateau Delineation Pathline Analysis Run 483
(root mean square error = 2.122 meters)**

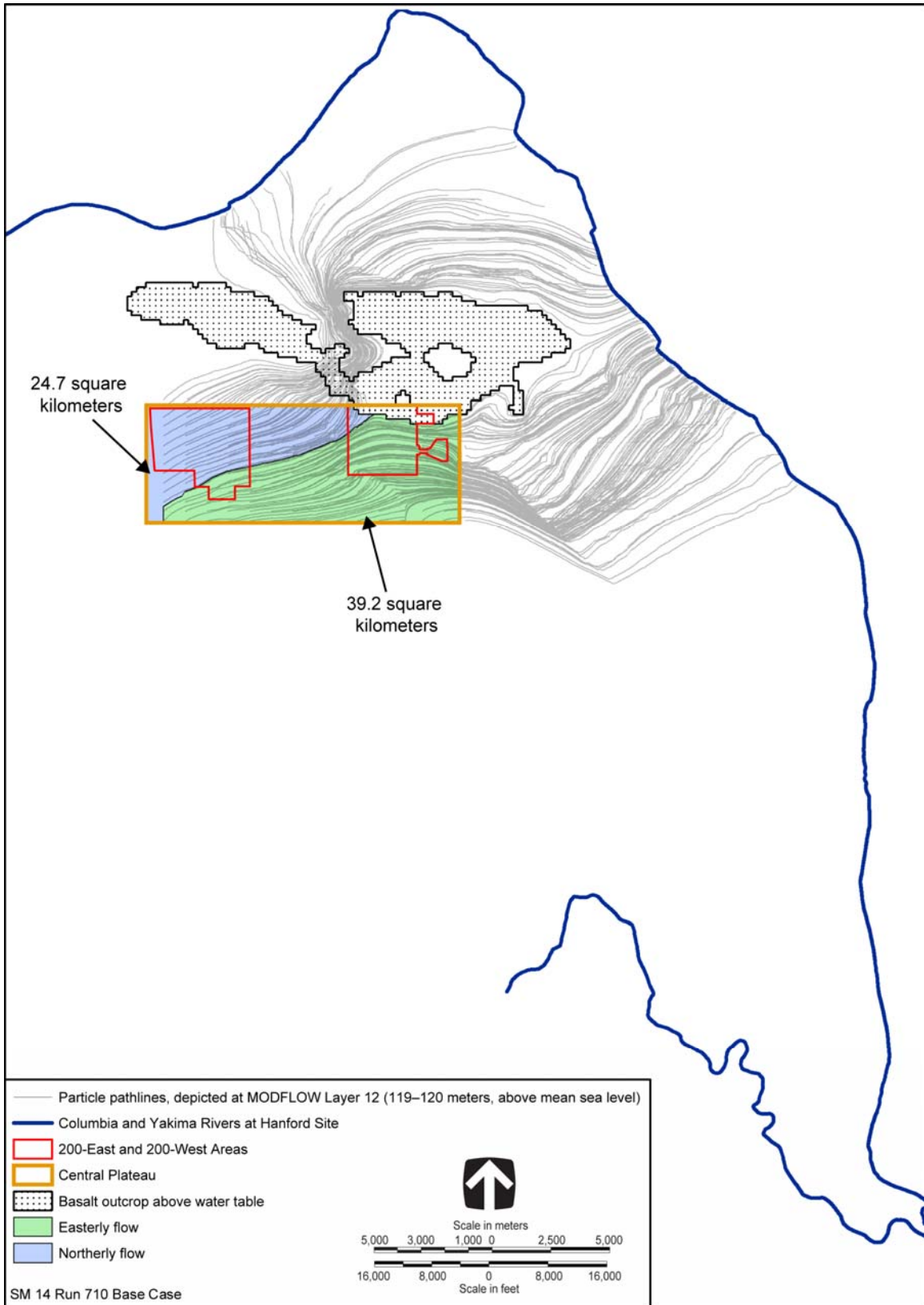


Figure L-72. Central Plateau Delineation Pathline Analysis Run 710 (root mean square error = 2.116 meters) – Selected as Base Case Flow Model

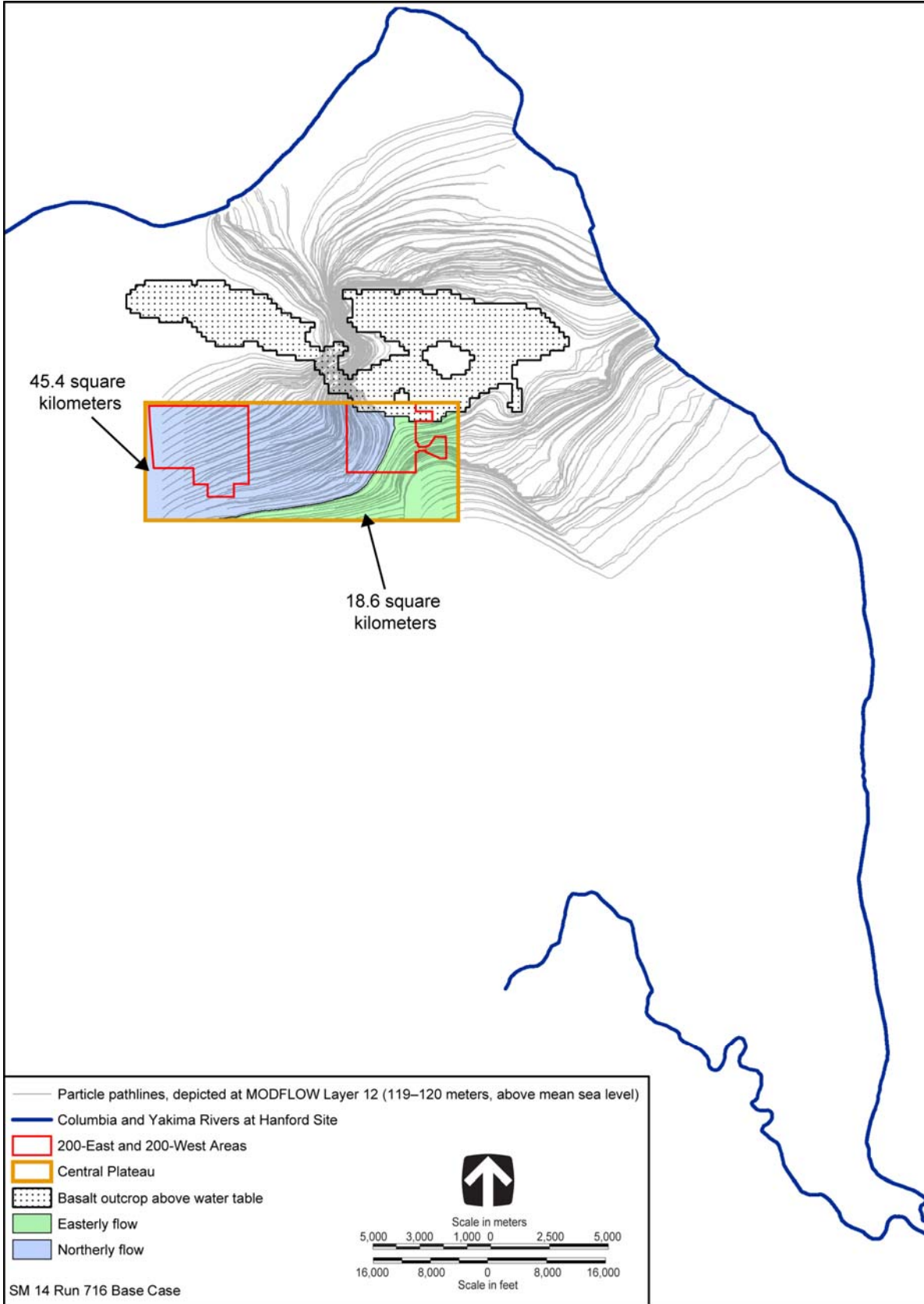


Figure L-73. Central Plateau Delineation Pathline Analysis Run 716 (root mean square error = 2.110 meters)

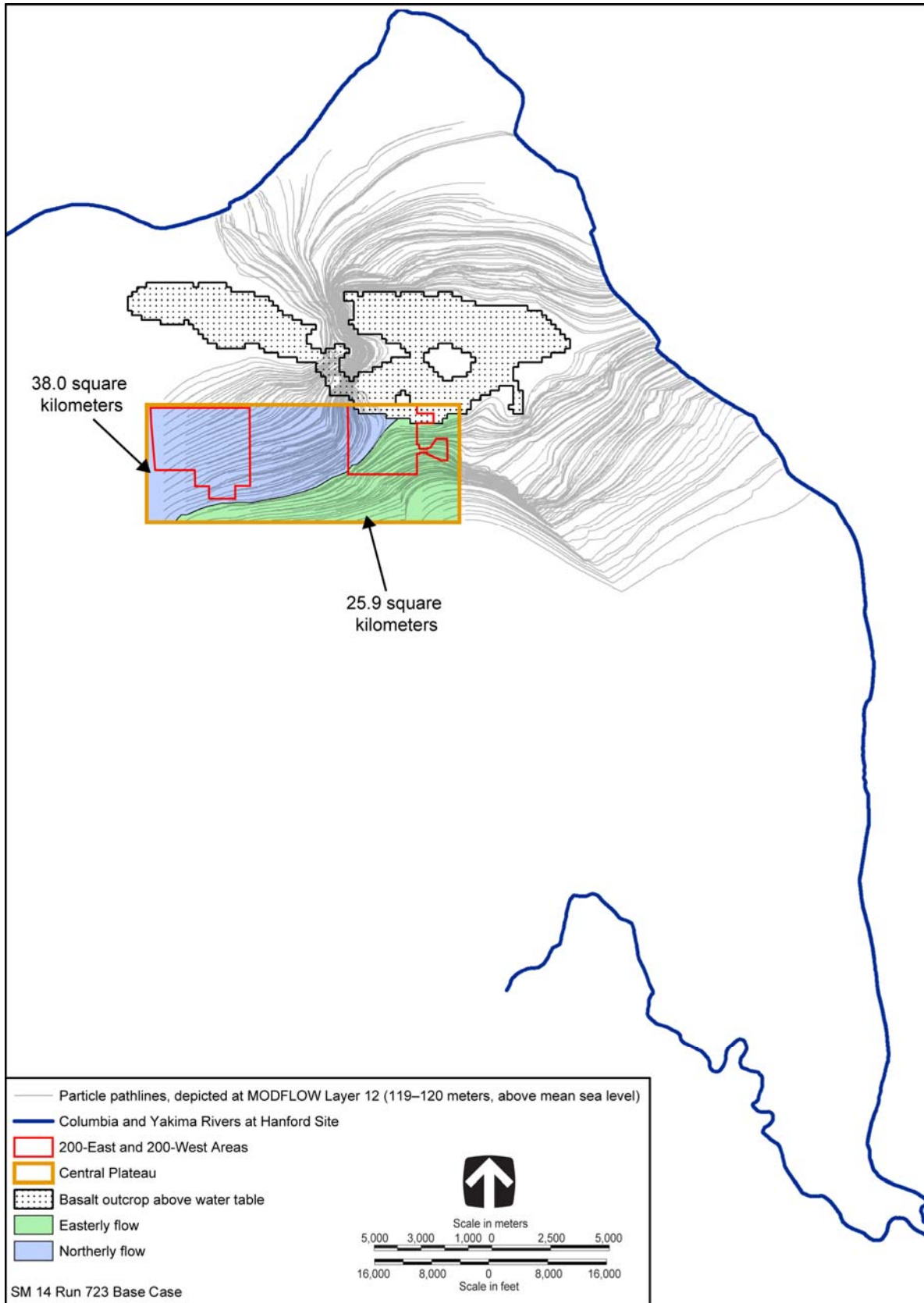


Figure L-74. Central Plateau Delineation Pathline Analysis Run 723 (root mean square error = 2.090 meters)

Table L–22 provides a summary of the percentages of particle pathlines flowing to the east and to the north for the top 26 Base Case model runs.

Table L–22. Summary of Top 26 Base Case Model Runs – Northerly Versus Easterly Flow

Run Number	Area of Northerly Flow (square kilometers)	Area of Easterly Flow (square kilometers)	Northerly Flow (percent)	Easterly Flow (percent)
710	24.7	39.2	39	61
690	26.8	37.1	42	58
712	27.0	37.0	42	58
734	29.1	34.9	45	55
376	32.4	31.5	51	49
449	32.5	31.4	51	49
306	33.2	30.8	52	48
G1543	33.6	30.3	53	47
483	35.0	28.9	55	45
422	36.3	27.6	57	43
612	36.9	27.0	58	42
682	37.3	26.7	58	42
637	37.4	26.5	59	41
671	37.9	26.0	59	41
723	38.0	25.9	59	41
023	39.5	24.5	62	38
725	41.5	22.4	65	35
709	43.3	20.7	68	32
645	43.6	20.3	68	32
716	45.4	18.6	71	29
455	45.6	18.4	71	29
631	45.8	18.1	72	28
680	49.7	14.3	78	22
340	53.1	10.9	83	17
698	54.3	9.7	85	15
659	56.2	7.7	88	12

Note: To convert square kilometers to square miles, multiply by 0.3861.

Based on the results of this analysis, run 710, which results in the largest area and highest percentage of easterly flow from particles released in the 200 Areas, was selected as the Base Case flow model.

L.10.2 Alternate Case

The Alternate Case flow model is encoded identically to the Base Case flow model with the following exceptions:

- The TOB cutoff elevation, which is the lowest elevation through which water can flow, is lowered by 3 meters (9.8 feet) in the Gable Gap Area in the Alternate Case flow model. See Section L.4.3.2.1 for a discussion of the basalt surface.
- The hydraulic conductivity values assigned in the Alternate Case model were calibrated independently, resulting in a set that is different from the hydraulic conductivity values assigned in the Base Case flow model.

The Monte Carlo optimization described in Section L.9 focused on identifying sets of hydraulic conductivity values that result in simulated head values over time and across the model domain that reasonably match observed heads over time and across the model domain. For the Alternate Case flow model, the Monte Carlo optimization identified 32 model runs, each with different sets of hydraulic conductivity values, where model simulations of head values reasonably match observed heads. These 32 model runs were evaluated further to determine which one best met the following additional selection criteria:

- The majority of the particles released to the water table within the Core Zone Boundary (200 Area Central Plateau of Hanford) move to the north through Gable Gap rather than to the east toward the Columbia River.
- Particles released to the water table in the 200 Areas (representing a historical tritium release) result in particle pathlines that qualitatively match the observed 200-East and 200-West Area tritium plumes, without considering the effects of dispersion.
- Performance of the tritium plume particle pathlines for the selected Alternate Case flow model should reasonably match performance of the tritium plume particle pathlines for the selected Base Case flow model (see Section L.10.1.3.1).

After this additional evaluation, the Alternate Case flow model was selected. The selected model must meet the calibration acceptance criteria described in Section L.6.2. Table L-23 summarizes the calibration acceptance criteria along with the Alternate Case flow model’s performance for each criterion.

Table L-23. Summary of Alternate Case Flow Model Performance Compared to Calibration Acceptance Criteria

Flow Model Calibration Acceptance Criteria	Alternate Case Flow Model Performance
Residual distribution should be reasonably normal.	Residual distribution is reasonably normal (see Figure L-75).
The residual mean should be approximately 0.	Residual Mean = -0.078 meters (-0.255 feet).
The number of positive residuals should approximate the number of negative residuals.	Positive residuals approximately equal negative residuals (see Figure L-75).
The correlation coefficient (calculated versus observed) should be greater than 0.9.	Correlation coefficient = 0.98 (see Figure L-76)
The root mean square (RMS) error (calculated versus observed) should be less than 5 meters (16.4 feet), approximately 10 percent of the gradient in the water table elevation.	RMS error = 2.058 meters (see Figure L-76).
Residuals in the 200-East Area should be distributed similarly to those in the 200-West Area.	Residuals in the 200-East and 200-West Areas are distributed similarly (see Figures L-77 and L-78).
The residuals should be evenly distributed over time.	Residuals are approximately evenly distributed over time (see Figures L-79, L-80, L-81, and L-82).
The residuals should be evenly distributed across the site.	Residuals are approximately evenly distributed across the site (see Figures L-83, L-84, and L-85).
The calibrated parameters should compare reasonably well with field-measured values.	Calibrated hydraulic conductivity values are listed in Table L-24 and compare reasonably with field-measured values for material types to which the model is sensitive (i.e., Hanford formation and Ringold Formation material types). Figure L-53 provides field-measured values from aquifer pumping tests (Cole et al. 2001).
Parameters should be reasonably uncorrelated.	Hydraulic conductivity parameters are reasonably uncorrelated (see Table L-24 for the key to model material type zones and Table L-25 for the correlation coefficient matrix).

Note: To convert meters to feet, multiply by 3.281.

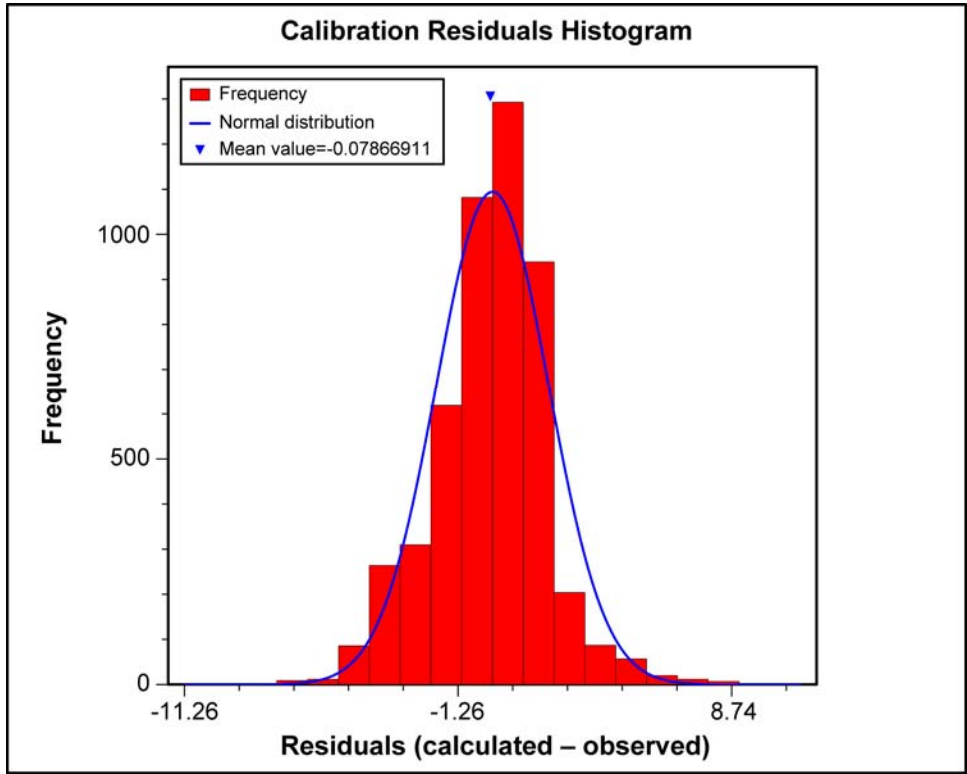


Figure L-75. Alternate Case Flow Model Residual Distribution

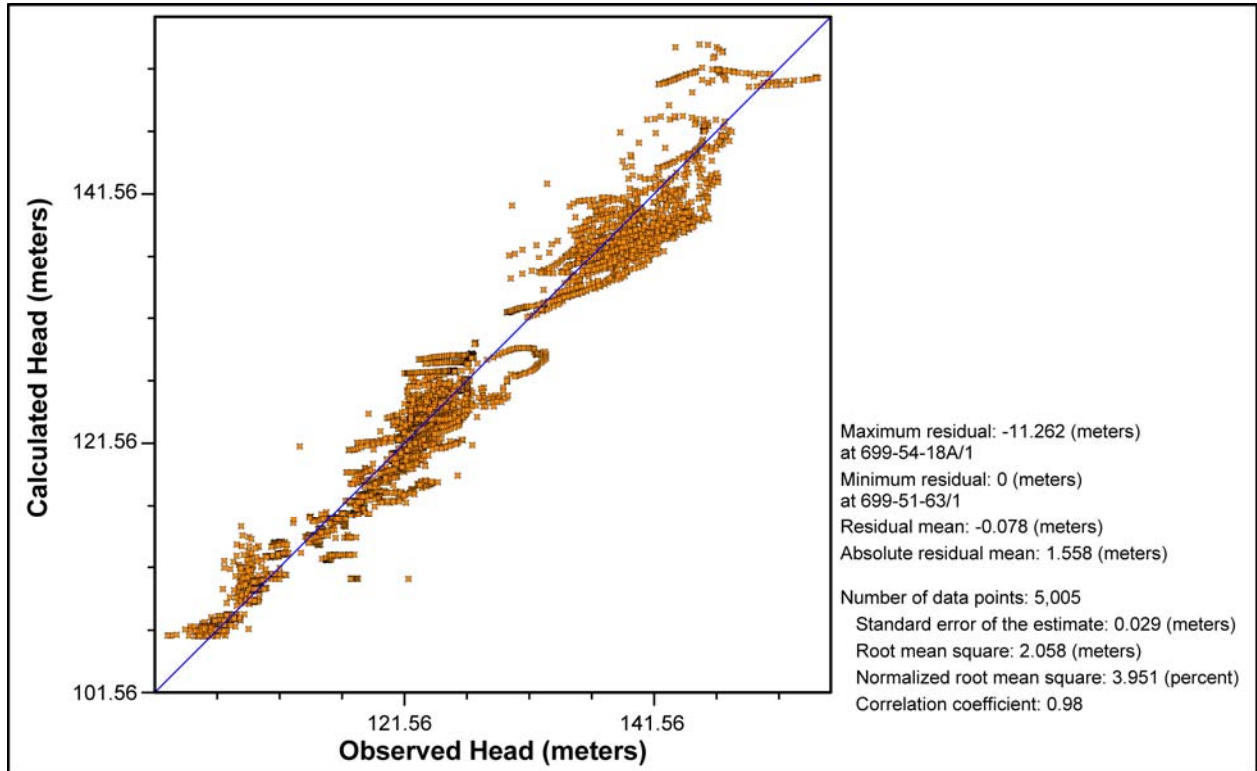


Figure L-76. Alternate Case Flow Model Calibration Graph and Statistics

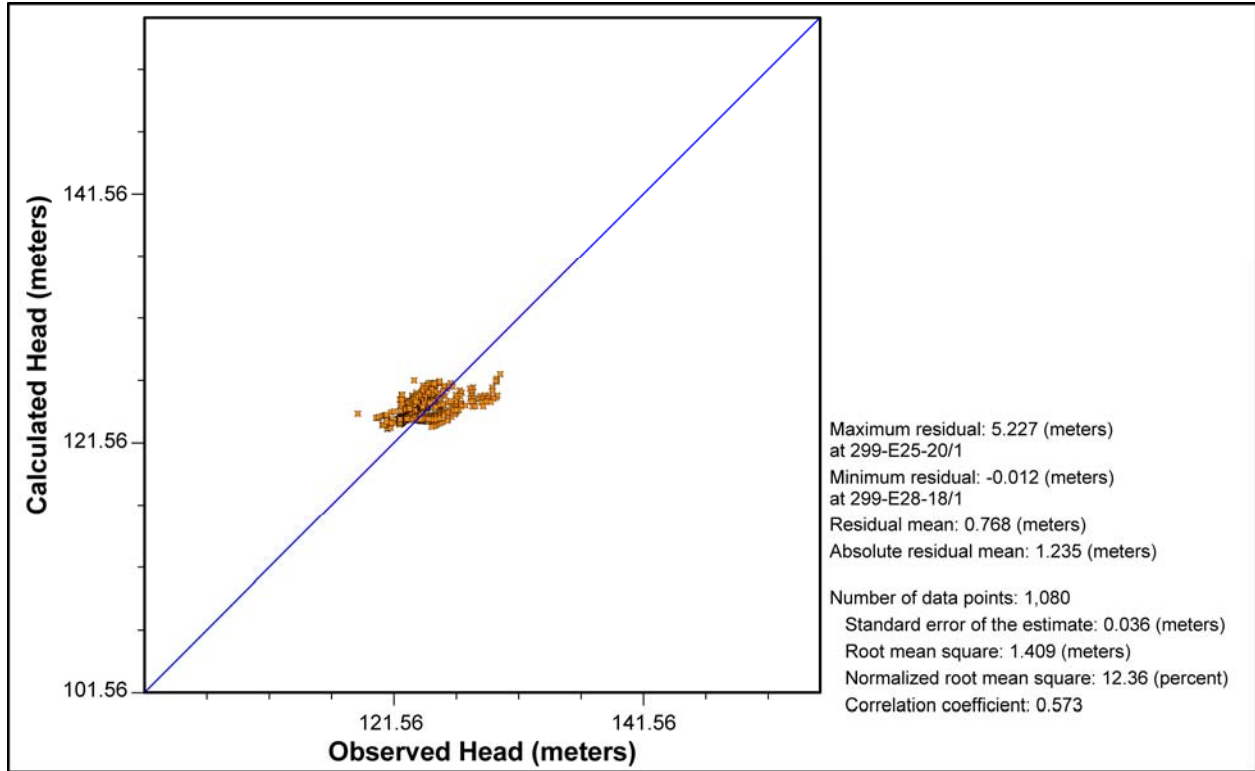


Figure L-77. Alternate Case Flow Model Residuals – 200-East Area

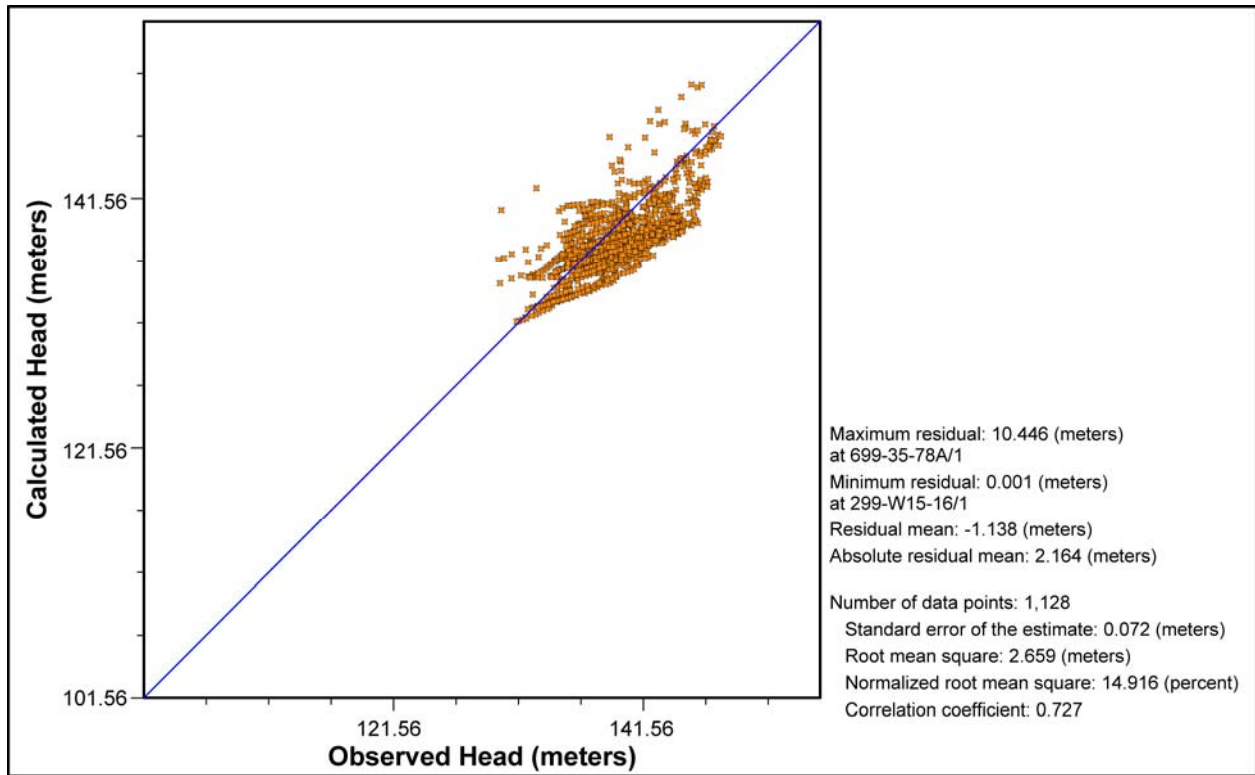


Figure L-78. Alternate Case Flow Model Residuals – 200-West Area

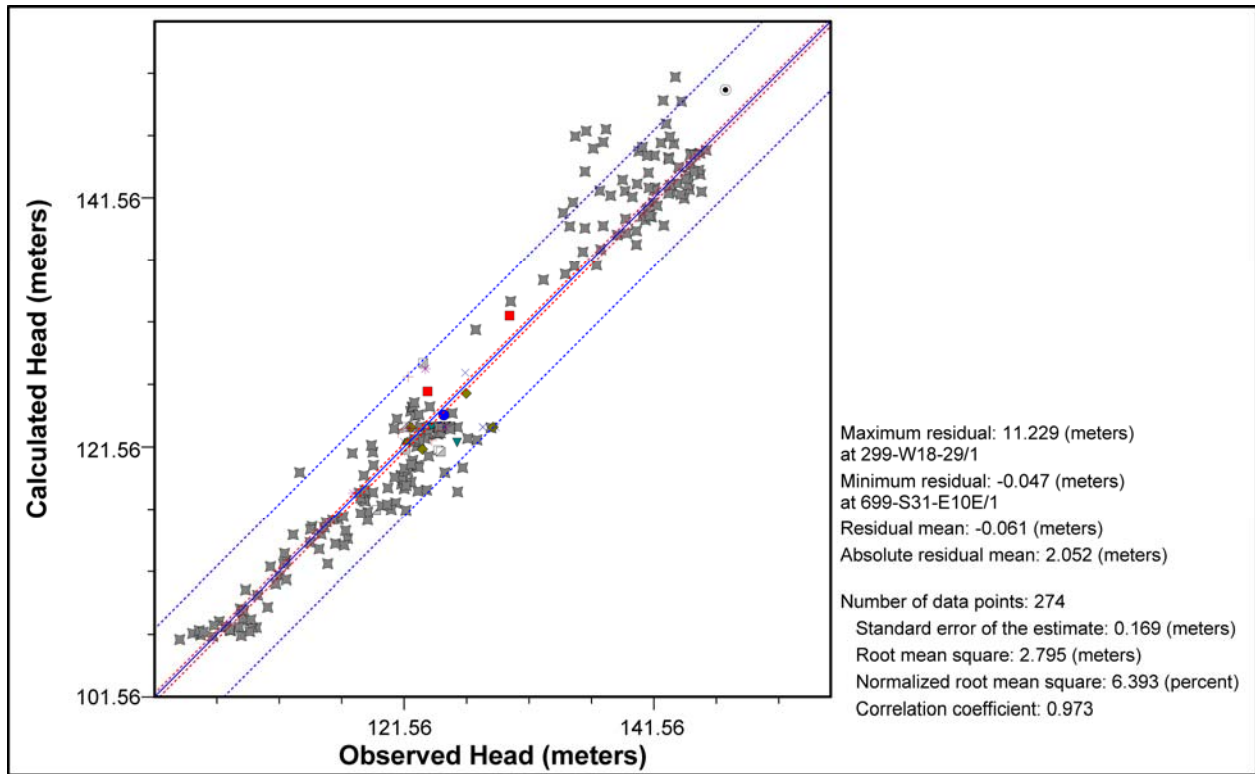


Figure L-79. Alternate Case Flow Model Residuals – Calendar Year 1955

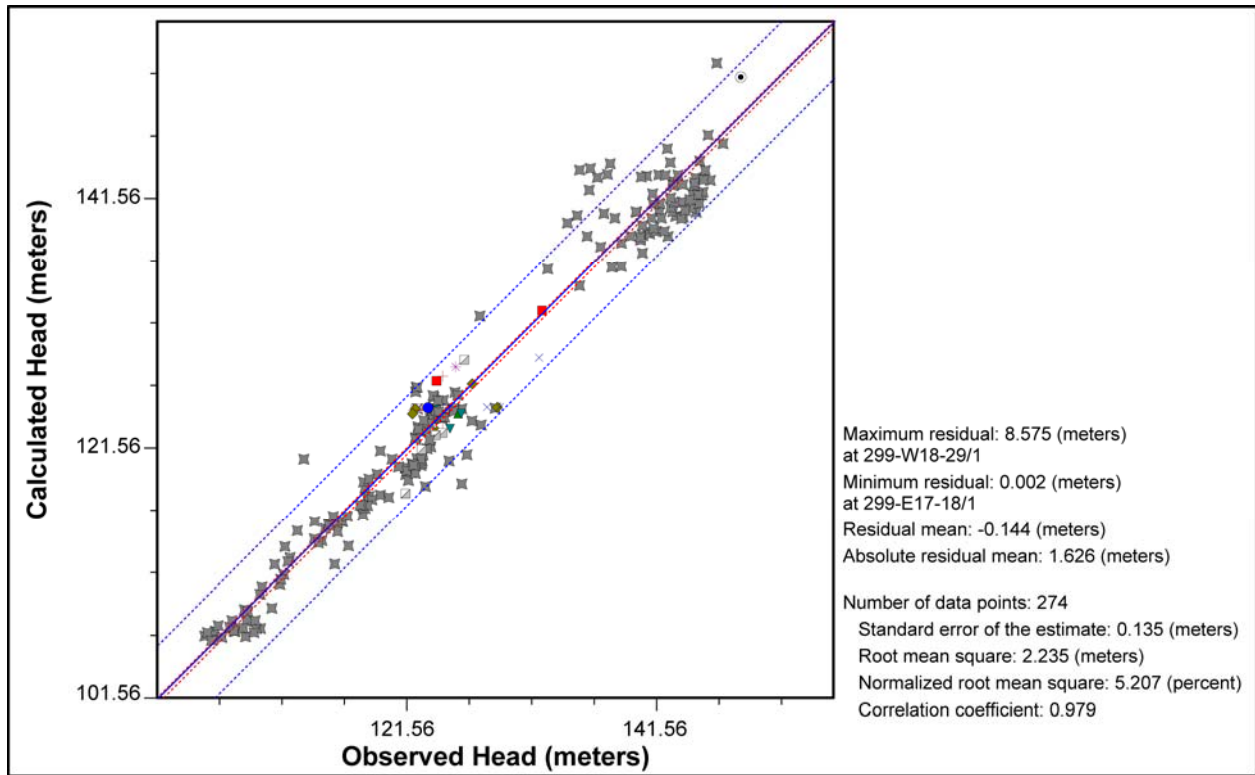


Figure L-80. Alternate Case Flow Model Residuals – Calendar Year 1975

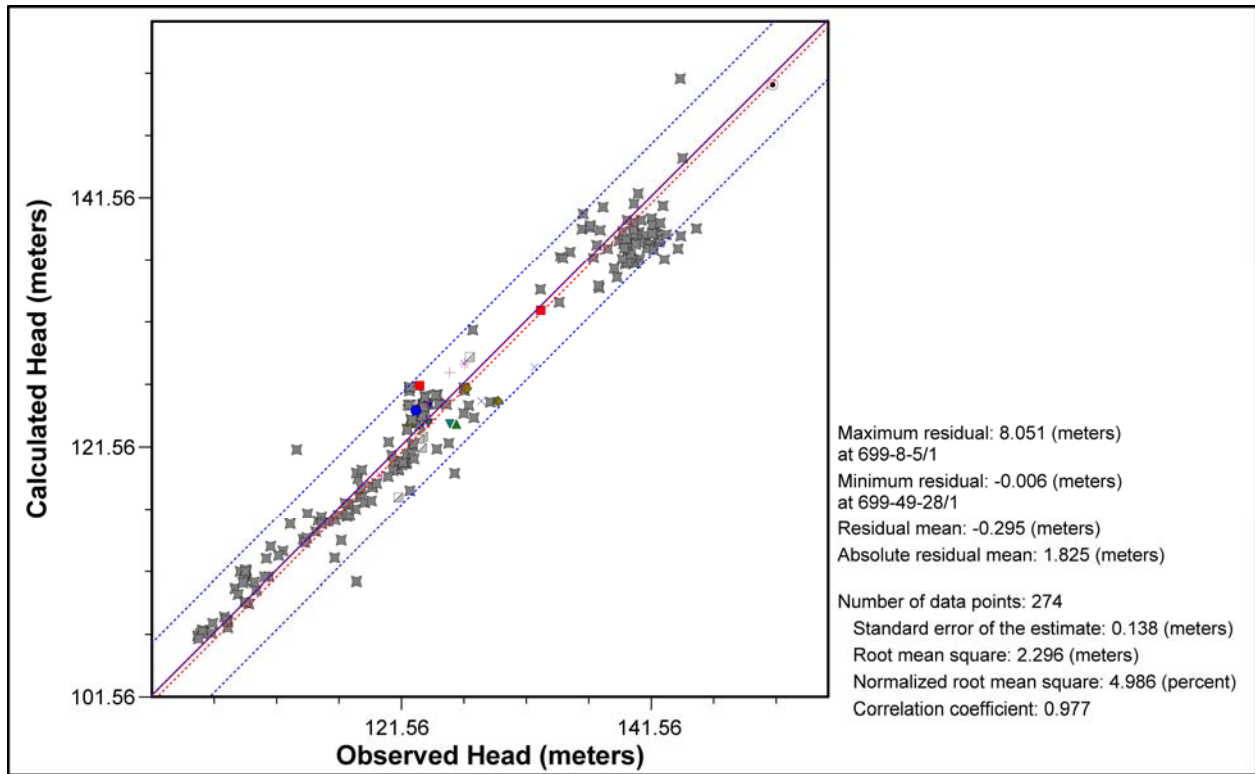


Figure L-81. Alternate Case Flow Model Residuals – Calendar Year 1995

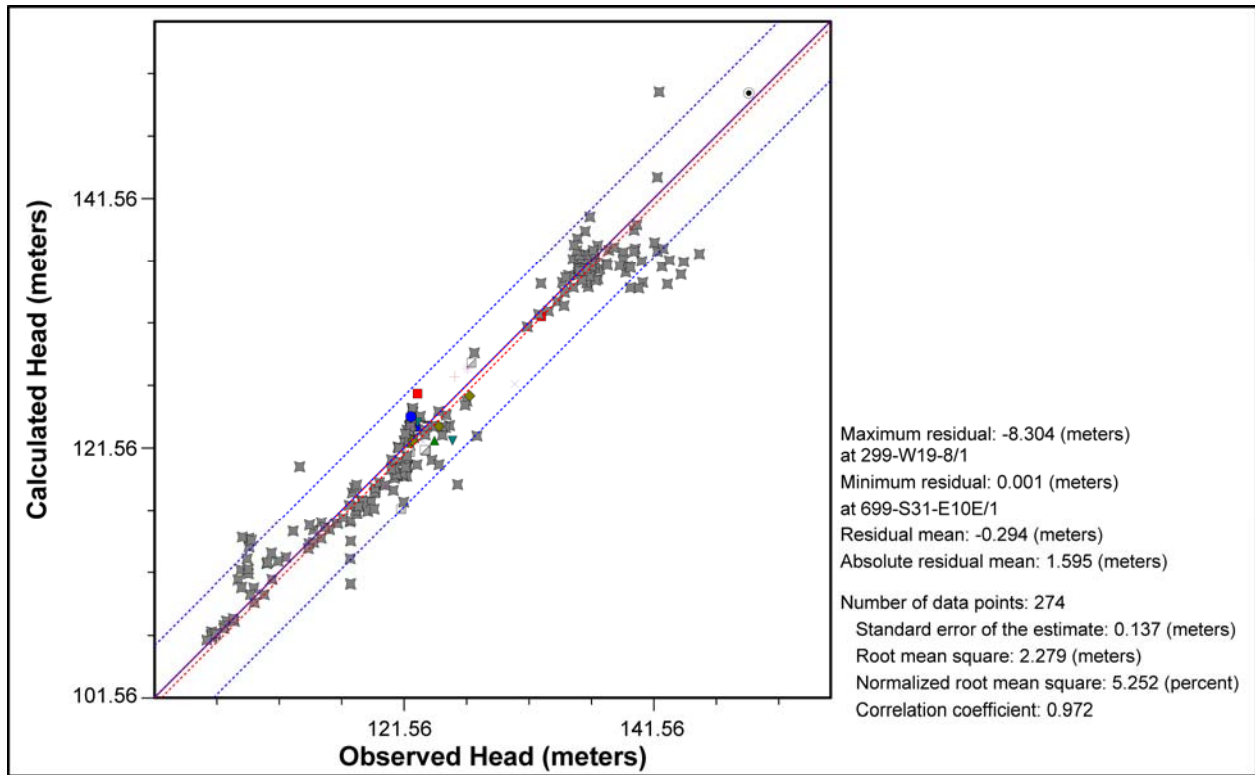


Figure L-82. Alternate Case Flow Model Residuals – Calendar Year 2015

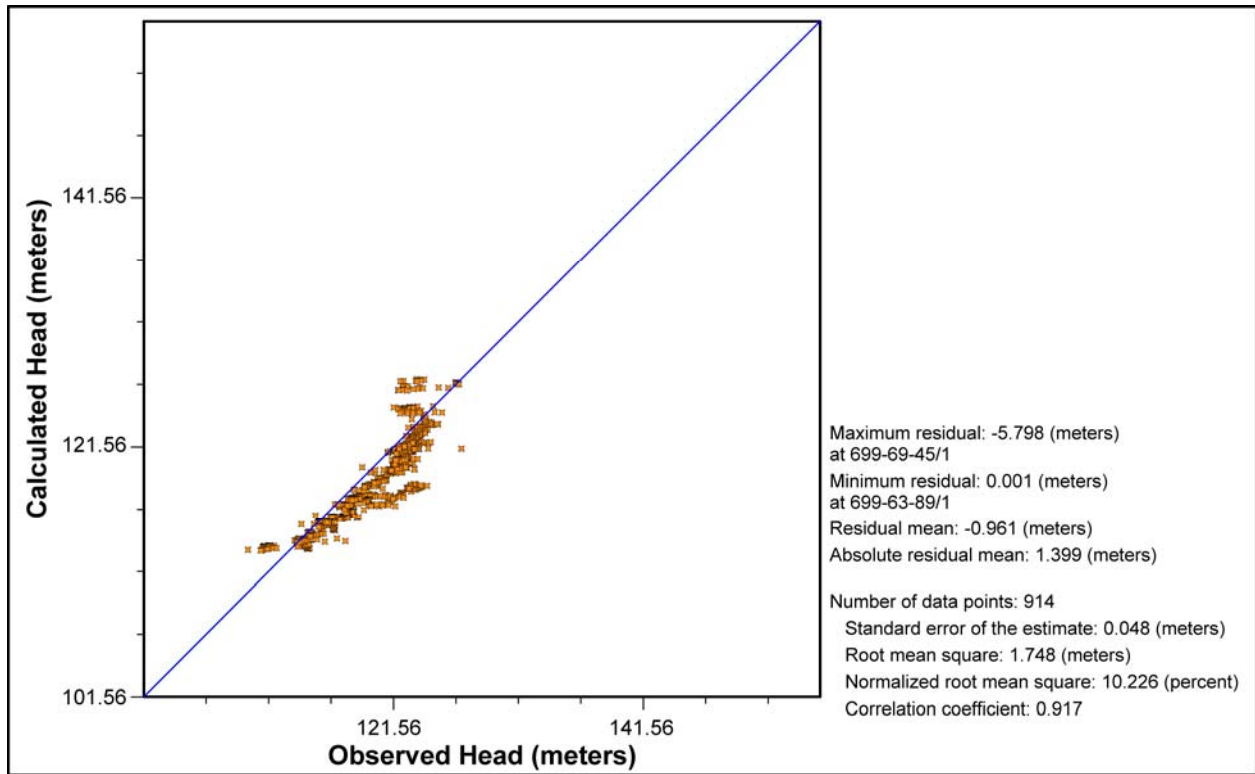


Figure L-83. Alternate Case Flow Model Residuals in Northern Region of Model

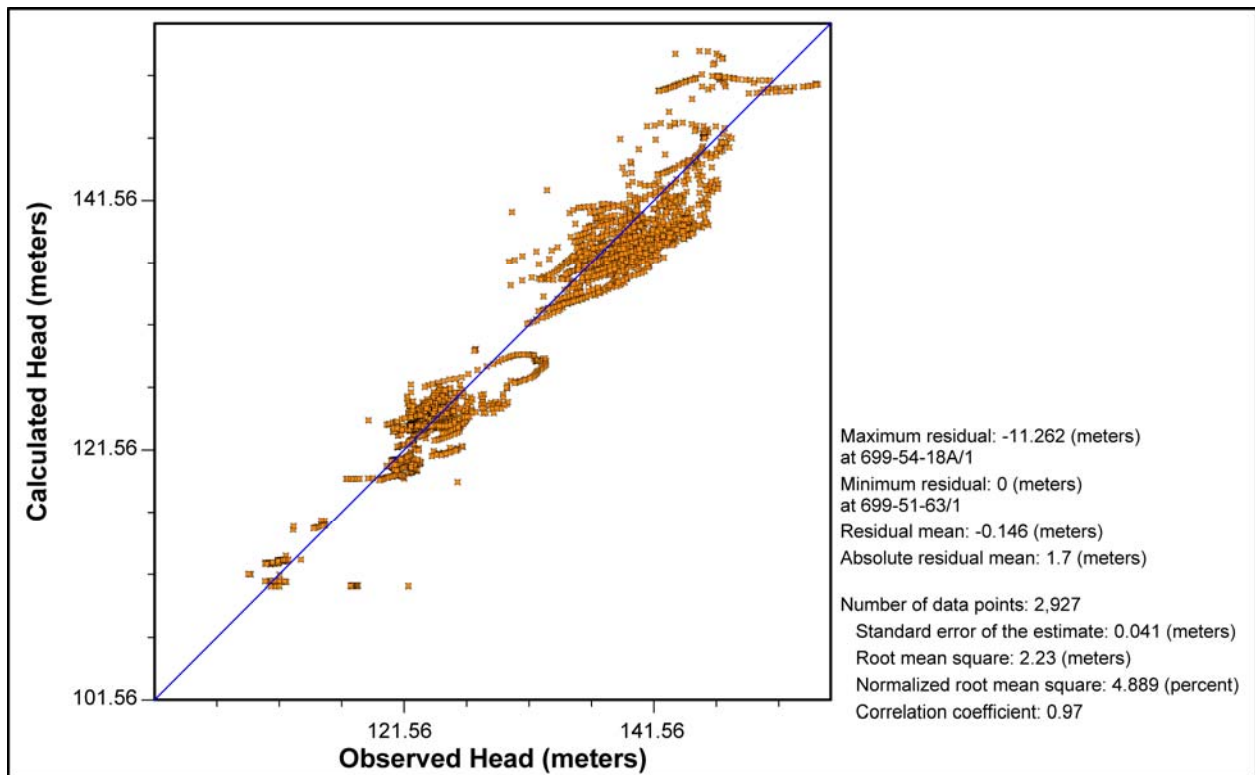


Figure L-84. Alternate Case Flow Model Residuals in Central Region of Model

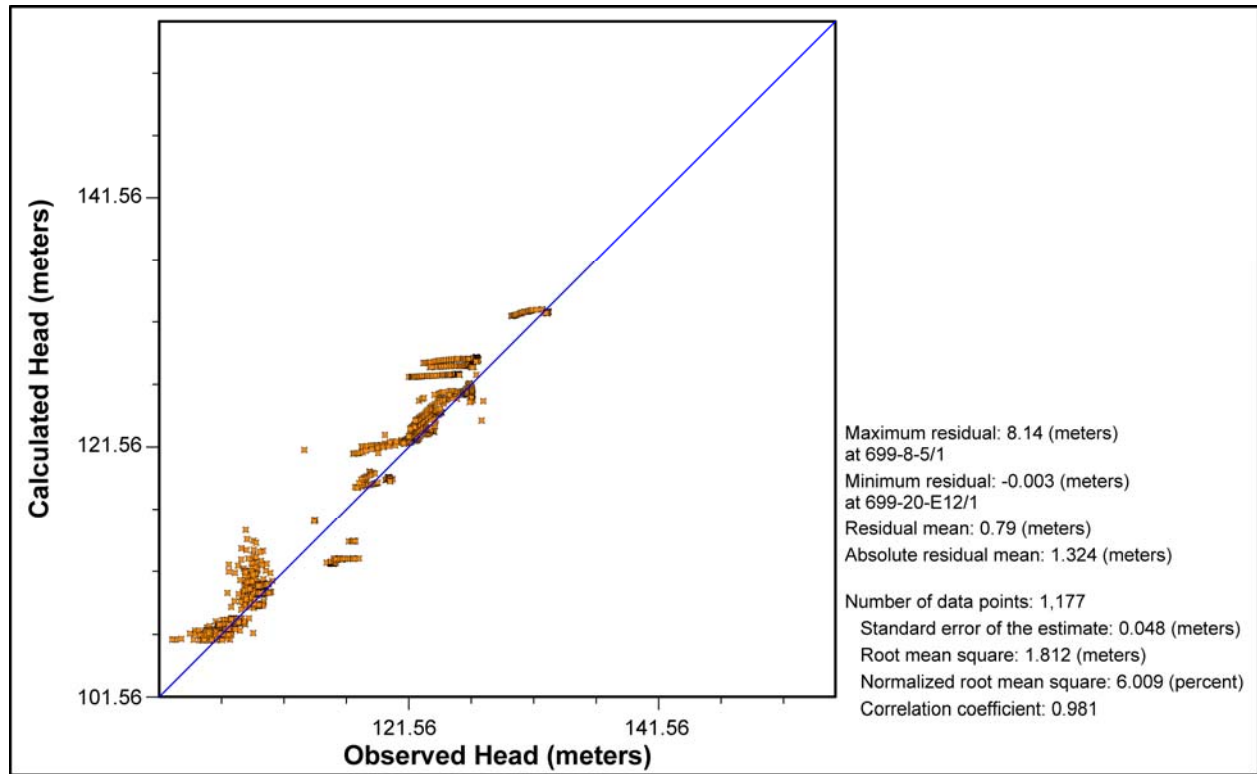


Figure L-85. Alternate Case Flow Model Residuals in Southern Region of Model

Table L-24. Alternate Case Flow Model Calibrated Hydraulic Conductivity Values

Material Type (Model Zone)	Hydraulic Conductivity (K _x) ^a	Hydraulic Conductivity (K _y) ^b	Hydraulic Conductivity (K _z) ^c
Hanford mud (1)	0.481	0.481	0.0481
Hanford silt (2)	21.8	21.8	2.18
Hanford sand (3)	30.4	30.4	3.04
Hanford gravel (4)	222.1	222.1	22.21
Ringold Sand (5)	0.83	0.83	0.083
Ringold Gravel (6)	18.7	18.7	1.87
Ringold Mud (7)	1.958	1.958	0.1958
Ringold Silt (8)	0.77	0.77	0.077
Plio-Pleistocene sand (9)	84.2	84.2	8.42
Plio-Pleistocene silt (10)	6.87	6.87	0.687
Cold Creek sand (11)	39.4	39.4	3.94
Cold Creek gravel (12)	5.6	5.6	0.56
Highly conductive Hanford gravel (13)	4331	4331	433.1
Activated basalt (14)	0.001	0.001	0.0001

^a Hydraulic conductivity with respect to the x axis, meters per day.

^b Hydraulic conductivity with respect to the y axis, meters per day.

^c Hydraulic conductivity with respect to the z axis, meters per day.

Note: To convert meters to feet, multiply by 3.281.

Table L–25. Alternate Case Hydraulic Conductivity Parameter Correlation Coefficient Matrix

Model Zone	1	2	3	4	5	6	7	8	9	10	11	12	13
1	1.00	0.08	-0.01	0.14	-0.08	-0.20	0.33	0.11	0.29	-0.14	0.01	0.07	-0.03
2	0.08	1.00	0.00	-0.01	-0.05	-0.01	-0.05	0.01	0.02	-0.17	0.10	0.02	-0.11
3	-0.01	0.00	1.00	0.12	-0.06	-0.11	-0.12	-0.08	0.20	-0.11	0.19	-0.12	0.21
4	0.14	-0.01	0.12	1.00	-0.13	-0.31	-0.23	-0.23	-0.18	-0.11	0.06	-0.18	0.26
5	-0.08	-0.05	-0.06	-0.13	1.00	-0.54	-0.04	0.10	-0.07	0.18	-0.21	0.08	-0.23
6	-0.20	-0.01	-0.11	-0.31	-0.54	1.00	-0.23	-0.08	0.08	-0.09	0.03	0.03	-0.04
7	0.33	-0.05	-0.12	-0.23	-0.04	-0.23	1.00	0.13	0.16	-0.17	-0.09	0.08	-0.27
8	0.11	0.01	-0.08	-0.23	0.10	-0.08	0.13	1.00	-0.05	-0.06	-0.13	0.34	-0.22
9	0.29	0.02	0.20	-0.18	-0.07	0.08	0.16	-0.05	1.00	0.00	-0.01	0.04	-0.05
10	-0.14	-0.17	-0.11	-0.11	0.18	-0.09	-0.17	-0.06	0.00	1.00	-0.18	-0.12	0.12
11	0.01	0.10	0.19	0.06	-0.21	0.03	-0.09	-0.13	-0.01	-0.18	1.00	0.09	-0.07
12	0.07	0.02	-0.12	-0.18	0.08	0.03	0.08	0.34	0.04	-0.12	0.09	1.00	-0.42
13	-0.03	-0.11	0.21	0.26	-0.23	-0.04	-0.27	-0.22	-0.05	0.12	-0.07	-0.42	1.00

The Alternate Case flow model is most sensitive to the hydraulic conductivity values of the Ringold Gravel, the Hanford gravel, and the highly conductive Hanford gravel. The Alternate Case hydraulic conductivity of Ringold Gravel is about 20 meters per day (65.6 feet per day) (see Table L–24). The histogram of hydraulic conductivity distribution for the Ringold Formation as measured in aquifer pump tests is shown in the upper right-hand corner of Figure L–53. The majority of the field measured hydraulic conductivities are between 10 and 30 meters per day (between 32.8 and 98.4 feet per day), in reasonable agreement with the Base Case value. Alternate Case hydraulic conductivities for the Hanford gravel and the highly conductive Hanford gravel are about 220 meters per day (722 feet per day) and about 4,000 meters per day (13,124 feet per day), respectively (see Table L–24). The histogram of hydraulic conductivity for the Hanford Formation as measured in aquifer pump tests is shown in the upper left-hand corner of Figure L–53. Note that the range of measured hydraulic conductivities for the Hanford Formation is much broader than the Ringold Formation. Measured hydraulic conductivities for the Hanford Formation show a maximum of about 300 meters per day (984 feet per day), with a secondary occurrence between 3,000 and 5,000 meters per day (between 9,843 and 16,405 feet per day). This suggests that the inclusion of the highly conductive Hanford gravel in the conceptual model reflects an important component of the hydraulic conductivity distribution at the site.

In addition to the calibration acceptance criteria, water (or mass) balance and a long-term steady state condition must be achieved in the calibrated flow model. Cumulative mass water balance data are shown in Figure L–86, indicating a cumulative mass balance error of approximately –1.4 percent. Total water balance and storage data as a function of time are shown in Figure L–87. These data show storage values relative to the total water balance and indicate that storage-in is approximately equal to storage-out in model year 140 (calendar year 2080). This confirms that a long-term steady state condition is achieved. Note that, in Figure L–87, there is a spike in “Total Storage In” and “Total In” at about model year 82. This spike is the result of a stress period change to the final long-term stress period. As a result, the model is moving from a relatively long time step at the end of the previous stress period to a relatively short time step at the beginning of the final stress period.

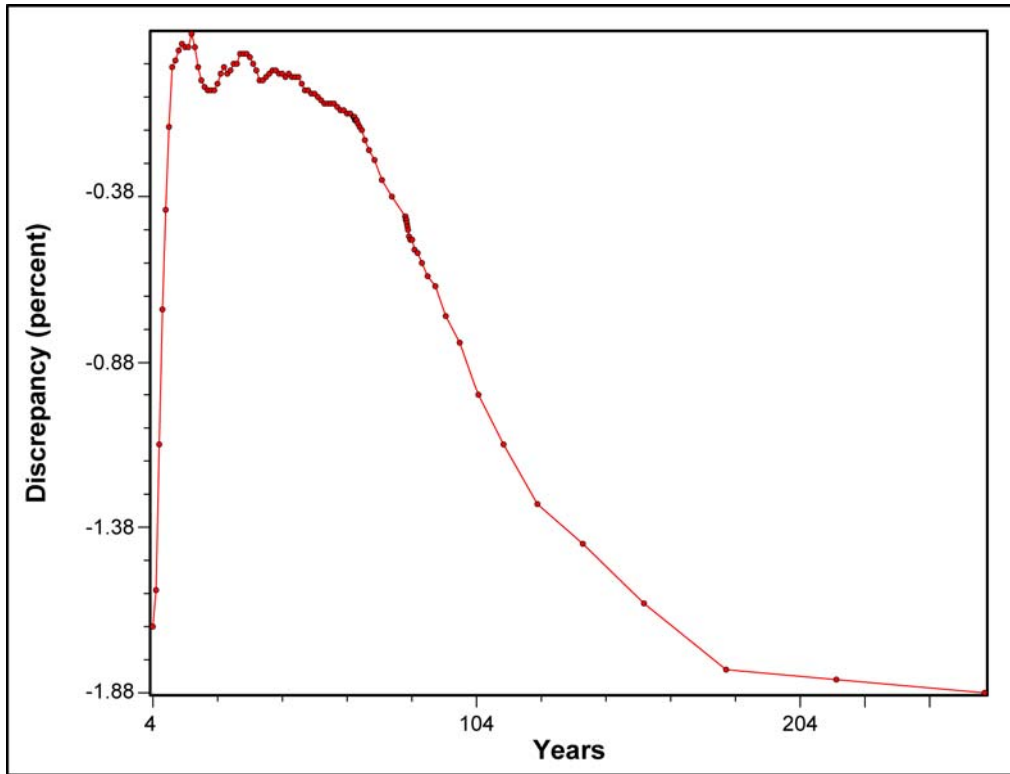


Figure L-86. Alternate Case Flow Model Cumulative Water Balance Discrepancy – Year 0 (Calendar Year 1940)

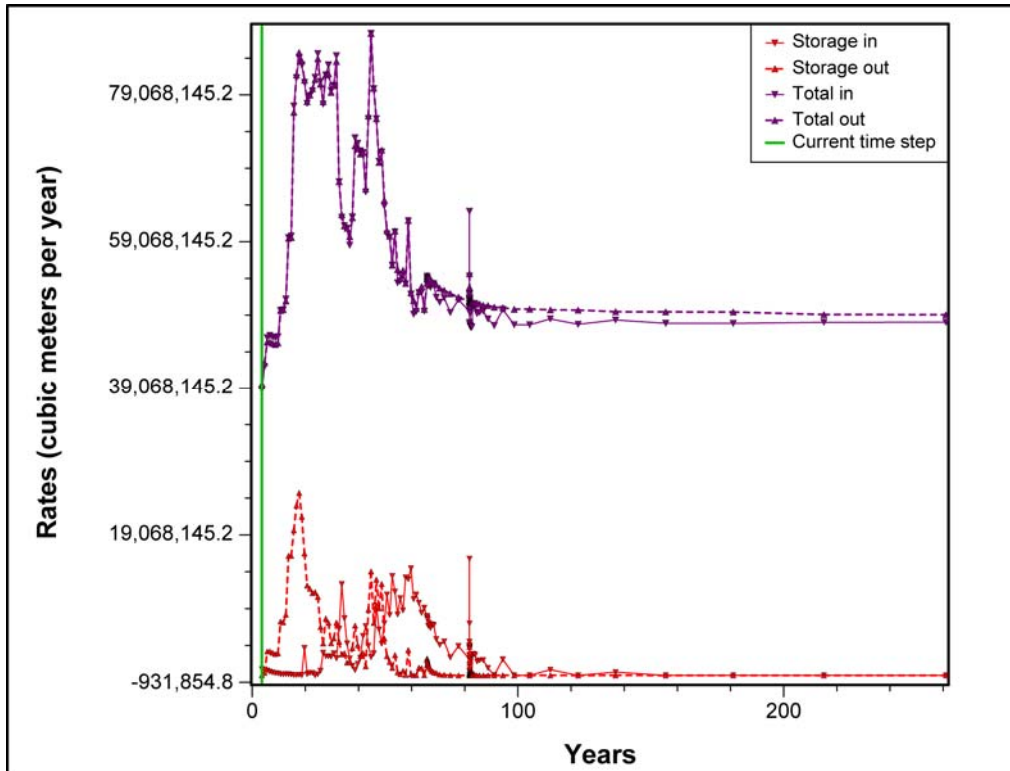


Figure L-87. Alternate Case Flow Model Total Water and Storage Rates Over Time – Year 0 (Calendar Year 1940)

L.10.2.1 Potentiometric Distribution

A goal for the Alternate Case flow model is to produce a potentiometric distribution of heads that shows a steep water table in the 200-West Area due to the low conductivity material types in that area and a relatively flat water table in the 200-East Area where high conductivity material types are present. The pre-Hanford potentiometric surface is assumed to be approximately the same as the post-Hanford long-term steady state condition, with water table mounding occurring below areas where and near times when Hanford operational discharges were released at the ground surface. Figures L-88 through L-90 are Alternate Case flow model simulations of the potentiometric surface in calendar years 1944 (pre-Hanford), 1975 (Hanford operations), and 2200 (post-Hanford), respectively.



**Figure L-88. Alternate Case Flow Model
Potentiometric Head Distribution –
Calendar Year 1944**



**Figure L-89. Alternate Case Flow Model
Potentiometric Head Distribution –
Calendar Year 1975**

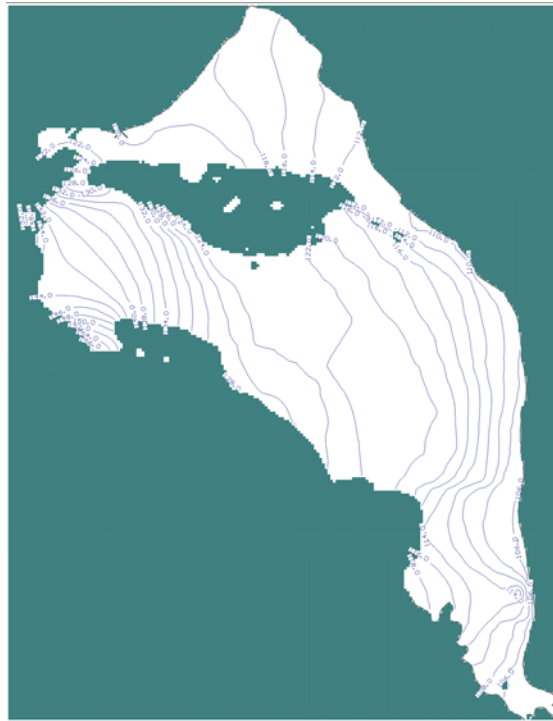


**Figure L-90. Alternate Case Flow Model
Potentiometric Head Distribution –
Calendar Year 2200**

L.10.2.2 Velocity Field

The Alternate Case flow model is variable in both magnitude and direction over time and across the model domain. This magnitude and direction variability near the BY Cribs in the 200-East Area is shown in Figures L-91 and L-92. The BY Cribs are in close proximity to Gable Gap, which is the location within the model that has a lower TOB encoded for the Alternate Case flow model. This lower TOB in the Gable Gap area is the distinguishing feature between the Base Case flow model and the Alternate Case flow model. See Figures L-63 and L-64 for comparable Base Case flow model velocity data at the BY Cribs. Comparing the velocity data between the Base Case and Alternate Case flow models at the BY Cribs indicates that the velocity directions and magnitudes in the Gable Gap area are sensitive to the elevation of the TOB in this area.

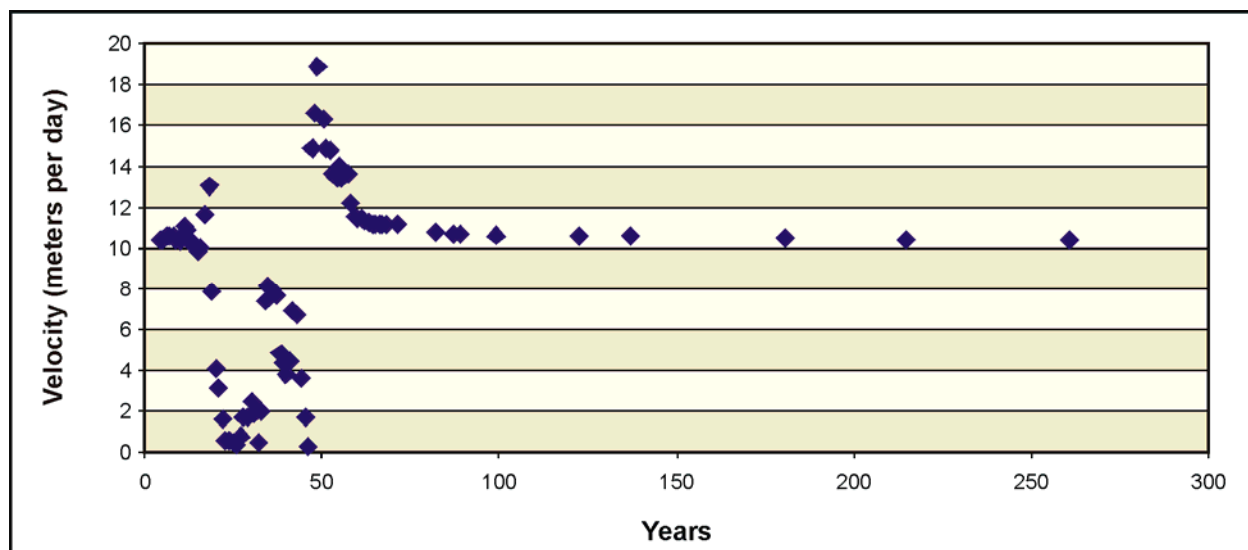


Figure L-91. Alternate Case Flow Model Velocity Magnitude at BY Cribs (200-East Area) – Year 0 (Calendar Year 1940)

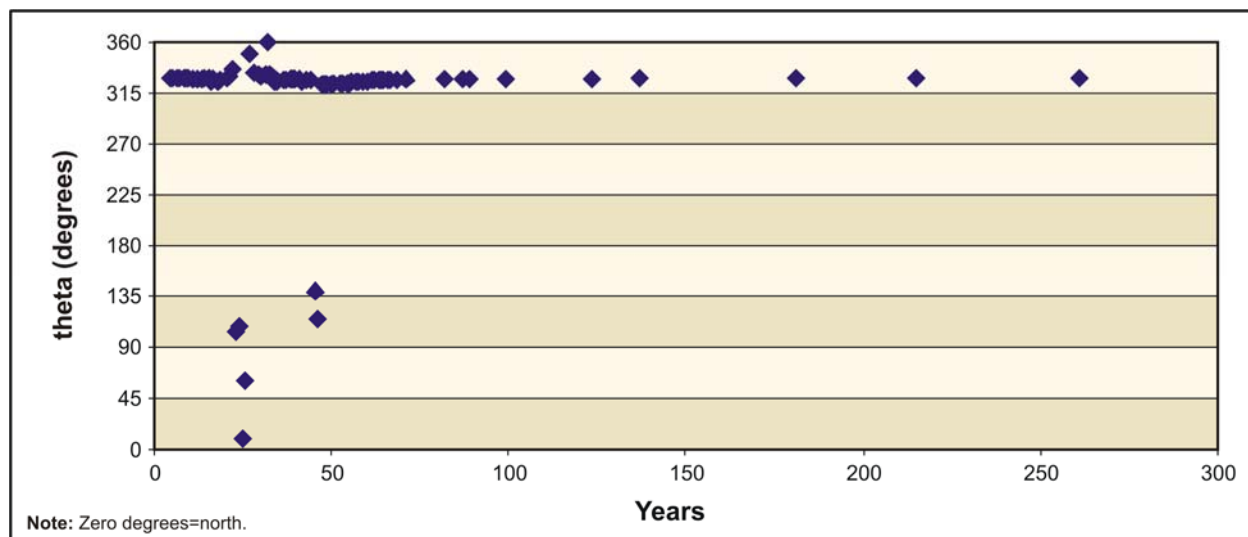


Figure L-92. Alternate Case Flow Model Velocity Direction at BY Cribs (200-East Area) – Year 0 (Calendar Year 1940)

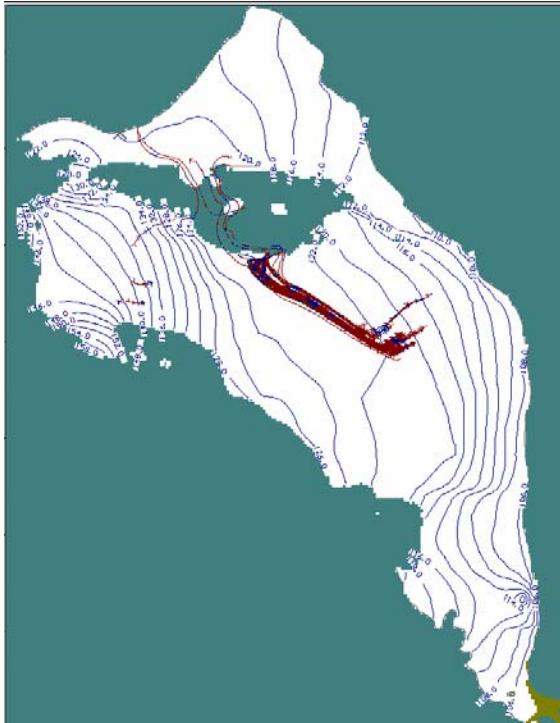
L.10.2.3 Pathline Analyses

Pathline analysis was performed on the top 32 model runs (see Section L.10.2) to narrow this field of models that performed well relative to RMS error to a single Alternate Case flow model. Two pathline analyses, the tritium plume pathline analysis and the Central Plateau delineation pathline analysis, were performed on each of the top 32 models.

L.10.2.3.1 Hydrogen-3 (Tritium) Plume Pathline Analysis

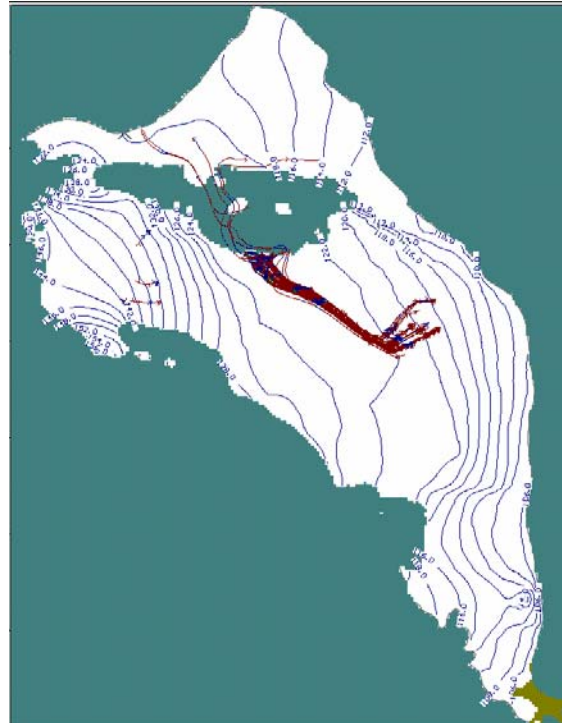
Tritium plume pathline analysis included a MODFLOW and MODPATH model run for each of the top 32 model cases, releasing particles in the 200-East and 200-West Areas representing an actual tritium release and comparing the particle pathlines to the general shape of the observed tritium plumes. This analysis is somewhat limited because no dispersion is applied to the particle pathlines so that spreading of the plume to its actual extents is constrained. This analysis does provide a qualitative means to compare

this final set of possible models to one another and aid in selecting the Alternate Case flow model. Figures L-65 and L-66 provide an interpretation of the field-observed tritium plume (Hartman, Morasch, and Webber 2004) to which the model-simulated pathlines were compared. Figures L-93 through L-96 provide the MODFLOW/MODPATH results of 4 of the top 32 model runs, including the model run selected as the Alternate Case flow model. Additionally, for the Alternate Case flow model, since the tritium plume pathline analysis covers the calibration period (1948–2006), it is important that the tritium plume result for the Alternate Case flow model qualitatively match the tritium plume result for the Base Case flow model. Figure L-68 shows the tritium plume pathline analysis results for the Base Case flow model. This analysis concluded that many of the top 32 model runs could be selected as the Alternate Case flow model if the selection were based only on the tritium plume pathline analysis.



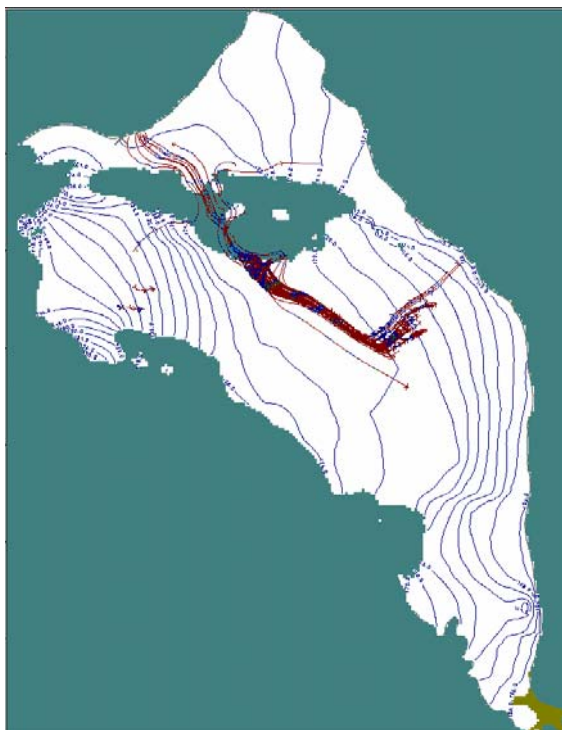
Note: To convert meters to feet, multiply by 3.281.

**Figure L-93. Hydrogen-3 (Tritium) Plume Pathline Analysis Run 407
(root mean square error = 2.065 meters)**



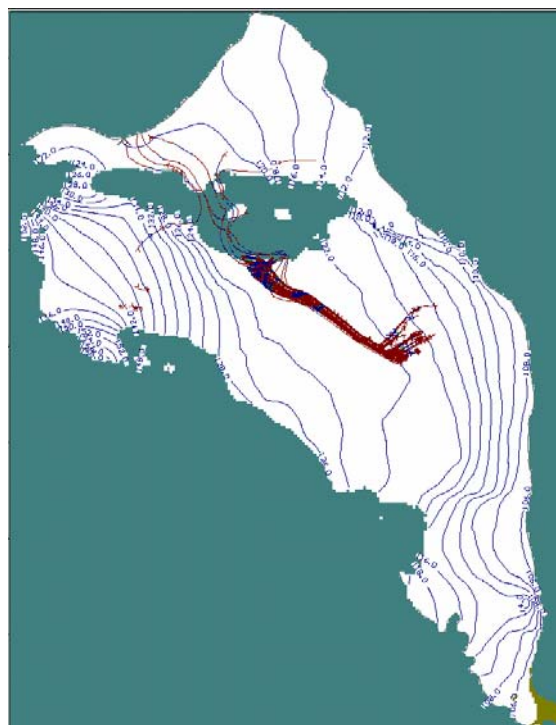
Note: To convert meters to feet, multiply by 3.281.

**Figure L-94. Hydrogen-3 (Tritium) Plume Pathline Analysis Run 195
(root mean square error = 2.056 meters) –
Selected as Alternate Case Flow Model**



Note: To convert meters to feet, multiply by 3.281.

**Figure L-95. Hydrogen-3 (Tritium)
Plume Pathline Analysis Run 238
(root mean square error = 2.048 meters)**



Note: To convert meters to feet, multiply by 3.281.

**Figure L-96. Hydrogen-3 (Tritium)
Plume Pathline Analysis Run 304
(root mean square error = 2.036 meters)**

L.10.2.3.2 Central Plateau Delineation Pathline Analysis

The *Technical Guidance Document* (DOE 2005) directed that the Alternate Case flow model would flow predominantly northward from the 200 Areas of Hanford. The purpose of the central plateau delineation pathline analysis was to determine for each of the top 32 model runs the amount of particles released in the 200 Areas that would move to the north through Gable Gap and the amount of particles that would move to the east toward the Columbia River. This analysis included a MODFLOW and MODPATH model run for each of the top 32 model cases, releasing a uniformly distributed set of particles across the central plateau. The central plateau is depicted as a rectangular-shaped boundary that includes all of the 200-East and 200-West Areas as well as other areas between and outside of the 200 Areas. This analysis provides a quantitative means to compare this final set of possible models to one another and aid in selecting a single Alternate Case flow model. Figures L-97 through L-100 provide the MODFLOW/MODPATH results of 4 of the 32 model runs, including the model run selected as the Alternate Case flow model (see Figure L-98).

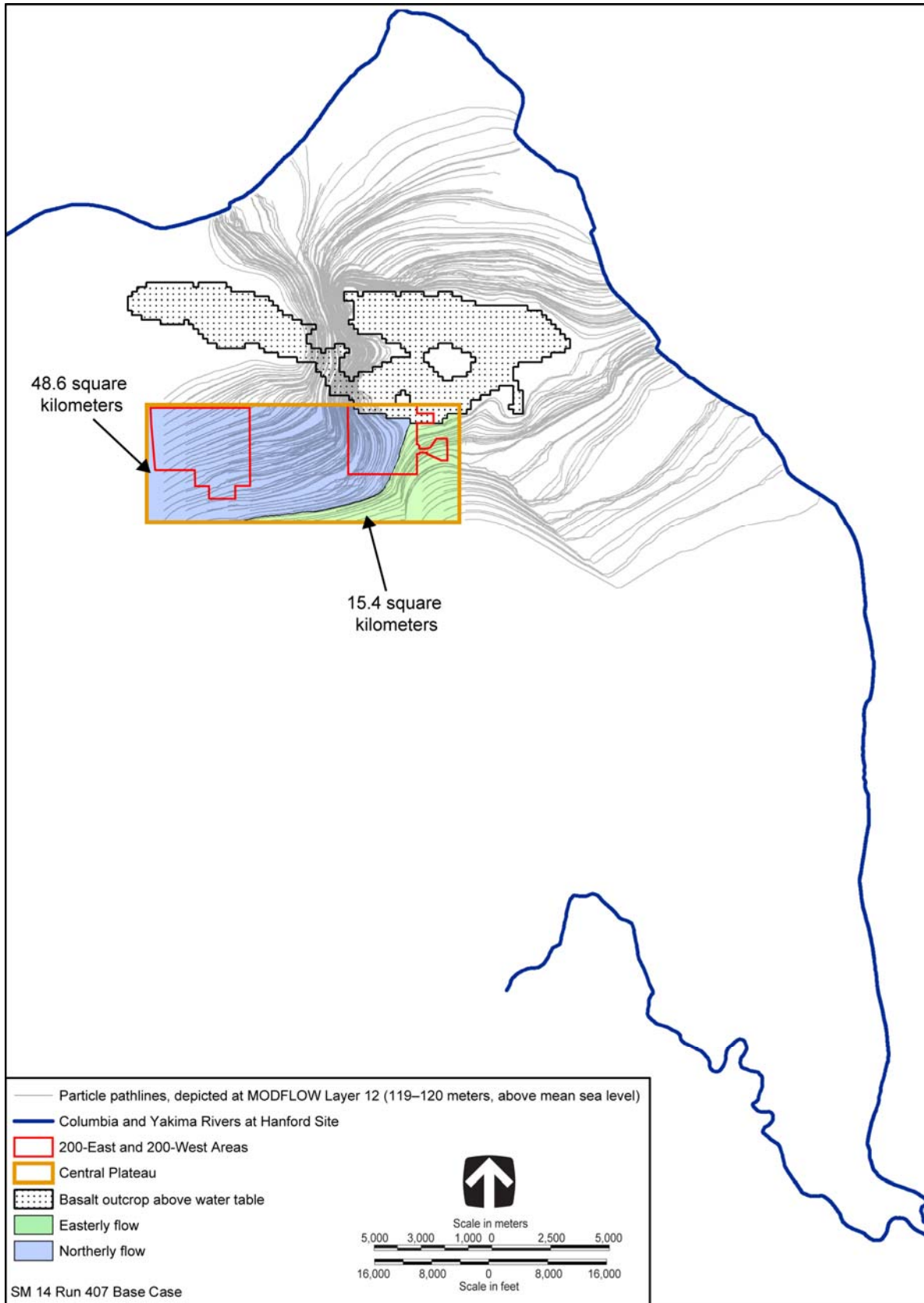


Figure L-97. Central Plateau Delineation Pathline Analysis Run 407 (root mean square error = 2.065 meters)

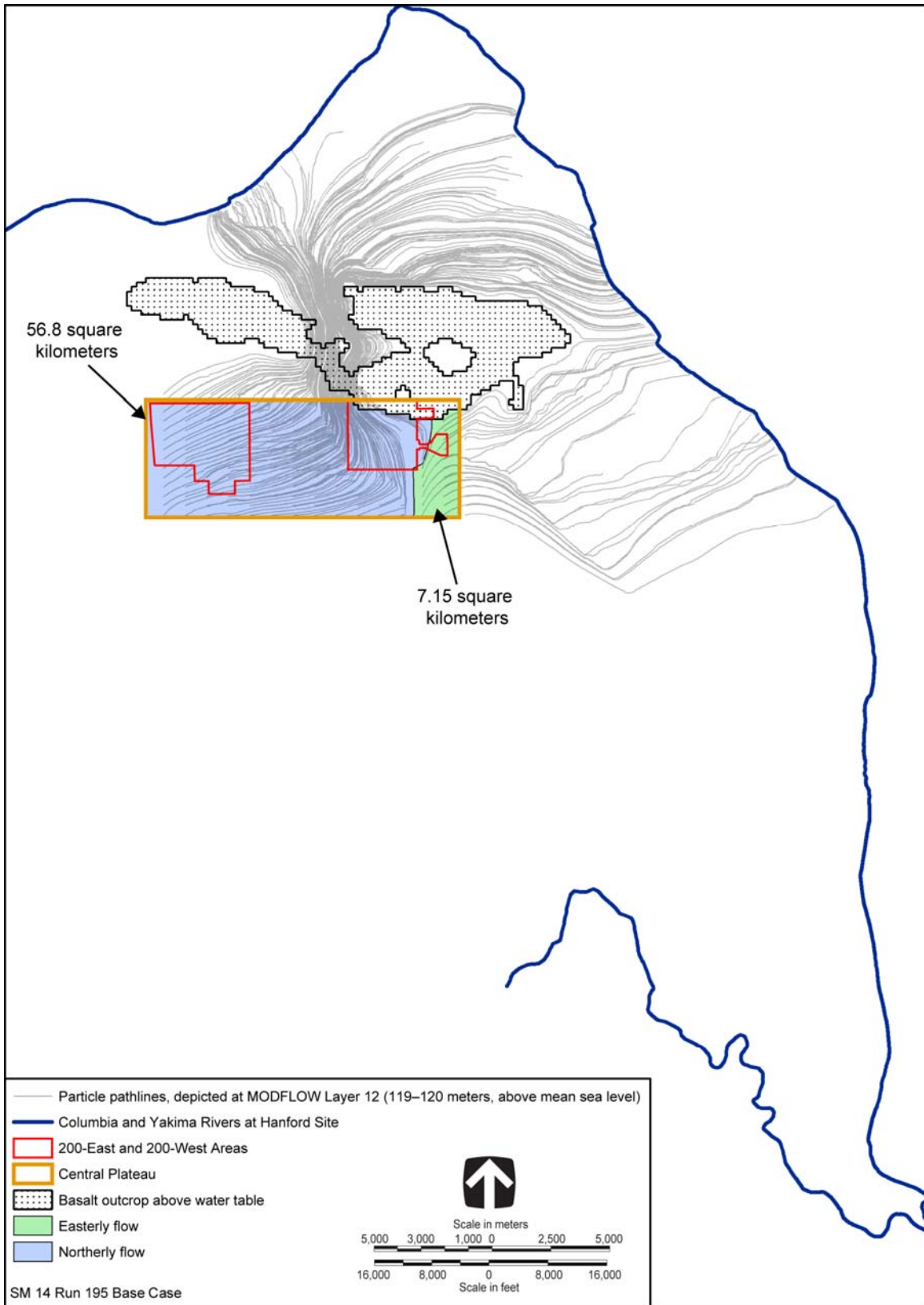


Figure L–98. Central Plateau Delineation Pathline Analysis Run 195 (root mean square error = 2.056 meters) – Selected as Alternate Case Flow Model

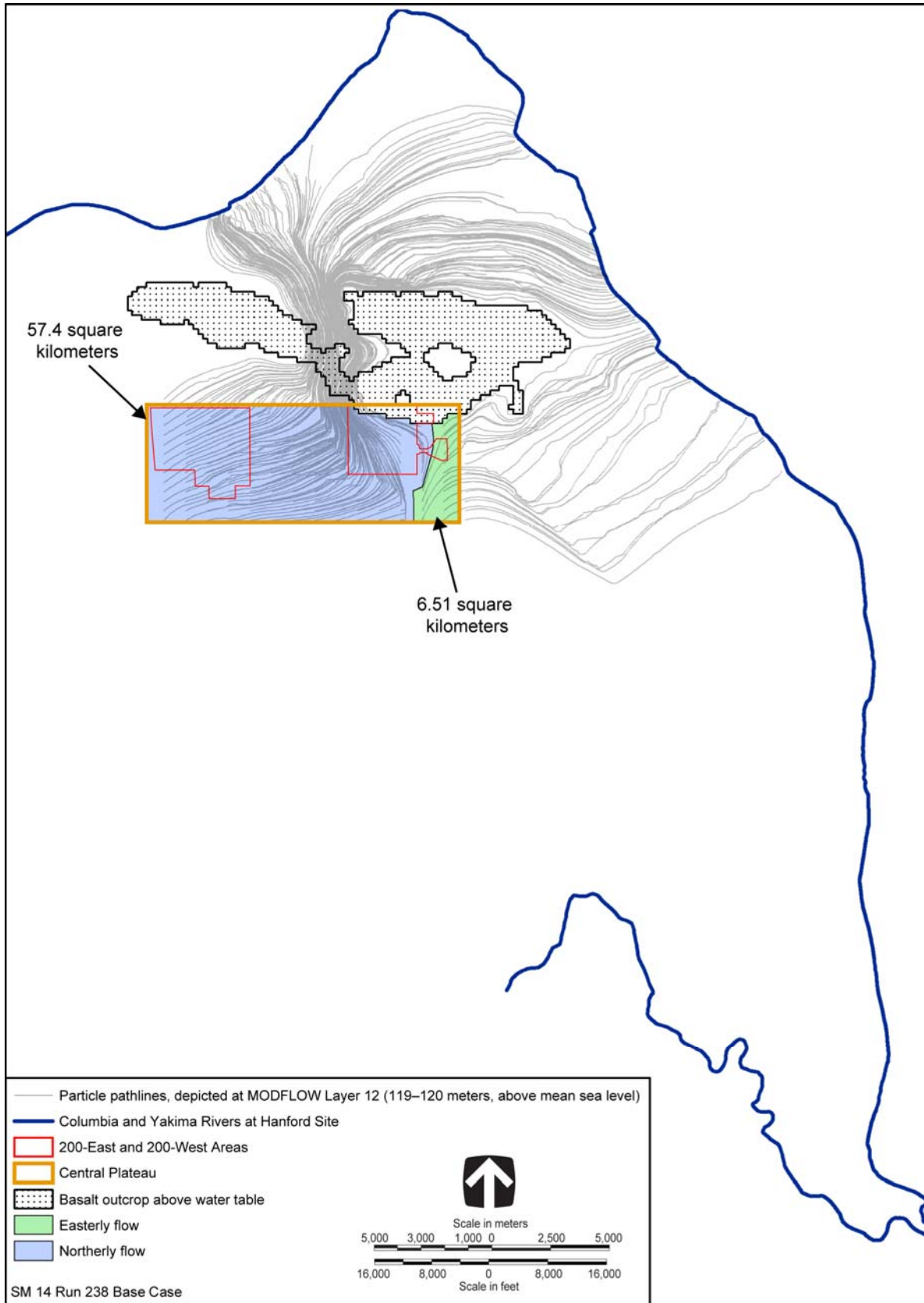


Figure L-99. Central Plateau Delineation Pathline Analysis Run 238 (root mean square error = 2.048 meters)

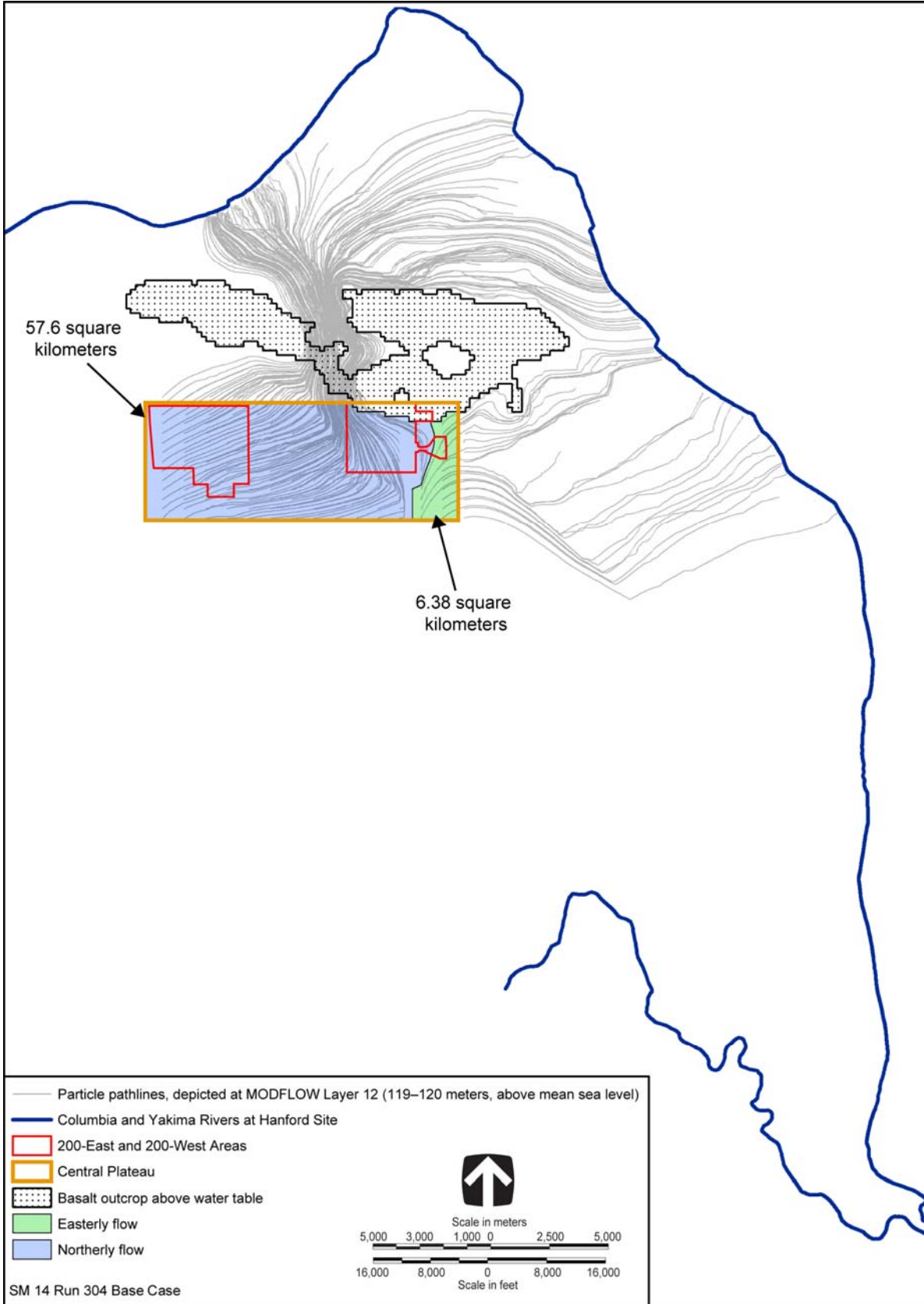


Figure L–100. Central Plateau Delineation Pathline Analysis Run 304 (root mean square error = 2.036 meters)

Table L–26 provides a summary of the percentage of particle pathlines flowing to the east and to the north for the top 32 Alternate Case model runs.

**Table L–26. Summary of Top 32 Alternate Case Model Runs – Northerly Versus
Easterly Flow**

Run Number	Area of Northerly Flow (square kilometers)	Area of Easterly Flow (square kilometers)	Northerly Flow (percent)	Easterly Flow (percent)
075	61.5	2.4	96	4
210	61.0	3.0	95	5
321	60.8	3.1	95	5
120	60.6	3.3	95	5
148	59.0	5.0	92	8
290	58.4	5.6	91	9
043	58.2	5.8	91	9
118	57.7	6.2	90	10
304	57.6	6.4	90	10
215	57.4	6.5	90	10
238	57.4	6.5	90	10
286	57.1	6.8	89	11
020	57.1	6.8	89	11
214	57.0	7.0	89	11
109	56.9	7.1	89	11
195	56.8	7.2	89	11
133	56.7	7.2	89	11
060	56.6	7.3	89	11
039	56.6	7.4	88	12
185	56.6	7.4	88	12
126	56.5	7.5	88	12
369	56.4	7.5	88	12
380	56.4	7.6	88	12
198	56.2	7.8	88	12
390	54.4	9.5	85	15
353	54.0	10.0	84	16
033	53.8	10.1	84	16
212	49.4	14.6	77	23
407	48.6	15.4	76	24
066	48.6	15.4	76	24
059	44.2	19.7	69	31
068	43.5	20.4	68	32

Note: To convert square kilometers to square miles, multiply by 0.386.

Based on the results of this analysis, coupled with the qualitative matching of the Alternate Case flow model tritium plume pathline analysis with the Base Case flow model results, run 195 was selected as the Alternate Case flow model.

L.11 FLOW FIELD EXTRACTION

To support analysis of potential contaminant transport patterns in the saturated zone, the MODFLOW groundwater flow model developed for this *TC & WMEIS* is being used as the basis for particle-tracking simulations. The selected particle-tracking code does not directly read MODFLOW output files to calculate the velocities required as input to particle tracking; instead, the MODFLOW files must be independently processed to generate these velocities.

The Base Case and Alternate Case flow model data files were processed by extracting hydraulic heads and velocities at each active cell within the model domain at selected times. The times selected for extracting the head and velocity data files are included in Table L-27.

Table L-27. Selected Times for Extracting the Base Case and Alternate Case Head and Velocity Data Files

Stress Period	Time Step	Model Year	Calendar Year
1	5	4	1943
2	10	5	1944
3	10	6	1945
4	10	7	1946
5	10	8	1947
6	10	9	1948
7	10	10	1949
8	10	11	1950
9	10	12	1951
10	10	13	1952
11	10	14	1953
12	10	15	1954
13	10	16	1955
14	10	17	1956
15	10	18	1957
16	10	19	1958
17	10	20	1959
18	10	21	1960
19	10	22	1961
20	10	23	1962
21	10	24	1963
22	10	25	1964
23	10	26	1965
24	10	27	1966
25	10	28	1967
26	10	29	1968
27	10	30	1969
28	10	31	1970
29	10	32	1971
30	10	33	1972
31	10	34	1973
32	10	35	1974
33	10	36	1975
34	10	37	1976
35	10	38	1977

**Table L-27. Selected Times for Extracting the Base Case
and Alternate Case Head and Velocity Data Files
(continued)**

Stress Period	Time Step	Model Year	Calendar Year
36	10	39	1978
37	10	40	1979
38	10	41	1980
39	10	42	1981
40	10	43	1982
41	10	44	1983
42	10	45	1984
43	10	46	1985
44	10	47	1986
45	10	48	1987
46	10	49	1988
47	10	50	1989
48	10	51	1990
49	10	52	1991
50	10	53	1992
51	10	54	1993
52	10	55	1994
53	10	56	1995
54	10	57	1996
55	10	58	1997
56	10	59	1998
57	10	60	1999
58	10	61	2000
59	10	62	2001
60	10	63	2002
61	10	64	2003
62	10	65	2004
63	10	66	2005
64	70	67	2006
64	90	67.9	2006.9
64	100	68.6	2007.6
64	110	69.5	2008.5
64	120	70.8	2009.8
64	130	72.5	2011.5
64	140	74.8	2013.8
64	150	77.9	2016.9
64	160	82	2021
65	230	83.2	2022.2
65	250	84.1	2023.1
65	270	85.8	2024.8
65	280	87.2	2026.2
65	290	88.9	2027.9
65	300	91.3	2030.3

Table L–27. Selected Times for Extracting the Base Case and Alternate Case Head and Velocity Data Files
(continued)

Stress Period	Time Step	Model Year	Calendar Year
65	310	94.5	2033.5
65	320	98.8	2037.8
65	330	104.6	2043.6
65	340	112.4	2051.4
65	350	122.8	2061.8
65	360	136.9	2075.9
65	370	155.7	2094.7
65	380	181.1	2120.1
65	390	215.2	2154.2
65	400	261	2200

The Base Case and Alternate Case flow models have achieved a long-term steady state condition as of model year 140 (calendar year 2080). Four additional time steps after model year 140 (through model year 261, calendar year 2200) were extracted for use in groundwater transport modeling. Appendix O contains simulations of groundwater plumes for both the operational and post-operational timeframes to illustrate the effects of the uncertainty in predominant flow field direction on contaminant transport simulations.

L.12 SUMMARY

A three-dimensional transient flow model was developed to support the *TC & WMEIS* analyses of alternatives and cumulative impacts. The flow model was developed using the MODFLOW 2000 engine within the Visual MODFLOW framework. The site conceptual model consists of an unconfined, heterogeneous aquifer bounded at the bottom by an impermeable basalt surface. Water enters the model from mountain-front recharge along Rattlesnake Mountain, from the Yakima River, from areal recharge, and from operational discharges, primarily at the Central Plateau of Hanford. Water leaves the model via the Columbia River and several pumping wells. The operational discharges and pumping well withdrawals vary with time, providing the transient drivers to the model.

Standard data gathering and encoding techniques were used to develop the model extents, gridding, TOB topography, location and elevation of the Columbia and Yakima Rivers, lithology, and artificial discharges and withdrawals. These elements of the model were encoded directly from site-specific data. The background areal recharge was encoded using the *Technical Guidance Document* (DOE 2005). Initial estimates for GHB heads and conductances, riverbed conductances, and material properties were encoded and refined through a flow calibration process.

Initial calibration suggested that the model was extremely sensitive to GHB heads and conductances. These items were calibrated manually using water-level data for a selected subset of wells near the GHB locations. Initial calibration also suggested that the model was relatively insensitive to the riverbed conductances, as long as these values were reasonably high. Gradient-based PEST calibration was initially used to estimate the material properties (the primary model sensitivity was to hydraulic conductivity). The results from the gradient-based calibration suggested that this method seriously overestimated the confidence in the calibration parameters and that the topology of the objective function was characterized by many local minima.

For the purposes of this *TC & WMEIS*, an accurate estimate of the uncertainty in the model is an important objective. Accordingly, an effort was made to better estimate the span of parameter space that

provided acceptable agreement with historic field measurements of water-level data using Monte Carlo optimization. The parameter space was searched at random, with over 5,000 realizations of hydraulic conductivity values tested. The results of the Monte Carlo optimization were that the model is primarily sensitive to the values of hydraulic conductivity for five of the material types and that acceptable ranges for these hydraulic conductivities could be established.

At the start of the model development effort, it was anticipated that the model could be extremely sensitive to the TOB elevation in the Gable Gap area. The *Technical Guidance Document* (DOE 2005) directed that an Alternate Case should be developed to investigate this sensitivity. A geostatistical analysis of the available elevations of the unconfined aquifer/TOB contact was performed. The mean surface was used in the Base Case model, and the 95th percentile lower confidence limit surface was used in the Alternate Case model. Results showed that both the Base Case and Alternate Case models could yield reasonable agreement with measured water-level data during the operational period (1944–2006) and that long-term post-Hanford flow directions from the sources in the Core Zone were primarily to the east for the Base Case and primarily to the north for the Alternate Case.

Flow fields were extracted from both the Base and Alternate Cases for use with contaminant transport modeling for the long-term groundwater impacts analyses (see Appendix O). These flow fields contain magnitude and direction of the pore water velocity field throughout the active model domain. Finally, the Base Case model was used in conjunction with modeling results from the Bureau of Reclamation to estimate the effects of leakage from the proposed Black Rock Reservoir (see Appendix V), a reasonably foreseeable future condition.

L.13 REFERENCES

Byrnes, M.E., and M.S. Miller, 2006, *Remedial Investigation Report for 200-ZP-1 Groundwater Operable Unit*, DOE/RL-2006-24, Draft A, U.S. Department of Energy, Richland, Washington, April.

Cole, C.R., M.P. Bergeron, C.J. Murray, P.D. Thorne, S.K. Wurstner, and P.M. Rogers, 2001, *Uncertainty Analysis Framework – Hanford Site-Wide Groundwater Flow and Transport Model*, PNNL-13641, Pacific Northwest National Laboratory, Richland, Washington, November.

Connelly, M.P., B.H. Ford, and J.V. Borghese, 1992, *Hydrogeologic Model for the 200 West Groundwater Aggregate Area*, WHC-SD-EN-TI-014, Rev. 0, Westinghouse Hanford Company, Richland, Washington.

DOE (U.S. Department of Energy), 1994, *Limited Field Investigation Report for the 100-HR-3 Operable Unit*, DOE/RL-93-43, Rev. 0, Richland, Washington, September.

DOE (U.S. Department of Energy), 2005, *Technical Guidance Document for Tank Closure Environmental Impact Statement, Vadose Zone and Groundwater Revised Analyses*, Final Rev. 0, Office of River Protection, Richland, Washington, March 25.

Ecology, EPA, and DOE (Washington State Department of Ecology, Olympia, Washington; U.S. Environmental Protection Agency, Washington, D.C.; and U.S. Department of Energy, Richland, Washington), 1989, Hanford Federal Facility Agreement and Consent Order, 89-10, as amended, accessed through <http://www.hanford.gov/tpa/tpahome.htm>, May 15.

Fetter, C.W., 1988, *Applied Hydrogeology*, 2nd ed., Merrill Publishing Company, Columbus, Ohio.

Freeze, R.A., and J.A. Cherry, 1979, *Groundwater*, Prentice-Hall Inc., Englewood Cliffs, New Jersey.

Fruchter, J.S., J.E. Amonette, C.R. Cole, Y.A. Gorby, M.D. Humphrey, J.D. Isok, F.A. Spane et al., 1996, *In Situ Redox Manipulation Field Injection Test Report – Hanford 100-H Area*, PNNL-11372, Pacific Northwest National Laboratory, Richland, Washington, December.

Hartman, M.J., L.F. Morasch, and W.D. Webber, eds., 2004, *Hanford Site Groundwater Monitoring for Fiscal Year 2003*, PNNL-14548, Pacific Northwest National Laboratory, Richland, Washington, March.

Hill, M.C., 1990, *Preconditioned Conjugate-Gradient 2 (PCG2), A Computer Program for Solving Ground-Water Flow Equations*, Water-Resources Investigations Report 90-4048, U.S. Geological Survey, Denver, Colorado.

Johnston, K., J.M. Ver Hoef, K. Krivoruchko, and N. Lucas, eds., 2001, *Using ArcGIS Geostatistical Analyst*, Environmental Systems Research Institute, Inc., Redlands, California.

Khaleel, R., and E.J. Freeman, 1995, *Variability and Scaling of Hydraulic Properties for 200 Area Soils, Hanford Site*, WHC-EP-0883, Rev. 0, Westinghouse Hanford Company, Richland, Washington, October.

National Research Council, 1996, *The Hanford Tanks: Environmental Impacts and Policy Choices*, Committee on Remediation of Buried and Tank Wastes, Board on Radioactive Waste Management, Commission on Geosciences, Environment, and Resources, National Academy Press, Washington, D.C.

PNNL (Pacific Northwest National Laboratory), 2006, HydroDat_DataReq239.xls, HydroDat_DataReq239_WithOrigDate.xls, qry_DataRequest239.txt, September.

Rohay, V.J., K.J. Swett, and G.V. Last, 1994, *1994 Conceptual Model of the Carbon Tetrachloride Contamination in the 200 West Area at the Hanford Site*, WHC-SD-EN-TI-248, Rev. 0, Westinghouse Hanford Company, Richland, Washington.

Rohay, V. J., K.J. Swett, V.M. Johnson, G.V. Last, D.C. Lanigan, and L.A. Doremus, 1993, *FY93 Site Characterization Status Report and Data Package for the Carbon Tetrachloride Site*, WHC-SD-EN-TI-202, Rev. 0, Westinghouse Hanford Company, Richland, Washington.

SAIC (Science Applications International Corporation), 2006, *Cumulative Impacts Analysis, Inventory Development*, Rev. 4, Germantown, Maryland, October 2.

Schalla, R., R.W. Wallace, R.L. Aaberg, S.P. Airhart, D.J. Bates, J.V.M. Carlile, C.S. Cline et al., 1988, *Interim Characterization Report for the 300 Area Process Trenches*, PNL-6716, Pacific Northwest Laboratory, Richland, Washington, September.

Spane, F.A., Jr., and P.D. Thorne, 2000, *Analysis of the Hydrologic Response Associated with Shutdown and Restart of the 200-ZP-1 Pump-and-Treat System*, PNNL-13342, Pacific Northwest National Laboratory, Richland, Washington, September.

Spane, F.A., Jr., P.D. Thorne, and D.R. Newcomer, 2001a, *Results of Detailed Hydrologic Characterization Tests – Fiscal Year 1999*, PNNL-13378, Pacific Northwest National Laboratory, Richland, Washington, January.

Spane, F.A., Jr., P.D. Thorne, and D.R. Newcomer, 2001b, *Results of Detailed Hydrologic Characterization Tests – Fiscal Year 2000*, PNNL-13514, Pacific Northwest National Laboratory, Richland, Washington, May.

Spane, F.A., Jr., P.D. Thorne, and D.R. Newcomer, 2002, *Results of Detailed Hydrologic Characterization Tests – Fiscal Year 2001*, PNNL-14113, Pacific Northwest National Laboratory, Richland, Washington, November.

Spane, F.A., Jr., D.R. Newcomer, and P.D. Thorne, 2003, *Results of Detailed Hydrologic Characterization Tests – Fiscal Year 2002*, PNNL-14186, Pacific Northwest National Laboratory, Richland, Washington, February.

Thorne, P.D., M.P. Bergeron, M.D. Williams, and V.L. Freeman, 2006, *Groundwater Data Package for Hanford Assessments*, PNNL-14753, Rev. 1, Pacific Northwest National Laboratory, Richland, Washington, January.

USGS (U.S. Geological Survey), 2004, *MODFLOW 2000 Engine, Version 1.15.00*, August 6.

WHI (Waterloo Hydrogeologic, Inc.), 2005, *HydroGeo Analyst v. 3.0 User's Manual – Database Utilities*, Borehole Logging/Reporting, 2D Mapping and Cross Sections, and 3D Visualization, Waterloo, Ontario, Canada.

WHI (Waterloo Hydrogeologic, Inc.), 2006, *Visual MODFLOW v. 4.2 User's Manual: For Professional Applications in Three-Dimensional Groundwater Flow and Contaminant Transport Modeling*, Waterloo, Ontario, Canada.

Williams, M.D., V.R. Vermeul, J.E. Szecsody, and J.S. Fruchter, 2000, *100-D Area In Situ Redox Treatability Test for Chromate-Contaminated Groundwater*, PNNL-13349, Pacific Northwest National Laboratory, Richland, Washington, September.

Code of Federal Regulations

10 CFR 1021, U.S. Department of Energy, “National Environmental Policy Act Implementing Procedures.”

40 CFR 1500–1508, Council on Environmental Quality, Regulations for Implementing the Procedural Provisions of the National Environmental Policy Act.

40 CFR 1502.1, Council on Environmental Quality, “Environmental Impact Statement: Purpose.”

40 CFR 1502.2(b), Council on Environmental Quality, “Environmental Impact Statement: Implementation.”

Federal Register

62 FR 8693, U.S. Department of Energy, 1997, “Record of Decision for the *Tank Waste Remediation System, Hanford Site, Richland, WA*,” February 26.

United States Code

42 U.S.C. 4321 et seq., National Environmental Policy Act of 1969.